# Synthesis and Characterization of Methacrylate Based Copolymers

**Mamoon Mohammad Alokour**

Submitted to the
Institute of Graduate Studies and Research
in partial fulfillment of the requirements for the degree of

Doctor of Philosophy
in
Chemistry

Eastern Mediterranean University
September 2019
Gazimağusa, North Cyprus

Approval of the Institute of Graduate Studies and Research

Prof. Dr. Ali Hakan Ulusoy
Acting Director

I certify that this thesis satisfies all the requirements as a thesis for the degree of Doctor of Philosophy in Chemistry.

Prof. Dr. İzzet Sakallı
Chair, Department of Chemistry

We certify that we have read this thesis and that in our opinion it is fully adequate in scope and quality as a thesis for the degree of Doctor of Philosophy in Chemistry.

Prof. Dr. Elvan Yılmaz
Supervisor

Examining Committee

1. Prof. Dr. Mustafa Gazi

2. Prof. Dr. Oğuz Okay

3. Prof. Dr. Hayal Bülbül Sönmez

4. Prof. Dr. Elvan Yılmaz

5. Asst. Prof. Dr. Emine Vildan Burgaz

# ABSTRACT

Random copolymers of poly(ethylene glycol methacrylate) (PEGM), and diethyl amino ethyl methacrylate (DEAEM) were synthesized at low, and high conversions by photoinitiation. Crosslinked poly(PEGM-co-DEAEM) samples were obtained, and characterized by FTIR, SEM, DSC, TGA, and elemental analyses. Swelling behavior of the copolymers revealed that the copolymers acted as superabsorbent hydrogels. The monomer reactivity ratios were calculated using Fineman Ross, Extended Kelen Tüdøs, and Mayo Lewis methods that gave $r_1$(PEGM)=0.90, $r_2$(DEAEM)=0.14 at low conversions. At high conversions $r_1$ and $r_2$ values were calculated as 1.01 and 0.40, respectively. Adsorption isotherms of methyl orange(MO) onto hydrogels were studied using Langmuir, Freundlich, and Temkin models. The experimental data fitted well with the Langmuir equation. The maximum adsorption capacity for MO was 212.7 mg $g^{-1}$ at pH=3. The adsorption data gave best fit with the pseudo-second order kinetic model. Thermodynamic evaluation showed spontaneous nature for MO adsorption onto poly(PEGM-co-DEAEM ) hydrogels.

Poly(2-hydroxyethyl methacrylate ) was grafted onto poly(vinyl cinnamate) by photoinitiation using benzophenone ($Ph_2CO$) as initiator, at 360 nm wavelength, and at a total power of 7670 $\mu W.cm^{-2}$. The grafting process was optimized by changing the concentration of HEMA, $Ph_2CO$, chemical crosslinker ethylene glycol dimethacrylate (EGDMA), and UV irradiation time. The polyVCi-*graft*-polyHEMA films obtained were characterized by FTIR and SEM. The contact angle measurments revealed enhancement of wettability of the polyVCi backbone via the

grafting with polyHEMA. TGA analysis confirmed thermal stablility of the films. Swelling behaviors of films were examined in both water and ethanol. Successful photo-encapsulation of flurbiprofen into the film matrixes was confirmed. The PolyVCi-*graft*-PolyHEMA films proved to be suitable release matrixes for flurbiprofen demonstrating pulsatile release behavior. Zero-order model fitted the flurbiprofen release mechanism. This mechanism was ensured through its Ritger-Peppas "*n*" value (1.00 to 1.41), which indicates super case II release kinetics.

**Keywords:** Methacrylate hydrogels, monomer reactivity ratio, photoinitiated copolymerization, superabsorbent hydrogels, dye adsorption, photoinitiated grafting, poly(vinyl cinnamate) films, Flurbiprofen, pulsatile release, lag time.

# ÖZ

Poli(etilen glikol metakrilat) (PEGM) ve dietil amino etil metakrilat (DEAEM) yapıtaşlarından oluşan rasgele kopolimerler UV başlatıcı ile düşük ve yüksek verimler ile sentezlendi. Elde edilen çapraz bağlı polimerler FTIR, SEM, DSC, TGA ve elemental analiz yöntemleri ile karakterize edildi. Sulu ortamda şişme davranışlarının incelenmesi sonucu elde edilen kopolimer hidrojellerin süperabsorban malzemeler oldukları belirlendi. Monomer reaktiflik oranları Fineman Ross, Extended Kelen Tüdøs, and Mayo Lewis metodları ile düşük verimde $r_1$(PEGM)=0.90, $r_2$(DEAEM)=0.14 ve yüksek verimde 1.01 and 0.40 olarak hesaplandı. Metil oranj'ın (MO) hidrojeller üzerine adsorplanması çalışılarak Langmuir, Freundlich, and Temkin modellerine göre incelendi. Veriler Langmuir modeline yüksek uyum sağladı. En yüksek MO adsorplama kapasitesi pH=3'te 212.7 mg $g^{-1}$ olarak bulundu. Adsorpsiyon davranışının psödo ikinci dereceden kinetik davranış gösterdiği belirlendi. Adsorpsiyon davranışının termodinamik bakımdan spontane olduğu saptandı.

Poli(2-hidroksietil metakrilat) (poliHEMA) poli(vinil sinnamat) (poliVCi) üzerine UV başlatıcı ile benzofenon kullanılarak aşılandı. Aşılanma davranışı HEMA, benzofenon, çapraz bağlayıcı ve radyaysona maruz bırakılan zaman açısından optimize edildi. Elde edilen film örnekler FTIR, SEM ve TGA yöntemleri ile karakterize edildi. Kontak açısı ölçümleri poliVCi yüzeyinin poliHEMAile aşılandıktan sonra daha hidrofilik bir karakter elde ettiğini gösterdi. Filmelrin hem suda hem de etanolde şişme davranışı gösterdiği gözlemlendi. Filmlere flurbiprofen enkapsüle edilerek flurbiprofen salım davranışınincelendi ve sıfırıncı dereceden

salım kinetiği belirlendi. Bu durum Ritger-Peppas n (1.00-1.41) değerine göre de konfirme edildi. Aynı zamanda aralıklı salım davranışı gözlemlendi.

**Anahtar Kelimeler:** Metakrilat hidrojel, monomer reaktiflik oranı, fotokopolimerizasyon, süperabsorban hidrojel, boya adsorpsiyonu, fotoaşılama, poli(vinil sinnamat) flürbiprofen, aralıklı salım , gecikme zamanı.

# DEDICATION

***I would like to dedicate this thesis to my father`s soul, and to my mother for her patience and loving heart until the completion of this page of my life.***

# ACKNOWLEDGMENT

First and foremost, thanks to Allah the most gracious, the most merciful, and peace be upon his messenger.

I would like to thank my supervisor Prof. Dr. Elvan Yilmaz for her endless support, guidance, and supervision. I would like to thank her for providing a very comfortable working atmosphere. In fact, no words can express my deep and honest appreciation for her effort during my PhD period. I am so lucky to be one of her students; she helped me to create my academic personality. I wish her happiness with health.

I am also grateful to my committee members: Prof. Dr. Mustafa Gazi, Prof. Dr. Oğuz Okay, Prof. Dr. Hayal Bülbül Sönmez, and Asst. Prof. Dr. Emine Vildan Burgaz for their time and sincere efforts. Special thanks for my dear Prof. Dr. Osman Yılmaz for his support, assistance and his encouragement.

I would like to thanks to the all staff in the chemistry department, and I would like to acknowledge EMU for providing financial support via BAP-C-04-18-02 project.

Special thanks to my friends who have helped me in many different ways. I would like to thank my friends (Khalid, Karar, Faisal, Ayo, and many other friends) for their support and help during my study.

My special thanks for Abdallah Alshhab for encouraging and helping me, and for being such a brother. My special thanks to my dear precious Gülnihal Tokgöz for being there and helping, encouraging me within my study and in my life.

My Jordanian friends Zaid Alrjoob, Bilal, Loai, Abdelalhakeem, Tareq, Ahmad, Younes, Ibrahim and Emad, who I cannot forget I really appreciate everything you did towards within my study period.

Finally, words alone cannot express the thanks I owe to my mother, brothers and sisters for their encouragement and endless support.

# TABLE OF CONTENTS

# LIST OF TABLES

# LIST OF FIGURES

# Chapter 1

# INTRODUCTION

The aim of this study is to synthesize new methacrylate copolymers by UV initiation via free radical mechanism and to examine their physiochemical properties and possible applications.

The thesis is divided into two parts. Part I describes and discusses synthesis of new crosslinked polymers of poly(PEGM-*co*-DEAEM), at low and high conversions, by photoinitiation using benzophenone as the photoinitiator. The PEGM/DEAEM pair provides hydrophilic and pH responsive matrixes for different hydrogel applications. The copolymer compositions were determined by elemental analysis and monomer reactivity ratios were calculated using Fineman Ross, Extended Kelen Tüdøs**,** and Mayo Lewis methods. The copolymer hydrogels synthesized were characterized with respect to thermal stability, swelling behavior, and morphology. Finally, to study the adsorption behavior of an anionic dye, methyl orange (MO) onto the copolymer hydrogels was investigated using Langmuir, Freundlich, and Temkin models.

Part II explains synthesis of poly(vinyl cinnamate)-*graft*-poly(2-hydroxyethyl methacrylate) (PolyVCi-*graft*-PolyHEMA) films by UV initiation via free radical mechanism and the physicochemical properties of the films synthesized. PolyVCi/polyHEMA pair was chosen due to their potential to blend the more hydrophilic nature of polyHEMA and hydrophobicity of polyVCi polymer. The

study aims to optimize the grafting conditions, and to study the effect of presence/absence of a chemical crosslinker, ethylene glycol dimethacrylate (EGDMA) on the physiochemical properties of the crosslinked films. In addition the swelling behavior in water and in ethanol was investigated, and the potential of the films as loading and release matrixes for flurbiprofen as a model compound was evaluated.

## 1.1 Hydrogel

Crosslinked hydrophilic polymers form three-dimensional network structures known as hydrogels. Hydrogels are soft and elastic materials that swell in aqueous media by absorbing huge quantities of water to attain an equilibrium swelling degree determined by the polymer characteristics such as the nature and degree of crosslinking, the initial monomer concentration present during gel formation, and the type of the hydrophilic groups present in the polymer structure. Hydrogels can be classified according to source, crosslinker type, and composition.

### 1.1.1 Classifications and Applications of Hydrogels

Depending on the source, hydrogels can be classified as natural, synthetic and hybrid, in other words containing both natural and synthetic components [1].

Proteins such as collagen, fibrin, and gelatin are biodegradable polymer used in studies early as natural hydrogel. Later, polysaccharides such as chitosan, starch, and alginate were formed into hydrogels [2]. Natural polysaccharides are favored over synthetic polymers due to their availability, biodegradability, biocompatibility, and nontoxicity [3].

Synthetic hydrogels are synthesized using chemical polymerization techniques, such as free radical polymerization of a vinyl polymer in the presence of a crosslinker.

The first swollen network was developed in 1954 as a copolymer of 2-hydroxyethyl methacrylate (HEMA) and ethylene dimethacrylate (EDMA) [4]. It was designed for contact lenses' applications. Examples of synthetic and degradable polymers are polylactide, poly(ethylene glycol), poly(2-hydroxy ethyl methacrylate), poly(2-hydroxypropyl methacrylamide), poly-glycolide, poly(glycolides-co-lactide) and poly(ε-caprolactone) [5].

Hybrid hydrogels are designed to combine the advantages of both synthetic and natural polymers to achieve the required properties. For example, polysaccharides can maintain their biodegradability nature and have their mechanical properties enhanced through grafting with vinyl monomers [3]. On the other hand, synthetic hydrogels can improve their bioactivity by incorporation of bio functional oligopeptide sequences, proteins (e.g. collagen), and other biological molecules [6, 7, 8].

Chemically crosslinked hydrogels have a network structure in which polymer chains are linked together by covalent bonds that can be obtained either through monomer grafting or by using a crosslinker. Crosslinkers are molecules that hold two or more reactive ends such as glutaraldehyde, adipic acid dihydrazide, and *N*,*N*-(3-dimethylaminopropyl)-*N*-ethyl carbodiimide (EDC). They interact easily with functional groups of polymers like primary amine ($NH_2$), carboxyl (COOH), sulfhydryl (–SH), and carbonyl (CHO). Phenolic and genipin are examples of crosslinking agents that can be used currently in food packaging materials. High energy irradiation like gamma, UV, electron beam, and microwave are used with vinyl group compounds to end up with chemically crosslinked hydrogels [9]. In

addition to chemically crosslinking, enzymatic crosslinking is another method suitable for biomedical applications. Some enzymes used for this purpose are tyrosinase and transglutaminase [10].in physical hydrogels, crosslinking is achieved via entangle chains or chains interacting by ionic forces, hydrogen bonding, or the chains interact hydrophobically [11].

Hydrogels may consist of a homopolymer, or a (copolymer), or may be in the form of interpenetrating polymer network (IPN). As an example of homopolymer hydrogel is poly(2-hydroxyethyl methacrylate) (polyHEMA) which was synthesized by free radical mechanism [12], polyvinyl pyrrolidone which was synthesized via irradiation technique [13], and Poly-acrylic acid [14].

Copolymer hydrogels are those hydrogels which are built as random, alternating, or block forms [15]. A biodegradable tri-poly (ethylene glycol)-(α-caprolactone)-(ethylene glycol) hydrogel was used in drug delivery applications [16, 17], and poly(ethylene glycol)-*co*-poly(xylitol sebacate) hydrogel which was used as 3D printing ink for tissue engineering [18].

IPNs are defined as the intimate mixtures of two polymers [19]. These networks contain both crosslinked and noncrosslinked polymers. IPNs are prepared by immersing a pre-polymerized hydrogel in a solution that contains other monomers, initiator, and a crosslinker. When a linear polymer penetrates into a crosslinked network "semi-IPN" structure may form [20]. Examples of IPN hydrogels are poly(diallyldimethyl ammonium chloride)/poly acrylic acid (PDADMAC/PAA) [20], and temperature sensitive poly(n-isopropylacrylamide)-poly(2-hydroxyethyl methacrylate) hydrogel [21].

Hydrogels may respond to different environmental conditions such as pH [22, 23], temperature [24, 25], thermo-pH [26], enzyme [27], light [28], and electric [29] by changing a given physicochemical property such as volume or conformation.

Other classification parameters, which may not have been mentioned here, could exist. Figure 1.1 shows the classification of hydrogels according to different point of views.

While the hydrogel properties can be improved via copolymerization, or nanoparticles incorporation, hydrogels can be used in environmental, medical, pharmaceutical, and agricultural applications. For example, they find uses as drug delivery systems, tissue engineering matrixes and as components of regenerative medicines. Other examples include coal dewatering, food additives, pharmaceuticals, biosensor applications, and others shown in Table 1.

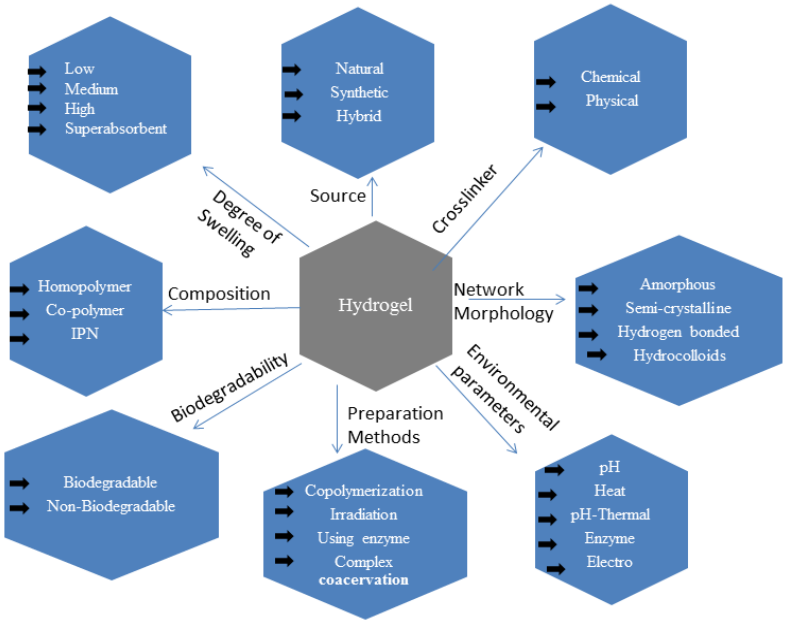


Figure 1.1: Classifications of Hydrogels

Table 1.1: Examples of hydrogels and their applications

| **Hydrogel** | **Applications** |
|---|---|
| **Poly Vinyl Alcohol** | Packaging [30] |
| **Chitosan** | Tissue Engineering [31] |
| **Polyacrylamide/guar gum graft copolymer** | Heavy metal removal [32]<br>Water transport and drug release [33]<br>Sorbent material for chromium ion (Cr (VI) [32] |
| **Guar gum** | Biomedical application [34]<br>Drug delivery [35] |
| **Glycol chitosan** | Drug delivery [36] |
| **Hydroxamated alginates** | Drug delivery [37] |
| **Alginate bead** | Drug delivery [38] |
| **Poly(acrylic-co-vinyl sulfonic) acid** | Drug delivery [39] |
| **Chitosan/poly(acrylamide-co-acrylic acid)** | Waste water treatment [40] |

## 1.2 Superabsorbent Hydrogels

Superabsorbent hydrogels are loosely crosslinked hydrophilic polymers which show high swelling capacity, where they can absorb water till thousands times of their own dry masses. They are high swelling rate, and good strength of the swollen gel compared to conventional hydrogels. These materials were initially made in the United States as water retention agents in agriculture. In general, different approaches can be used to synthesize superabsorbent hydrogels such as polymerization of synthetic monomers, polymerization of functionalized natural/synthetic polymers, and copolymerization of functionalized polymers [41].

Free radical polymerization of synthetic monomers was broadly carried out in order to obtain superabsorbent hydrogels. Vinyl monomers such as methacrylate, acrylamide, and acrylate, were used in superabsorbent hydrogel preparation due to their hydrophilic nature [42]. Several methods were used to enhance the poor mechanical properties of the obtained hydrogels such as crosslinking the surface of the hydrogel, increasing the crosslinking density, and incorporating microsized and/or nanosized particles into the hydrogel matrix [43].

Functionalized biopolymers such as polysaccharides represent the natural based superabsorbent hydrogels. The polar function groups such as hydroxyl and carboxyl on the polysaccharides backbone are the reactive sites used in superabsorbent hydrogels synthesis [44]. The esterification process of cotton cellulose [45], chitin [46], and starch [47], with succinic anhydride, using of 4-dimethylaminopyridine as the esterification agent, was effectively used to prepare biodegradable superabsorbent hydrogels. Chemically modified arabic gum, polyacrylamide, and polyacrylate were used together for the synthesis of superabsorbent hydrogels that found a place in dye adsorption applications [48].

In general, copolymerization with functionalized polymers, and oligomers, or monomers via radical-induced, graft copolymerization, are common approaches for superabsorbent hydrogel synthesis [49, 50].

Superabsorbent hydrogels can be prepared by UV irradiation without any chemical crosslinker. Poly(2-acrylamido-2-methyl-1-propanesulfonic acid) superabsorbent hydrogel was successfully obtained via UV irradiation in aqueous solution and showed large swelling capacities exceeding 1000 times their original weight [51].

Poly(poly(ethylene glycol) methacrylate-*co*-diethyl amino ethyl methacrylate) hydrogels were synthesized by photoinitiation and showed large swelling capacities exceeding 2000 times their original masses in acidic medium within an hour [52].

Superabsorbent hydrogels are used in soil due to their ability to enhance the fertilizer absorption, extend the water retention, and reduce the water required for irrigation [53]. They find many other applications in controlled release of drugs, fertilizers, pesticides, agrochemicals or pharmaceuticals, artificial snow for skiing regions, and in baby napkins because of their high swelling rate [54]. Super-porous superabsorbent hydrogels are used in controlled drug delivery systems [55, 56].

## 1.3 Copolymerization

Copolymerization involves simultaneous polymerization of two or more monomers. Copolymerization is carried out to achieve a copolymer with desired properties resulted from combining two polymers with different chemical and physical properties. The properties of the obtained copolymer will depend on the composition and sequence distribution of each monomer in the copolymer [57].

### 1.3.1 Types of Copolymers

#### 1.3.2.1 Statistical Copolymers

Statistical copolymers are random copolymers in which the monomers are distributed randomly in the chain and defined as poly[(monomer one)-*ran*-(monomer two)]. The low cost methods, such as standard free radical and controlled radical polymerization methods are usually used to obtain random copolymers.

The macroscopic level of random copolymers prepared by both methods is almost the same, but the molecular level is different. During normal free radical process

different chains undergo initiation, propagation, and termination processes, resulting in complex mixture of random copolymers with different chain lengths and different monomer compositions. Using the controlled radical polymerization method gives opportunity to enhance the homogeneity of the obtained copolymer [58].

#### 1.3.2.2 Block Copolymers

A block copolymer is made up of blocks of two or more linear monomers, it is defined as poly(monomer one)-*block*-poly(monomer two) [59]. Due to their specific microstructure, the block copolymers have superior properties compared to random copolymers. The block copolymers are not gradient copolymers where the comonomer composition regularly changes as a function of the copolymer chain length [60].

#### 1.3.2.3 Graft Copolymers

A graft copolymer is a branched copolymer that consists of sequences of one comonomer type grafted onto the polymer backbone consisting of another type of monomer and is defined as poly(monomer one)-*graft*-poly(monomer two) [59] .

During grafting active sites are formed on the substrate backbone together with activation of the monomer to be grafted via free radical or ionic initiation or by irradiation or enzymatic activity [61]. Figure 1.2 shows a general mechanism of free radical grafting copolymerization.

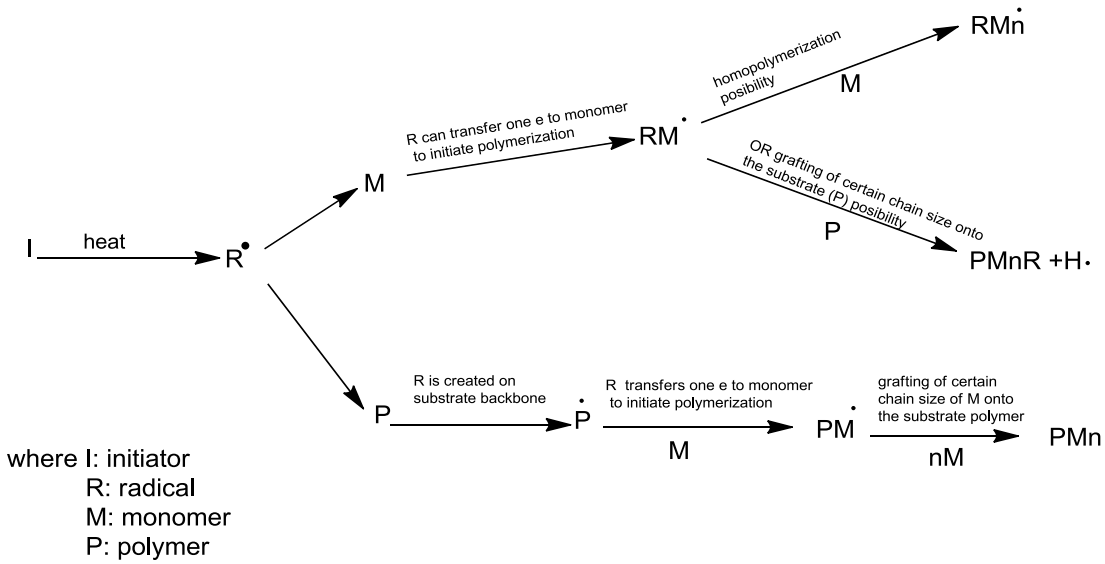


Figure 1.2: General mechanism of free radical grafting

UV irradiation (Figure 1.3) can be used in order to generate active sites on polymers either by mutual irradiation or pre irradiation. There are several advantages of using irradiation technique as it provides an optional usage of initiator, highly pure products, and makes the molecular weight of products controllable. In mutual irradiation both polymer and monomer are simultaneously irradiated [62], while in the pre irradiation process, the substrate polymer is exposed to UV irradiation and then treated with the monomer, in the absence of air ($O_2$) or in the presence of air to form peroxides following decomposition in the presence of the monomer [63]. Peroxides and hydroperoxides are common initiators for vinyl polymerization reactions to achieve graft copolymers. These groups should be either pre irradiated or thermally decomposed in order to create active sites on monomer or polymer backbone.

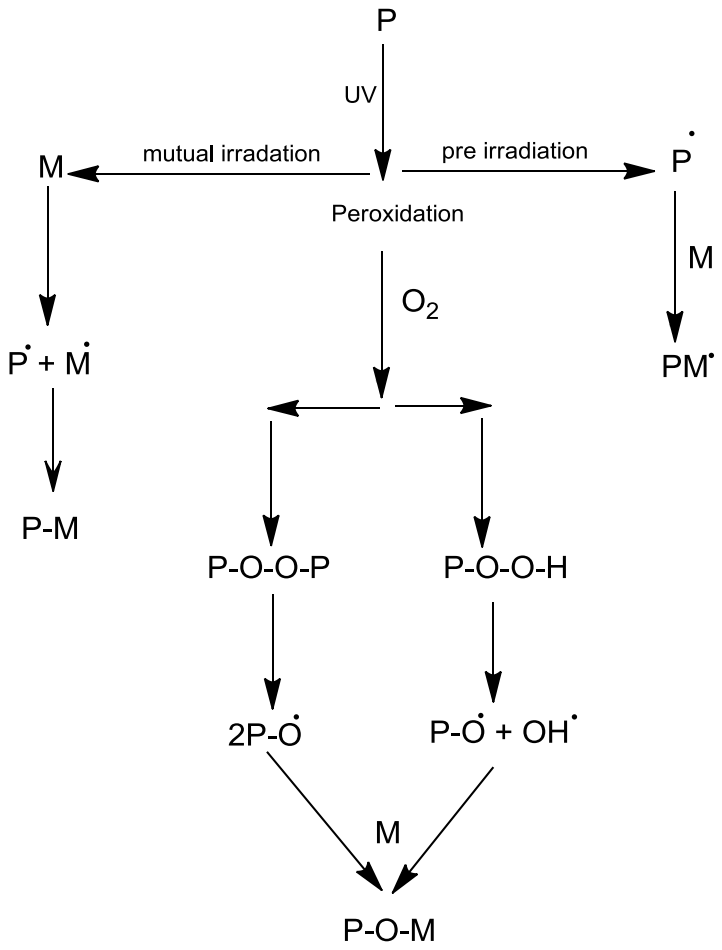

Figure 1.3: Photoinitiated grafting mechanisms.

### 1.3.2.4 Alternating Copolymers

An alternating copolymer holds two repeating units in equimolar amounts with regular alternating distribution [64]. It is defined as poly[(monomer one)-*alt*-(monomer two)]. Normally, electron acceptor systems of an acrylic monomer (acrylonitrile, methyl acrylate, methyl methacrylate, and methyl vinyl ketone) and an electron donor monomer (propene, isobutylene, vinyl chloride, and vinyl acetate) can be synthesized into an alternating polymer using a Lewis acid as catalyst [65].

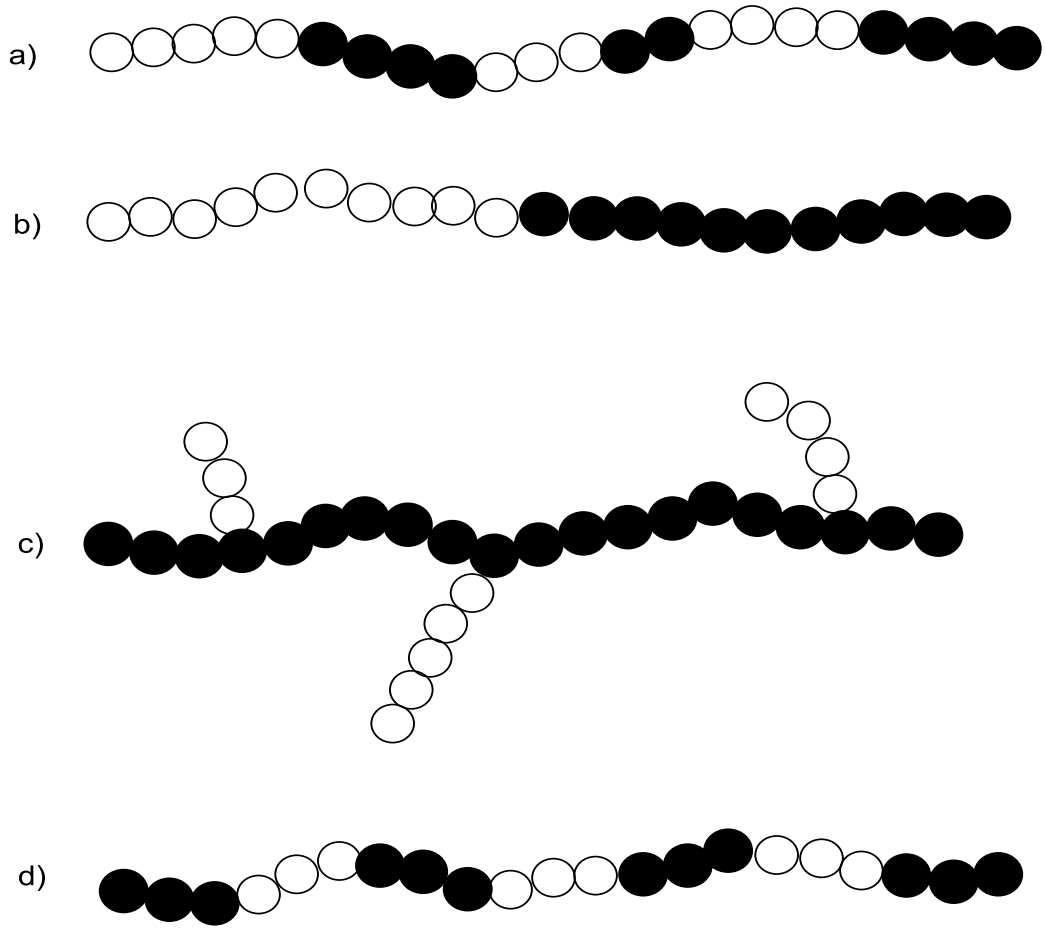


Figure 1.4: Representation of common copolymer a) random copolymers b) block copolymer c) graft copolymer d) alternating copolymer.

### 1.3.2 Copolymer Composition

In order to design a new copolymer with desired properties through free radical copolymerization, understanding the factors that control and determine the final structure of copolymer chains is needed. Copolymer composition and comonomer sequence distribution are unique features and main variables used to describe the copolymer chains.

Writing a set of differential equations, which represent rates at which each of the two monomers enters the copolymer chain by attacking the growing macro radical, will increase the ability of predicting the copolymer composition. As a result, kinetic model of the copolymerization process is needed. The following section examines

the general bases of the most important and the simplest copolymerization kinetic model.

### 1.3.2.1 Terminal Model; Monomer Reactivity Ratios

Two homopropagation and two crosspropagations reactions are considered in copolymerization process rather than one reaction that exists in homopolymerization. Knowing the homopolymerization rates of both monomers is not enough to determine the copolymerization composition. An assumption was created, indicating that the chemical reactivity of the propagating chain in a copolymerization depends only on the ultimate monomer unit. This is mentioned as the first order Markov or terminal model of copolymerization [64].

Consider the case for the copolymerization of the two monomers $M_1$ and $M_2$. Copolymerization of the two monomers ends up with two kinds of propagating species; one with $M_1$ at the propagating end and the other with $M_2$. These can be represented by $M_1$* and $M_2$* where the asterisk denotes an active chains end. If it is assumed that the reactivity of the propagating species is dependent only on ultimate unit i.e. the monomer unit at the end of the chain, four propagation reactions are available. Monomers $M_1$ and $M_2$ can each add either to a propagating chain ending in $M_1$ or to one ending in $M_2$, that is,

$$M_1^* + M_1 \xrightarrow{k_{11}} M_1^* \qquad (1.1)$$

$$M_1^* + M_2 \xrightarrow{k_{12}} M_2^* \qquad (1.2)$$

$$M_2^* + M_1 \xrightarrow{k_{21}} M_1^* \qquad (1.3)$$

$$M_2^* + M_2 \xrightarrow{k_{22}} M_2^* \qquad (1.4)$$

where $k_{11}$ is the rate constant for a propagating chain ending in $M_1$ adding to monomer $M_1$, $k_{12}$ that for a propagating chain ending in $M_1$ adding to monomer $M_2$,

$k_{21}$ that for a propagating chain ending in $M_2$ adding to monomer $M_1$, and $k_{22}$ that for a propagating chain ending in $M_2$ adding to monomer $M_2$. The propagation of a reactive center by addition of the same monomer (i.e., Reactions 1.1 and 1.4) is often referred to as homopropagation or self-propagation; propagation of a reactive center by addition of the other monomer (Reactions 1.2 and 1.3) is referred to as crosspropagation or a crossover reaction. All propagation reactions are assumed to be irreversible.

Writing differential equations that describe the rates of disappearance of monomers $M_1$ and $M_2$, and by assuming steady-state concentrations of the radical centers $M_I$* and $M_2$*, one arrives at a simple expression that relates the ratio of monomers in the copolymer (d[Ml]/d[M2]) to the concentrations of monomers in the feed mixture ([M1] and [M2])

$$\frac{d[M_1]}{d[M_2]} = \frac{[M_1](r_1[M_1]+[M_2])}{[M_2]([M_1]+r_2[M_2])} \tag{1.5}$$

where $r_1$ and $r_2$ are monomers reactivity ratios , defined as $r_1 = k_{11}/k_{12}$ and $r_2 = k_{22}/k_{21}$. This copolymerization equation (equation 5) can also be expressed in terms of mole fractions instead of concentrations. If $f_1$ is the mole fraction of $M_1$ in solution and $F_1$ is the mole fraction of $M_1$ in the copolymer then:

$$f_1 = 1 - f_2 = \frac{[M_1]}{[M_1]+[M_2]} \tag{1.6}$$

$$F_1 = 1 - F_2 = \frac{d[M_1]}{d[M_1]+d[M_2]} \tag{1.7}$$

Combining equations (1.5 - 1.7), the following instantaneous composition equation, also known as the Mayo-Lewis equation, is obtained:

$$F_1 = \frac{r_1 f_1^2 + f_1 f_2}{r_1 f_1^2 + 2 f_1 f_2 + r_2 f_2^2} \tag{1.8}$$

Equation 1.8 gives the copolymer composition as the mole fraction of monomer $M_1$ in the copolymer and is often more convenient to use than the previous form (Eq. 1.5) of the copolymerization equation.

## 1.4 Photopolymerization

Light can interact with light-sensitive materials, photoinitiators, to generate free radicals that can initiate polymerization to produce crosslinked hydrogels. Photopolymerization technique has three main components: monomer, photo initiator, and additives. Photopolymerization can be used to convert monomer to a hydrogel via free radical polymerization in a fast and controllable manner under ambient or physiological conditions. The crosslinking procedure typically requires seconds to a few minutes. Reaction parameters like photoinitiator amount, UV intensity, UV irradiation time, and a distance between the hydrogel and the UV light source should be accurately adjusted to end up with the required products.

Since photopolymerization is a fast, low energy consumption process, which allows working with pure monomer with no solvent, it has become popular among scientists. Many commercial applications of hydrogels produced by photo-polymerization are available [66]. Hydrogels resulting from photo- polymerization have been widely explored as biomaterials in drug delivery systems, scaffolds, and coatings [67]. Photopolymerization is suitable for thin film applications such as photocurable solvent-free paints, lacquers, inks and other coating formulations wherever fast drying or setting is important [68], curing of dental fillings [69], fabrication of 3D objects by stereolithography [70] , and in encapsulation of microelectronic components [71] .

## 1.5 Poly(diethyl amino ethyl methacrylate)

Poly[2-(diethylamino ethyl methacrylate)] PolyDEAEM (Figure 1.5) is a biodegradable and dual responsive polymer. It shows both pH and temperature responsive behavior. It has a pKa about 7.3, and shows pH-dependent swelling/collapse behavior in aqueous solution. Changing the pH can change its hydrophilicity/hydrophobicity behavior; when pH is less than 7.3 due to protonation of its tertiary amines, polyDEAEM is a cationic hydrophilic polymer. In contrast, at pH values more than 7.3, polyDEAEM becomes hydrophobic because its tertiary amino groups undergo deprotonation [72]. PolyDEAEM is a weak polybasic polymer with a good charge density. It is able to form cationic polyelectrolyte in aqueous solution and to bind with DNAs carrying negative charges. PolyDEAEM is cytotoxic but this disadvantage can be reduced through crosslinking or copolymerization with cross-linkers such as PEG, so its biocompatibility can be improved [73]. PolyDEAEM is a polymer with high potentials in nanomedicine, biotechnology, biomedicine and gene/drug delivery systems [74].

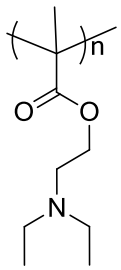


Figure 1.5: Poly[2-(diethylamino ethyl methacrylate)]

PolyDEAEM and its hydrogels through grafting or copolymerization have been synthesized by several ways, such as anionic polymerization [75], reversible addition fragmentation chain transfer polymerization (RAFT) [76, 77], atom transfer radical polymerization (ATRP) [74, 78], photoinitiated polymerization [52], as a part of this thesis work and by free radical polymerization [79].

## 1.6 Poly(poly(ethylene glycol)methacrylate

Poly(ethylene glycol) methacrylate polyPEGM, owns advantageous features as being a thermoresponsive polymer with biocompatibility, blood compatibility, and antifouling behaviors [80, 81].

Poly(ethylene glycol) (PEG) is nontoxic, and biocompatible macromolecule. It can be formed either as linear or branched macromolecule that can be dissolved in water or organic solvents. PEG can form hydrogels by crosslinking through ultraviolet irradiation or end functionalization with methacrylate and acrylate. Using its terminal hydroxyl group, PEG can covalently bind to other molecules [82].

Polyglycol esters are categorized as nonionic surfactants, which increase the possibility for numerous industrial applications. They are broadly used as non-ionic surfactants, thickening agents for creams, anti-static agents for plastics, and bases for cosmetics and pharmaceuticals.

Poly(ethylene glycol) is a promising substance for enhancing membrane hydrophilicity due to its high flexibility, excluded volume, and hydrophilicity. It is generally used for the antifouling modification of membranes [83]. The chemical structure of polyPEGM is shown in Figure 1.6. PolyPEGM is used as anti-adherent material to avoid the unnecessary bacterial adhesion of biodegradable polylactide (PLA) [84].

Flexible composite polymer electrolytes (CPEs) are easily fabricated with poly(ethylene glycol) methacrylate to be used in lithium battery systems [85]. In addition polyPEGM hydrolysable microspheres were synthesized for biomedical

applications [86]. Finally PEGM was successfully photocopolymerized with DEAEM to achieve crosslinked hydrogel for dye adsorption [52], as part of this thesis work.

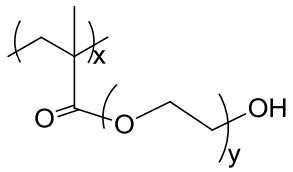


Figure 1.6: Poly(poly(ethylene glycol)methacrylate)

## 1.7 Poly(2-hydroxyethyl methacrylate )

Poly(2-hydroxyethyl methacrylate) polyHEMA has proved to be a promising polymer for applications in biomedical fields since it was first synthesized in 1960. These applications include the use of polyHEMA in the fields of contact lenses, artificial corneas and skins, drug delivery, and degradable scaffolds for tissue engineering [87]. PolyHEMA hydrogels have a wide range of appliactions due to their safety, biocompatibility, and thermal stability [88], polyHEMA has also been used as a carrier for numerous water-soluble anticancer medicines, like 5-fluorouracil, topical mitomycin-C, and doxorubicin [89], polyHEMA was also used in biomedicine and in electronic devices, due to its chemical and physicochemical stability and high biocompatibility [90]. PolyHEMA has been demostrated to be a good adsorbent for heavy metals [91]. PolyHEMA can be used as a polymer host for polymer electrolytes due to its compatibility to some organic solvents on account of the amphiphilic groups (-$OCH_2CH_2OH$) makes it an appropriate backbone for gel electrolytes [92].

Copolymer hydrogel established from 2-hydroxyethyl methacrylate (HEMA) and 2-(diisopropylamino)ethyl methacrylate (DPA) and , poly(HEMA-co-DPA), has found

a place in therapeutic contact lenses applications [93], and in specific ocular drug delivery systems like (Rhodamine 6G (Rh6G)) [94]. Figure 1.7 shows the chemical structure of polyHEMA.

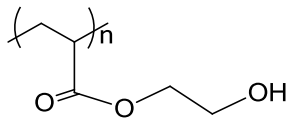


Figure 1.7: Chemical structure of Poly(2-hydroxyethyl methacrylate )

## 1.8 Poly(vinyl cinnamate )

Vinyl cinnamate, and especially its copolymers are well known for their photo responsive behavior including photoinitiated polymerization, photo crosslinking [95], and light induced bending of its gels [96].

Some of the cinnamoyl groups in poly(vinyl cinnamate) (polyVCi) (Figure 1.8) become excited under UV light, while some of them remain in ground state. These two forms react through photocycloaddition reaction and form crosslinked polymer, as schematically depicted in Figure 1.9. Photo responsive hydrogels/ nanogels of polyVCi can undergo UV induced bending or volume transition [97], which may find use in phototherapy, as drug carriers, or in medical imaging in addition to application in optoelectronics, and in photoresists tools such as circuits, printing substances, coatings, paint, compact discs, and cathode tubes. PolyVCi and its copolymers with hydrophilic polymers can form micelles in solution and molecular arrangement leading to liquid crystal behavior [98].

Studies on either homopolymerization or copolymerization of VCi are scarce in the literature. Homopolymerization to poly(vinyl cinnamate) (polyVCi) had been recorded [99], but its details are still missing. Detailed data and analysis on the

polymerization and copolymerization of vinyl cinnamate will be useful due to the photoresponsive nature of poly(vinyl cinnamate) that may lead to several biomedical, and physicochemical applications the following polymerization systems and polymer characteristics were reported in the studies given below.

Poly(vinyl cinnamate) (PolyVCi) was produced by the reaction between poly(vinyl alcohol) and cinnamic acid. However, this reaction is not a complete one. So polyVCi obtained is actually a copolymer of vinyl cinnamate and the alcohol [100]. Homopolymers of polyVCi were usually prepared after the synthesis the monomer itself via other small molecules whether by using the free radical method [99], or by cationic method, or the photopolymerization method.

Cinnamoyl moiety can dimerize using ultraviolet light to form a force-sensitive and highly strained bond that can be severed by the external application of a mechanical force [101]. Although polyVCi is a conjugated polymer, its usage is restricted due to some disadvantages such as lower strength, poor heat resistance, poor electrical properties. In order to synthesize polyVCi with better mechanical, thermal and electrical properties, incorporation of nanoparticles such as ZnO and NiO into the polyVCi composite was carried out [102,103].

Various poly(vinylalcohol-*co*-vinylcinnamate) derivatives including poly(vinylalcohol-*co*-vinylcinnamate), poly (vinylalcohol-*co*-vinyl-4 methoxycinnamate), and poly(vinylalcohol-*co*-vinyl-2,4,5-trimethoxycinnamate) were synthesized by grafting poly(vinylalcohol) with appropriate cinnamoyl groups. Amphiphilic copolymers have the ability to form micelle using suitable solvents [104].

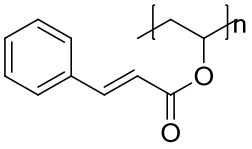


Figure 1.8: Poly(vinyl cinnamate

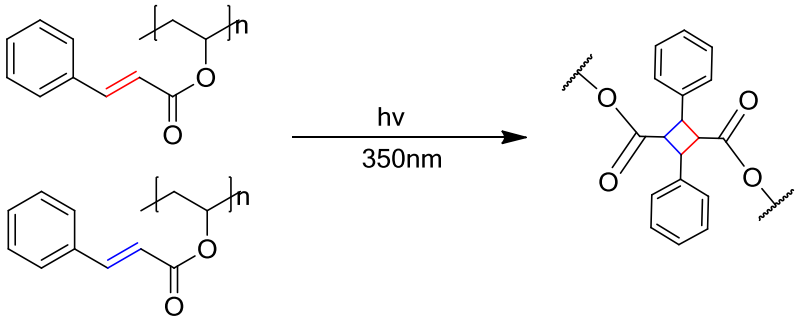


Figure 1.9: [2+2] cycloaddition of PolyVCi under UV irradiation

# Chapter 2

# PHOTOINITIATED SYNTHESIS OF POLY(POLY(ETHYLENE GLYCOL) METHACRYLATE-CO-DIETHYL AMINO ETHYL METHACRYLATE) SUPERABSORBENT HYDROGELS FOR DYE ADSORPTION

## 2.1 Introduction

Crosslinked hydrophilic polymers form three-dimensional network structures known as hydrogels. Hydrogels are soft and elastic materials that swell in aqueous media by absorbing large amounts of water to attain an equilibrium swelling degree determined by the polymer characteristics such as the nature and degree of crosslinking, the initial monomer concentration present during gel formation, and the type of the hydrophilic groups present in the polymer structure. Several external factors such as the ionic strength, pH of the medium, and the temperature are other factors that affect the degree of swelling [105,106,107]. Hydrogels are capable of adsorbing/absorbing of small molecules present in the external environment [108]. They also allow diffusion of entrapped molecules into the outer medium. Due to these properties, they have found applications in biomedicine, pharmacy [109] and in cleaning of the contaminated water and soil [105, 110].

Vinyl polymerization carried out in the presence of a crosslinker is one of the most common routes used to synthesize hydrogels. Besides chemical initiation, network polymers can be obtained by photoinitiation either by using multifunctional monomers, using polymers modified with crosslinkable functional groups or by using photosensitizers, which act by hydrogen abstraction from the polymer backbone [111]. Photoinitiation has got the advantage of avoiding use of chemical initiators in many cases. It also offers the possibility of controlling the degree of crosslinking, and the amount of the polymer yield by adjusting the dose of the radiation [112]. The photopolymerization of multifunctional (meth)acrylate monomers and oligomers have been reported to lead to the formation of highly cross-linked insoluble products [113].

Hydrogels with desired properties can be synthesized by copolymerization of different monomers. Copolymerization systems are characterized by the chemical composition of the copolymer, and the monomer reactivity ratios. These are important characteristics that allow design and synthesis of copolymers with required properties [114].

Nowadays, polymeric adsorbents synthesized via versatile polymerization techniques are needed to deal with the growing water pollution problem. Our waters are contaminated with heavy metals, dyes, pesticides, drugs and many others [115]. Around 15 % of dyes, for example, used in the paper, textile, plastics and other industries are released into water, causing pollution to the environment [116]. These are harmful substances causing adverse environmental and health effects [117]. Among many other techniques like membrane filtration, coagulation/flocculation, ion exchange biological treatment, ozone treatment, and photocatalytic degradation

used to clean wastewater from dyes, adsorption is a relatively easy, efficient and cost-effective method [118,119,120,121].

The subject of this study is the synthesis of cationic copolymer hydrogels of 2-(diethyl amino ethyl methacrylate) and poly(ethylene glycol methacrylate) and investigate their potential as dye adsorbents. Poly[2-(diethyl amino ethyl methacrylate)] PDEAEM is a pH sensitive polymer acting as a polycation under acidic conditions. Reports are available demonstrating the potentials of PDEAEM in nanomedicine, biotechnology, biomedicine and gene/drug delivery systems [122,123], as well as in waste water treatment acting as adsorbent [124]. Poly(ethylene glycol methacrylate) PEGM possesses useful features such as being a thermoresponsive polymer with biocompatibility, blood compatibility and antifouling behavior [81,125]. Examples of copolymers of both monomers with several different other monomers by several different techniques have been reported. For example, hyperbranched polymers of poly(diethyl amino ethyl methacrylate-block-polyethylene glycol methyl ether methacrylate-block ethylene dimethacrylate) were synthesized using atom transfer radical polymerization and tested for gene delivery [126]. Beads of 2-(diethyl amino)ethyl methacrylate-*co*-ethyleneglycol dimethacrylate(DEAEM-co-EGDMA) were synthesized by suspension polymerization method, in order to study their adsorption properties towards sulfamethoxazole [127]. Nanogels of poly(N,N-diethyl amino ethyl methacrylate)-*core*-polyethyleneglycol-shell (PDEAEM-core-PEG-shell) were synthesized by using a "surfactant-free" emulsion polymerization [128]. On the other hand, free radical copolymers of 2-(N,N-diethylamino)ethyl methacrylate (DEAEMA) and poly(ethylene glycol) methyl ether methacrylate with (PEGMA500) were prepared in

ethanol and their reactivity ratios were estimated as $r_{DEAEMA}$ = 0.81 ± 0.20 and $r_{PEGMA500}$ = 0.73 ± 0.18 by Tidwell and Mortimer method [129].

In this chapter, new crosslinked polymers of poly(PEGM-*co*-DEAEM) were obtained by photoinitiation using benzophenone as the photoinitiator and without using any additional chemical cross linker during polymerization. The copolymer compositions were determined by elemental analysis and the monomer reactivity ratios were calculated for the comonomer pair under given conditions. The thermal stability, swelling behavior, and morphology of the copolymers were characterized. Adsorption behavior of an anionic dye, methyl orange (MO) onto the copolymers synthesized was studied.

## 2.2 Experimental Part

### 2.2.1 Materials

Poly(ethylene glycol)methacrylate (PEGM) ($M_n$=360) (Aldrich), 2-(Di-ethylamino)ethyl methacrylate (DEAEM) (Aldrich), benzophenone (Aldrich), carbon tetrachloride ($CCl_4$) (Merck), methyl orange (MO) dye (Aldrich), were used without any further purification.

### 2.2.2 Synthesis of PolyDEAEM, PolyPEGM Homopolymers, and Poly(PEGM-co-DEAEM) Copolymers

Homopolymers and copolymers of PEGM, and DEAEM were synthesized by UV initiation using a Luzchem photoreactor LZC 4V equipped with 6 top and 8 side UVA lamps of 350 nm wavelength and 7670 $\mu W.cm^{-2}$ power. Only 3 top lamps were used during polymerizations that correspond to 1643 $\mu W.cm^{-2}$. Quartz tubes of 10 mL capacity were used. All samples were placed 15.0 cm distance from the lamps.

For homopolymerization, the monomer (1.0 mL) was dissolved in 2.5 mL of $CCl_4$ solvent, where the mole percent (mol%) of benzophenone to PEGM, and DEAEM monomers are (0.18%), and (0.09%) respectively. Homopolymerizations were carried out for 5 h to obtain products that will precipitate out of solution as crosslinked polymers, and in high yields.

For copolymerization, desired monomer feed ratio of the two monomers was dissolved in the solvent. The volume percent of monomers in solutions was kept as 28% and benzophenone was used as the photoinitiator with a mole percent of 0.05% with respect to both monomers. The procedure was carried out for 10 min at low conversions and 110 min for high conversion copolymerizations to end up with crosslinked polymers. Both homopolymer and copolymer gels formed were soaked in $CCl_4$ for (2-3) days and the solvent was refreshed every 6 h. The samples were always kept in closed containers while treated with $CCl_4$ under the hood, and were handled with gloves and a mask. They were then dried overnight under vacuum at 50 °C. The solvent was collected via a cold solvent trap, and was disposed of properly.

A set of nine feed ratios of PEGM and DEAEM, monomers were prepared with different monomer fractions of PEGM ($f_{PEGM}$), and DEAEM ($f_{DEAEM}$) by mole. In the photocopolymerization process (monomer feed ratio $f_{PEGM}/f_{DEAEM}$: 0.90/0.10, 0.80/0.20, 0.70/0.30, 0.60/0.40, 0.50/0.50, 0.40/0.60, 0.30/0.70, 0.20/0.80, and 0.10/0.90) were used. Copolymers were labeled according to feed ratios with respect to PEGM fraction. For example, a copolymer denoted as poly(PEGM-*co*-DEAEM) (1) indicates that $f_{PEGM} = 0.1$, and $f_{DEAEM} = 0.9$. The copolymers were characterized by FTIR, TGA, DSC, and SEM, analyses. The mole fractions of the monomers in the copolymer ($F_{PEGM}$, and $F_{DEAEM}$) were experimentally determined by elemental

analysis. Percent yield for each polymerization was calculated according to equation (2.1).

$$\%\ \text{Yield of Polymerization} = \frac{\text{mass of the copolymer(g)}}{\text{total mass of monomers(g)}} \text{X } 100\% \quad (2.1)$$

### 2.2.3 Characterization Techniques

The infrared absorption spectra (FTIR) of samples were taken using a Perkin Elmer Spectrum-Two spectrophotometer with ATR.

Thermal properties of the polymers were studied using a Perkin Elmer Diamond Differential Calorimeter and Perkin Elmer Pyris 1 at METU Central Laboratory in Ankara. The samples were studied under nitrogen atmosphere at 10 °C $min^{-1}$ heating rate.

The surface morphology of the samples was investigated by Quanta 400F field emission scanning electron microscope using Au-Pd coating.

The samples were analyzed for elemental composition using LECO, CHNS-932 instrument at METU Central Laboratory in Ankara. Each sample was studied in duplicate, and the average of the two values was reported.

Copolymer composition was calculated according to the following equations:

$$mass\ of\ DEAEM = weight\ fraction\ of\ DEAEM\ in\ the\ copolymer\ X\ \ mass\ of\ copolymer \quad (2.2)$$

where

$$weight\ fraction\ DEAEM = \frac{\%\ of\ Nitrogen\ atom\ in\ the\ copolymer}{\%of\ Nitrogen\ atom\ in\ Homopolymer} \quad (2.3)$$

$$mass\ of\ PEGM\ = mass\ of\ copolymer - mass\ of\ DEAEM \quad (2.4)$$

$$F_{DEAEM} = \frac{n\ DEAEM}{n\ DEAEM + n\ PEGM} \quad (2.5)$$

where,

$F_{DEAEM}$ represents the mole fraction of DEAEM monomer in the copolymer, and $n_{DEAEM}$, $n_{PEGM}$ are the number of moles of DEAEM, PEGM in the copolymer respectively.

$$F_{PEGM} = 1 - F_{DEAEM} \quad (2.6)$$

### 2.2.4 Equilibrium Swelling Behavior

Known mass of bulk samples of roughly cylindrical hydrogels of high conversion poly(PEGM-*co*-DEAEM)(3), poly(PEGM-*co*-DEAEM)(5), and poly(PEGM-*co*-PDEAEM) (7) were placed in water, 0.01 M NaOH, or 0.01 M HCl solution. The swollen samples were weighed at given time intervals after removing the excess water on the surface. Each sample was tested three times. The swelling capacity was determined using equation (2.7)

$$\%\ Swelling\ Degree = \frac{W_s - W_d}{W_d} \text{X } 100\% \quad (2.7)$$

where $W_d$ is the initial weight of dried gel and $W_s$ is the final weight of the swollen gel after a certain period of time.

### 2.2.5 Adsorption Isotherms

Distilled water was used to prepare dye solutions with the desired concentration. Adsorption isotherms were conducted at room temperature by a batch method. A 0.05 g of each of the copolymer samples poly(PEGM-*co*-DEAEM) (3), (5), and (7), which were obtained at high conversion conditions, was added into 50.0 mL of (20, 40, 60, 80, 100, and 200 mg $L^{-1}$) dye solution (pH=3.0). The pH adjustment was made by using 0.1 M HCl and 0.1 M NaOH solutions. The dye solutions and copolymers were added to a 100 mL Erlenmeyer flask at room temperature under an agitation speed of 200 rpm. The dye concentration was then determined by

measuring the absorbance of the solution at 464 nm, using a UV–vis spectrophotometer. The percent removal (%R) of dye and the amount of adsorption ($q_t$) were calculated according to equations (2.8) and (2.9) as given below.

$$\% R = \frac{(C_o - C_t)}{C_o} \times 100\% \quad (2.8)$$

$$q_t = \frac{(C_o - C_t)V}{W} \quad (2.9)$$

where $C_0$ and $C_t$ (mg $L^{-1}$) are the dye concentration in solution at initial time and at time t, respectively. The amount of dye adsorbed onto the adsorbent is given by $q_t$ (mg $g^{-1}$) at time t. In equation (2.9), V (L) is the volume of dye solution in liters and W (g) is the mass of the adsorbents in grams.

The adsorption equilibrium data were analyzed by Langmuir, Freundlich, and Temkin isotherms linear models [130,131,132] given below:

Langmuir equation:

$$\frac{C_e}{q_e} = \frac{1}{K_L q_{max}} + \frac{C_e}{q_{max}} \quad (2.10)$$

Freundlich equation:

$$\ln q_e = \frac{1}{n} \ln C_e + \ln K_F \quad (2.11)$$

Temkin equation:

$$q_e = \frac{RT}{b_T} \ln C_e + \frac{RT}{b_T} \ln K_T \quad (2.12)$$

where $C_e$ is the equilibrium adsorbate concentration (mg $L^{-1}$), $q_{max}$ is the monolayer maximum adsorption capacity (mg $g^{-1}$), $K_L$ is the Langmuir adsorption constant (L $mg^{-1}$) related to the free energy of adsorption, $K_F$ the adsorption capacity, n is adsorption intensity (how favorable is the adsorption process). $K_T$ is the equilibrium binding constant (L $mg^{-1}$), $b_T$ is Temkin constant, R is the gas constant (J $K^{-1}$ $mol^{-1}$), T is the room temperature (K).

### 2.2.6 Thermodynamics of Adsorption

The adsorption process was studied at three different temperatures (298, 308, and 318 K). The standard Gibbs free energy change $\Delta G^{\circ}$ (kJ $mol^{-1}$), standard enthalpy change $\Delta H^{\circ}$ (kJ $mol^{-1}$), and standard entropy change $\Delta S^{\circ}$ (J $mol^{-1}$ $K^{-1}$) were calculated using the dependence of thermodynamic equilibrium constant ($K_C$) on temperature using equations (2.13) – (2.15).

$$LnK_C = \frac{\Delta S^{\circ}}{R} + \frac{-\Delta H^{\circ}}{RT} \quad (2.13)$$

$$K_c = \frac{q_e}{C_e} \quad (2.14)$$

$$\Delta G^{\circ} = \Delta H^{\circ} - T\Delta S^{\circ} \quad (2.15)$$

where $q_e$ is the amount of adsorbed dye (mg $g^{-1}$) at equilibrium, $C_e$ is the equilibrium concentration of MO in the solution (mg $L^{-1}$). $K_C$ (L $g^{-1}$) is the equilibrium constant of the adsorption. R is the universal gas constant (8.314 $J.K^{-1}$ $mol^{-1}$). T is the temperature in Kelvin. The values of $\Delta S^{\circ}$ and $\Delta H^{\circ}$ are calculated from the intercept ($\Delta S^{\circ}/R$) and slope ($-\Delta H^{\circ}/R$) of the linear plot of ln $K_C$ against 1/T respectively.

### 2.2.7 Adsorption Kinetics

In order to describe the kinetics of MO adsorption onto poly(PEGM-*co*-DEAEM) (3), (5), and (7) hydrogels, the pseudo-first-order and pseudo-second-order kinetic models were examined. The pseudo-first-order equation can be expressed with equation (16).

$$\ln(q_e - q_t) = ln\, q_e - k_1 t \quad (2.16)$$

where $q_e$ and $q_t$ (mg $g^{-1}$) are the amounts of dye adsorbed at equilibrium and time t, $k_1$ ($min^{-1}$) is the rate constant of the pseudo-first-order kinetics.

The pseudo-second-order model assumes that the rate limiting step may be chemisorption, which can be given in equation (17).

$$\frac{t}{q_t} = \frac{1}{k_2 q_e^2} + \frac{t}{q_e} \quad (2.17)$$

where $k_2$ ( g $mg^{-1}$ $min^{-1}$) is the rate constant of pseudo-second-order model.

## 2.3 Results and Discussion

### 2.3.1 Copolymer Synthesis

The polymer yields for the homopolymer and copolymer samples obtained by photoinitiation using benzophenone as the photoinitiator are given in Table 2.1. The reactions were carried out in $CCl_4$ solvent. The percent yield of the homopolymers polyDEAEM, and polyPEGM that phase separated from solution due to crosslinking, were 50%, and 62% respectively within 5h polymerization time.

Copolymerization reactions were given enough time to allow crosslinking and precipitation of the product out of solution. For low conversion photoco-polymerizations, the conversion yield was kept in the range 1.20%-21.4% within 10 min polymerization time. The set of samples obtained at 10 min polymerization time are classified as low conversion samples. The high conversion samples were obtained at 110 min photopolymerization time with polymer yield values in the range 40.6%-67.9% except for poly(PEGM-*co*-DEAEM)(1) and (9) samples. No crosslinked polymer could be observed at 10 min polymerization time for the first copolymerization sample number (1). According to the monomer reactivity calculations given below, PEGM is the more reactive monomer. Hence, it can be concluded that when the fraction of PEGM is small in the comonomer mixture ($f_{PEGM}$ = 0.1), there is not enough amount of the more reactive monomer to obtain substantial copolymer yield within the time period given. When the molar fraction of PEGM is as high as 0.9, the polymerization rate is so high that it cannot be limited to a conversion yield lower than 20% within 10 minutes polymerization time.

One important characteristic of the samples obtained, whether homopolymer or copolymer, is that they are all insoluble in either organic solvents or in aqueous media. They swell in aqueous media and act as hydrogels. The formation of crosslinked polymers under the photopolymerization conditions given can be explained by the characteristics of the methacrylate/benzophenone monomer/initiator polymerization system. Benzophenone photoinitiator has been reported to undergo hydrogen abstraction from a hydrogen donor molecule upon UV irradiation [133]. The initiation of photopolymerization usually occurs through a donor molecule. The ketyl radical is expected to react with the growing chains by radical coupling reactions [134]. The DEAEM monomer, on the other hand, possesses hydrogen donating sites as well as a polymerizing methacrylate functional group [135]. Monomers having both initiating sites and a polymerizable group can lead to the formation of hyper branched polymers via so-called self-condensing vinyl polymerization. In this process, chain addition polymerization is combined with self-condensation of chains. Therefore, the nature of the photoinitiator, benzophenone, and the structure of the monomer DEAEM combined together leads to the formation of branched [136], and further crosslinked polymers. Furthermore, PEGM should also take part in the crosslinking via chain transfer reactions. The proposed polymerization and crosslinking mechanism are shown in (Figure 2.1). Presence of $CCl_4$ as the solvent increases the possibility of chain transfer reactions. All of these factors act together to form poly(PEGM-*co*-DEAEM) crosslinked copolymer hydrogels.

Table 2.1: Polymer Yields (%) for polyPEGM, polyDEAEM and poly(PEGM-co-DEAEM) Samples. (* t=5h)

| **Polymer Sample** | **Comonomer feed ratio $f_{PEGM}$:$f_{DEAEM}$** | **% Yield of polymerization t=10 min** | **% Yield of polymerization t=110 min** |
|---|---|---|---|
| **polyPEGM*** | 1.0:0.0 | - | 62.0 |
| **poly(PEGM-*co*-DEAEM) (1)** | 0.1:0.9 | - | 3.00 |
| **poly(PEGM-*co*-DEAEM) (2)** | 0.2:0.8 | 2.21 | 5.80 |
| **poly(PEGM-*co*-DEAEM) (3)** | 0.3:0.7 | 1.60 | 40.6 |
| **poly(PEGM-*co*-DEAEM) (4)** | 0.4:0.6 | 3.60 | 40.9 |
| **poly(PEGM-*co*-DEAEM) (5)** | 0.5:0.5 | 4.20 | 58.3 |
| **poly(PEGM-*co*-DEAEM) (6)** | 0.6:0.4 | 15.5 | 65.1 |
| **poly(PEGM-*co*-DEAEM) (7)** | 0.7:0.3 | 1.20 | 65.2 |
| **poly(PEGM-*co*-DEAEM) (8)** | 0.8:0.2 | 21.4 | 66.2 |
| **poly(PEGM-*co*-DEAEM) (9)** | 0.9:0.1 | - | 67.9 |
| **polyDEAEM*** | 0.0:1.0 | - | 50.0 |

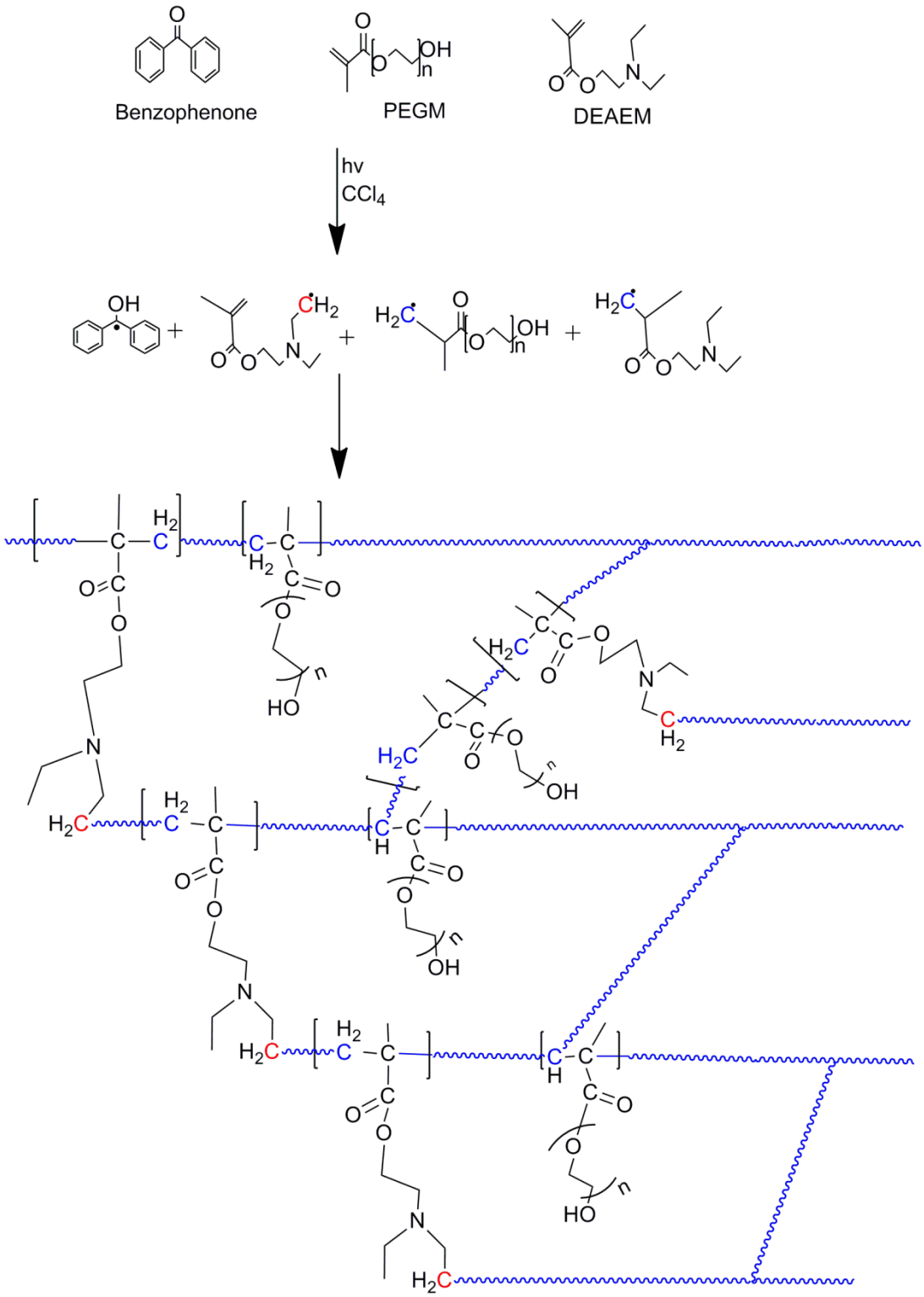


Figure 2.1: Synthesis of poly(PEGM-co-DEAEM) hydrogels.

### 2.3.2 FTIR Analysis

The FTIR spectrum of poly(diethylamino ethyl methacryalte), poly DEAEM, and poly(poly(ethylene glycol methacrylate)), polyPEGM, and their copolymer, poly(PEGM-*co*-DEAEM) (5) is shown in (Figure 2.2(a-c)), respectively. Both homopolymers have C-H stretching of the methylene groups in the region 2800 – 2900 $cm^{-1}$. Bending vibrations of the methylene groups are observed in the region 1380 –1450 $cm^{-1}$. In the spectrum of polyDEAEM given in (Figure 2.2(a)), the C=O stretching of the carbonyl group is at 1725 $cm^{-1}$, and the stretching vibrations C-O-C are identified in the region 1000 – 1100 $cm^{-1}$. Absorption band at 1000–1200 $cm^{-1}$ region corresponding to the $(CH_3CH_2)_2N$ group is observed in the spectrum of both the homopolymer, polyDEAEM and that of the copolymer (Figure 2.2(c)).

The absorption band in the region 2750-2950 $cm^{-1}$ refers to symmetric stretching vibration of $–NCH_2-$ for the tertiary amine of PolyDEAEM. A broad band is observed for both polyPEGM whose FTIR spectrum is given in (Figure 2.2(b)), and in the spectrum of the copolymer (Figure 2.2(c)) in the region 2450-2300 $cm^{-1}$ corresponding to the hydroxide group O-H. Photocopolymerization was confirmed by the clear changes observed in the region 1000-1200 $cm^{-1}$ represented by a broader absorption including overlap of C-O-C stretching, and in the region 2800-2900 $cm^{-1}$ exhibiting C-H stretching of methylene groups, and a more intense peak observed for C=O group at 1726 $cm^{-1}$ .

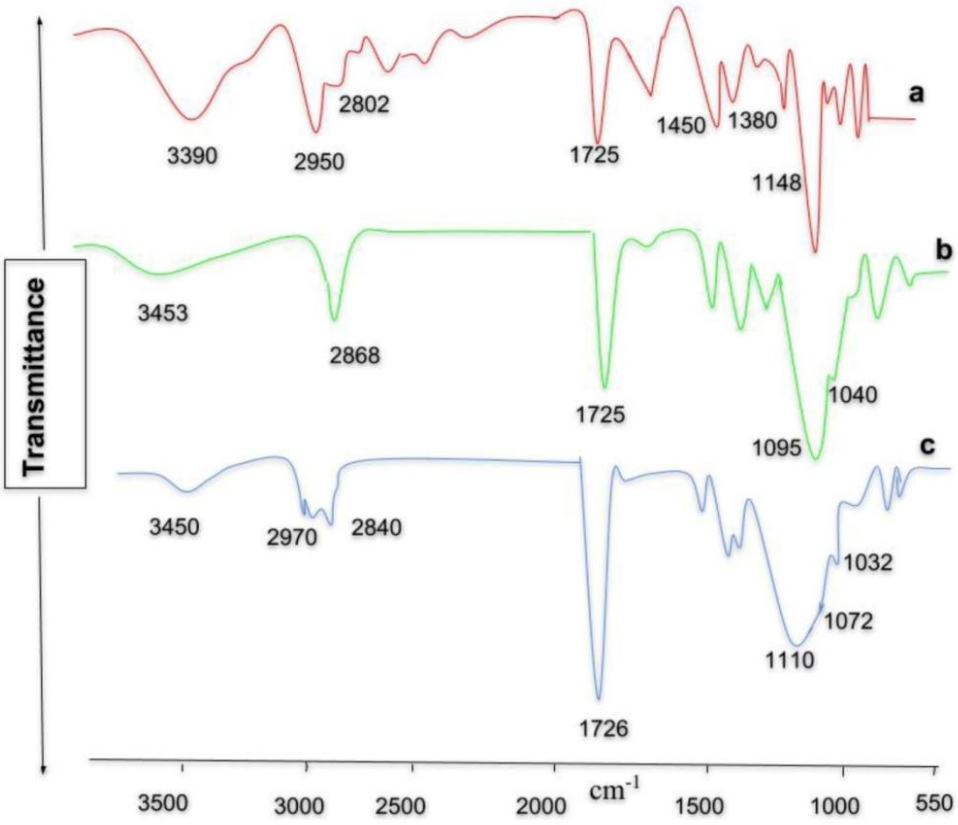


Figure 2.2: FTIR Spectrum for a) poly DEAEM, b) poly PEGM, c) poly( PEGM-co-DEAEM)(5).

### 2.3.3 Determination of the Copolymer Composition

The copolymer compositions were determined by elemental analysis. The nitrogen content of each sample was used to calculate the mole fraction of the DEAEM in the copolymer. The results confirm that the copolymerization has been successfully achieved at low, and at high conversions (Table 2.2, Table 2.3). The high conversion samples have slightly higher DEAEM fractions in the copolymer ($F_{DEAEM}$) than the corresponding low conversion samples, indicating that the reactivity of DEAEM increases at higher reaction times due to decreased PEGM fraction in the comonomer feed in time.

The effect of the solvent on the copolymer composition was investigated by carrying out the copolymerization for sample poly(PEGM-*co*-DEAEM)(5) in bulk, in carbon tetrachloride and in acetone. Table 2.4 shows elemental analysis results and the copolymer compositions for the sample poly(PEGM-*co*-DEAEM)(5) at high conversions in $CCl_4$, in acetone, and in bulk . As the solvent polarity changes from polar to nonpolar and when there is no solvent, $F_{DEAEM}$ increases from 0.186 to 0.376 to 0.689 respectively. In acetone, the monomers are solvated by the polar solvent molecules. DEAEM and PEGM molecules are not in close proximity, and hence PEGM can exhibit its higher reactivity. In a nonpolar solvent, namely in $CCl_4$, the monomers are poorly solvated by the solvent molecules and hence DEAEM monomer may establish stronger dipole-dipole interactions with the growing chain rather than with the solvent molecules. Consequently, DMAEM monomer finds a medium to incorporate into the growing copolymer chain. When it is in bulk, the effect is even more pronounced. In this case, the smaller molecule, DEAEM, has a higher mobility than PEGM, and hence may add to the growing copolymer chain more freely than PEGM.

Table 2.2: Elemental analysis for the copolymers at low conversions and their compositions.

| Sample | %C | %H | %N | $F_{PEGM}$ | $F_{DEAEM}$ |
|---|---|---|---|---|---|
| **polyPEGM** | 52.14 | 8.81 | - | - | - |
| **polyDEAEM** | 64.25 | 10.61 | 7.58 | - | - |
| **poly(PEGM-*co*-DEAEM) (2)** | 56.55 | 9.18 | 2.83 | 0.423 | 0.577 |
| **Poly(PEGM-*co*-DEAEM) (3)** | 53.62 | 8.76 | 2.11 | 0.531 | 0.468 |
| **Poly(PEGM-*co*-DEAEM) (4)** | 55.38 | 8.80 | 2.18 | 0.519 | 0.480 |
| **Poly(PEGM-*co*-DEAEM) (5)** | 54.41 | 8.89 | 1.48 | 0.642 | 0.357 |
| **Poly(PEGM-*co*-DEAEM) (6)** | 54.49 | 8.80 | 1.31 | 0.676 | 0.323 |
| **Poly(PEGM-*co*-DEAEM) (7)** | 52.11 | 7.87 | 0.38 | 0.892 | 0.107 |
| **Poly(PEGM-*co*-DEAEM) (8)** | 52.93 | 8.46 | 0.37 | 0.894 | 0.105 |
| **Poly(PEGM-*co*-DEAEM) (9)** | 52.76 | 8.11 | - | 1 | 0 |

Table 2.3: Elemental analysis for the copolymers at high conversions and their compositions.

| Sample | %C | %H | %N | $F_{PEGM}$ | $F_{DEAEM}$ |
|---|---|---|---|---|---|
| **poly(PEGM-co-DEAEM) (1)** | 59.15 | 8.79 | 4.86 | 0.196 | 0.803 |
| **Poly(PEGM-co-DEAEM) (3)** | 56.98 | 8.38 | 2.89 | 0.414 | 0.585 |
| **Poly(PEGM-co-DEAEM) (4)** | 56.30 | 8.41 | 2.44 | 0.479 | 0.520 |
| **Poly(PEGM-co-DEAEM) (5)** | 55.17 | 8.14 | 1.58 | 0.623 | 0.376 |
| **Poly(PEGM-co-DEAEM) (6)** | 53.91 | 8.08 | 1.24 | 0.690 | 0.309 |
| **Poly(PEGM-co-DEAEM) (7)** | 53.33 | 7.92 | 0.90 | 0.764 | 0.235 |
| **Poly(PEGM-co-DEAEM) (8)** | 53.28 | 7.97 | 0.62 | 0.830 | 0.169 |
| **Poly(PEGM-co-DEAEM) (9)** | 52.82 | 7.90 | 0.30 | 0.913 | 0.086 |

Table 2.4: Solvent effect on the copolymer composition.

| **Sample** | **Solvent** | **%C** | **%H** | **%N** | **$F_{PEGM}$** | **$F_{DEAEM}$** |
|---|---|---|---|---|---|---|
| Poly(PEGM-*co*-DEAEM) (5) | Bulk | 58.75 | 8.97 | 3.73 | 0.311 | 0.689 |
| Poly(PEGM-*co*-DEAEM) (5) | $CCl_4$ | 55.17 | 8.14 | 1.58 | 0.623 | 0.376 |
| Poly(PEGM-*co*-DEAEM) (5) | Acetone | 53.29 | 7.76 | 0.67 | 0.818 | 0.182 |

### 2.3.4 Monomer Reactivity Ratios

The copolymer composition was determined based on elemental analysis method. The monomer reactivity ratios were calculated for low conversion using Fineman-Ross (FR) [137] and Extended Kelen-Tüdøs (EKT) [138] methods, while Extended Kelen-Tüdøs (EKT), and Mayo Lewis [139] methods were used at high conversions. The linearized equation used for Finemann – Ross is

$$G = r_1 F - r_2 \tag{2.18}$$

where $G = X(Y-1)/Y$, $F = X^2/Y$ , $X = f_1/f_2$ and $Y = F_1/F_2$.

The slope gives $r_1$, the PEGM monomer reactivity ratio, and the intercept is $r_2$, the DEAEM monomer reactivity ratio. The FR plot is given in Figure 2.3(a).

Extended Kelen-Tüdøs (EKT) was used for both low and high conversions copolymers, and the effect of conversion was considered:

$$\eta = (r_1 + r_2/\alpha)\,\xi - r_2/\alpha \tag{2.19}$$

where:

$$F = (F_1/F_2)/[(log\ z_1)/(log\ z_2)]^2 \tag{2.20}$$

$$G = (F_1/F_2 - 1)/[(log\ z_1)/(log\ z_2)] \tag{2.21}$$

where $z_1 = f_{1,f}/f_{1,o}$ , $z_2 = f_{2,f}/f_{2,o}$ and $f_{1,o}$, $f_{1,f}$ , $f_{2,o}$, and $f_{2,f}$ are the initial and final mole fraction of monomer 1( PEGM) and monomer 2 (DEAEM), respectively. The partial molar conversion of monomer 2 is defined as:

$$\xi_2 = w\,(\mu + X)/(\mu + Y) \tag{2.22}$$

where w = weight conversion of polymerization, and μ= ratio of molecular weight of monomer 2 to that of monomer 1. The partial molar conversion of monomer 1 is:

$$\xi_1 = \xi_2(Y/X) \tag{2.23}$$

and

$$Z = \log(1-\xi_1)/\log(1-\xi_2) \tag{2.24}$$

where $F = Y/Z^2$, $G = (Y-1)/Z$, $\eta = G/(\alpha + F)$, $\xi = F/(\alpha + F)$ and $\alpha = \sqrt{F_{min}\,F_{max}}$. From [equation (2.19)], the intercept at $\xi = 0$ and $\xi = 1$ of the η versus ξ plot gives $-r_2/\alpha$ and $r_1$, respectively. The Extended Kelen-Tüdos plots for both low, and high conversion are given in [Figure 2.3(b,c)], respectively.

Mayo-Lewis (ML) method was used for the calculation of the monomer reactivity ratios at high conversion copolymers [139], ML plot for high conversion is given in Figure 2.3(d).

In all of these calculations, PEGM was considered as monomer 1, and DEAEM as monomer 2. The monomer reactivity ratios for both monomers at low and high conversions are given in (Table 2.5). The results obtained by Finemann-Ross (FR) and Extended Kelen-Tüdøs (EKT) methods at low conversions are in well agreement with each other. PEGM is the more reactive monomer with a monomer reactivity value of 0.90 by EKT method. DEAEM has a reactivity ratio of 0.15. At low conversions, $r_2$ (DEAEM) value is lower than $r_1$ (PEGM) showing that the DEAEM terminated growing chains prefers to add PEGM over adding to DEAEM. Similarly, PEGM terminated species active chains prefer adding to PEGM rather than DEAEM. Both $r_1$and $r_2$ values are less than 1, and ($r_1 \times r_2$=0.13) value is closer to zero than 1

indicating random copolymerization with alternating tendency. At high conversions, DEAEM has a considerably higher reactivity ratio ($r_2$=0.40) by EKT than at low conversions reflecting the effect of conversion on the comonomer feed ratio and consequently on the average copolymer composition. The multiplication of ($r_1 \times r_2$) equals 0.40 indicating random copolymerization. The copolymerization behavior of the PEGM/DEAEM comonomer pair is shown according to the mole fraction of monomer feed versus the copolymer composition in [Figure 2.4 (a,b)] at low and high conversions respectively. The deviation from ideal copolymerization behavior in favor of random copolymerization is clearly illustrated by the (F vs f) plots given in [Figure 2.4 (a,b)].

Table 2.5: Monomers reactivity ratios at low and high conversions, using different methods.

| **Method** | **$r_1$ (PEGM)** | **$r_2$ (DEAEM)** | **$r_1 \times r_2$** |
|---|---|---|---|
| **Low conversion** | | | |
| **FR** | 0.88 | 0.15 | 0.14 |
| **EKT** | 0.90 | 0.14 | 0.13 |
| **High conversion** | | | |
| **EKT** | 1.01 | 0.40 | 0.40 |
| **ML** | 0.82 | 0.70 | 0.58 |

Table 2.6: Tg values obtained by DSC for homopolymers and copolymers.

| **Sample** | **Tg (°C)** |
|---|---|
| **Poly PEGM** | -10.0 |
| **Poly DEAEM** | 16.0 |
| **Poly(PEGM-*co*-DEAEM)(4)** | 11.5 |
| **poly(PEGM-*co*-DEAEM) (8)** | 1.00 |

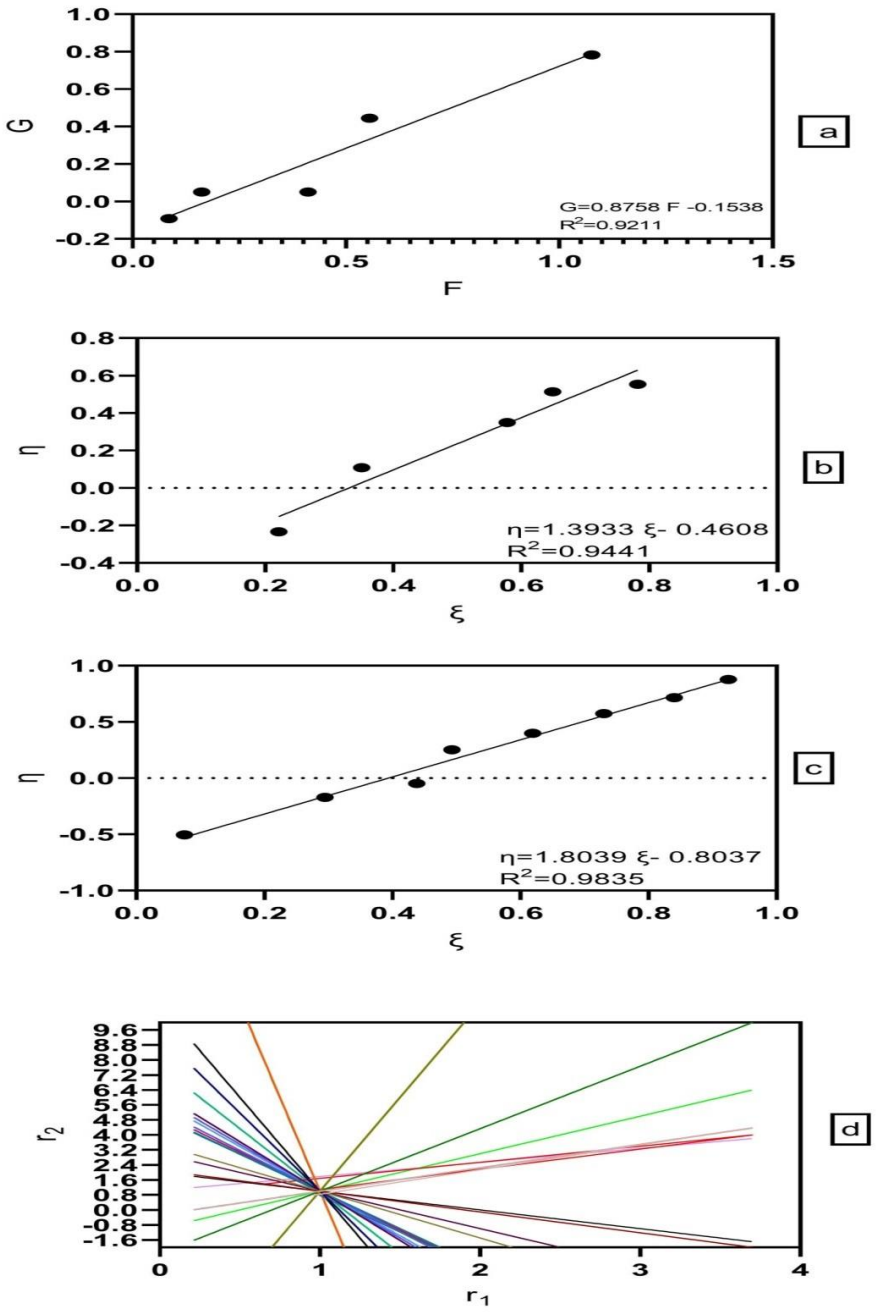


Figure 2.3: (a) FR at low conversion, (b) EKT at low conversion, (c) EKT at high conversion, and (d) ML at high conversion

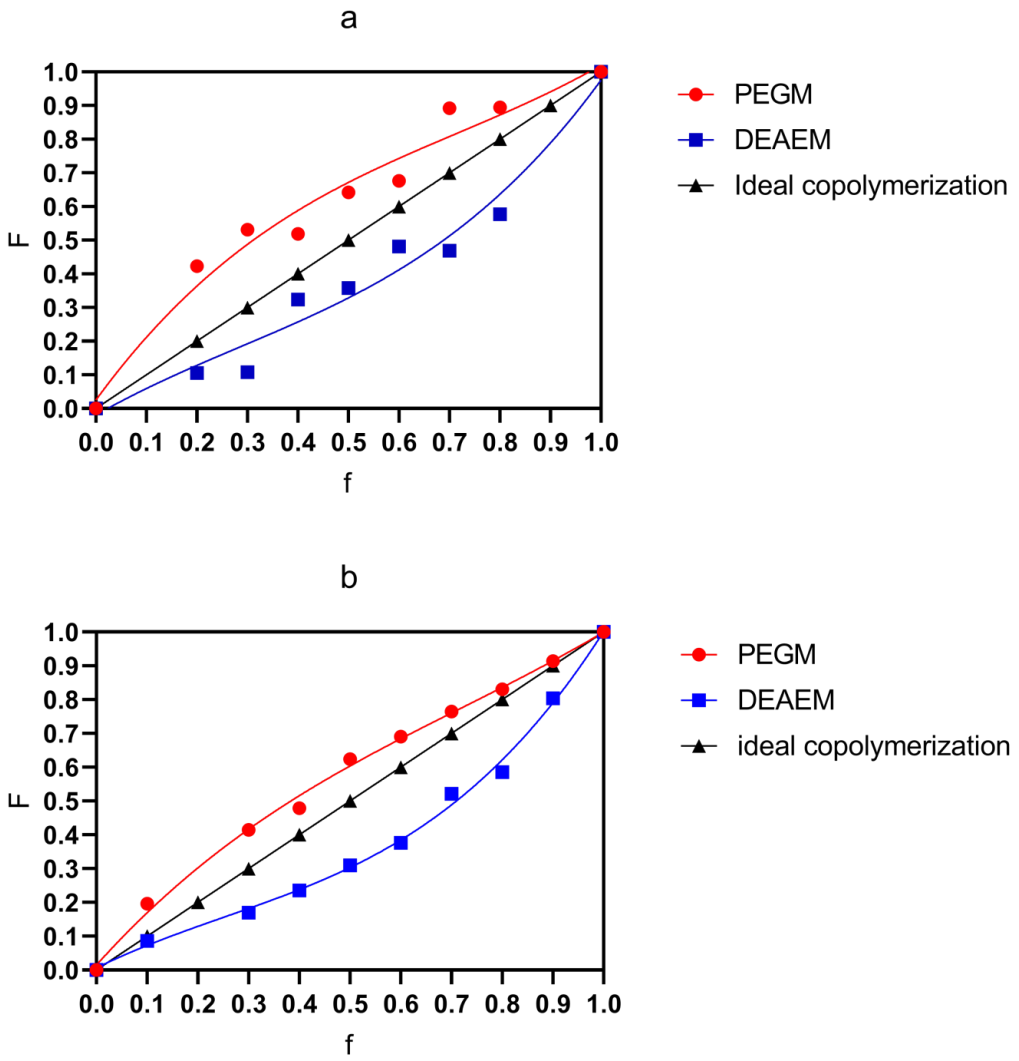


Figure 2.4: Variation of copolymer composition (F) as a function of mole fraction of PEGM in the initial comonomer feed (f) (a) low conversion and (b) high conversion.

### 2.3.5 Thermal Analysis of the Copolymers

Thermal properties of the polymers were characterized by DSC and TGA analyses. The influence of the PEGM molar ratio on the $T_g$ values of the copolymers was followed by DSC analysis. The $T_g$ values of the homopolymers and the copolymer samples are given in Table 2.6 The $T_g$ value of poly PEGM hydrogel is expected to be lower than 0 °C [80], and has been determined as -10.0 °C. The $T_g$ value of polyDEAEM is 16°C which is close to other values reported in the literature [140]. The measured $T_g$ values of the copolymer samples namely poly(PEGM-*co*-

DEAEM)(4), and poly(PEGM-*co*-DEAEM)(8) are 11.5 °C and 1.0 °C. Thus, increasing the amount of PEGM in the copolymers reduces the $T_g$ value. The PEGM used in this work has 6 ethoxy units on the side chain and is viewed as a flexible segment. Thus, the flexibility of the hydrogel is enhanced after introducing PEGM, which leads to the decrease in $T_g$ value. Similar results have been reported by other workers [129,141].

The thermogravimetric analysis of polyPEGM is shown in Figure 2.5(a). Around 4.0 % weight loss of polyPEGM was observed when the temperature rose to 120°C. This refers to evaporation of water from the sample. While 73% weight loss was observed from 120°C to 370°C, which was presumed as the decomposition of C-O backbone. A 23 % weight loss was observed from 370°C to 400°C, and this was presumed as the decomposition of the methacrylate component [142].

The homopolymer polyDEAEM has two decomposition peaks in the TGA curve shown in Figure 2.5(b). The main decomposition peak is observed around 370 °C and it is due to the loss of the diethyl amino ethyl groups. The second peak which is shorter than the first one, and is around 425 °C, it may relate to the elimination of $CO_2$ and CO groups and to the carbonization processes.

The main decomposition peak is attributed to the decomposition of the main chain, in both homopolymers. The general mechanism of the thermal degradation of the polymethacrylates involves the loss of the ester side group to form methacrylic acid followed by cross-linking [143]. It appears that diethyl amino ethyl groups provide higher thermal stability compared to the glycol groups. In other words, the thermolysis of the side groups of PEGM is favored.

TGA curves of copolymer samples obtained at low conversions and at high conversions are given in [Figure 2.5(c-e)], [Figure 2.5(f-h)], respectively. The copolymers, whether produced at low conversions or at high conversions show similar thermal stabilities. This refers to random distribution of the comonomers in the copolymer structure. However, the decomposition behavior shows similar characteristics to that of polyPEGM for the sample richer in polyPEGM and vice versa.

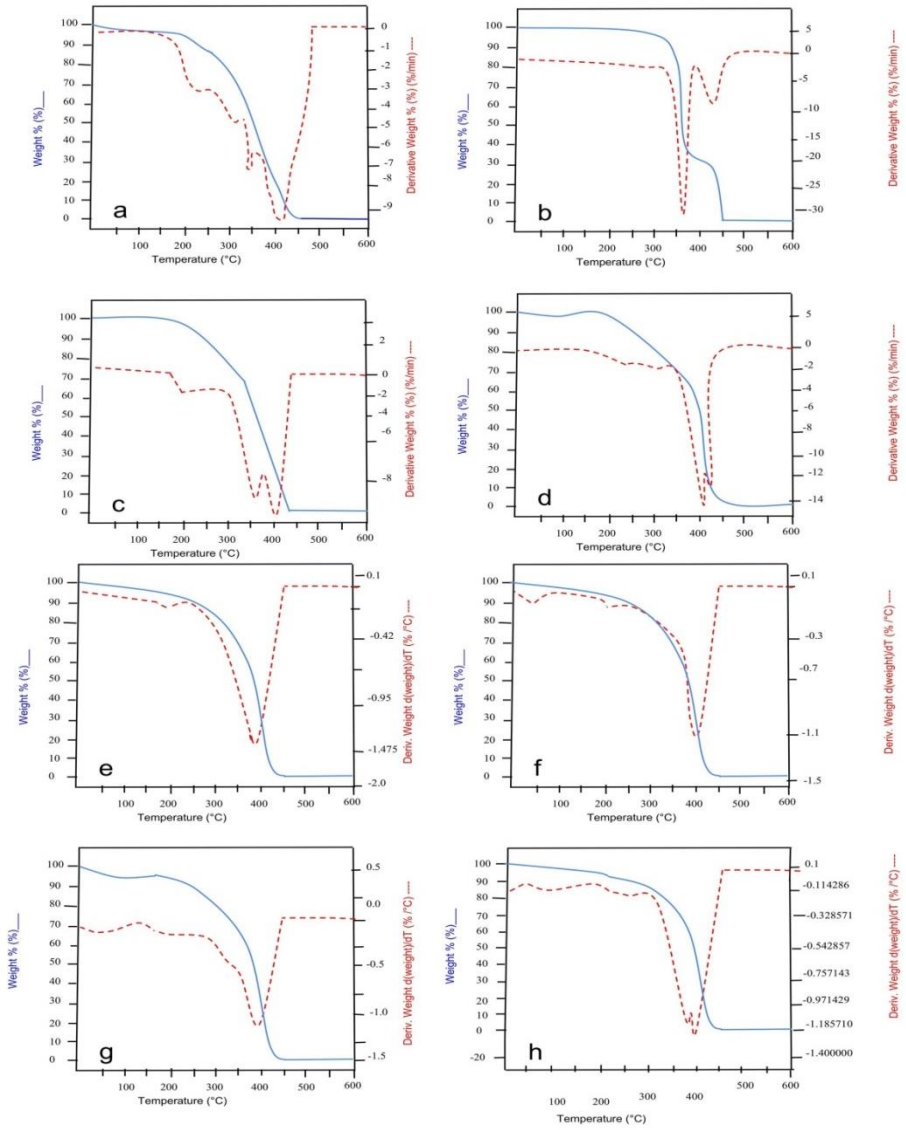


Figure 2.5: TGA curve of ( a) poly PEGM , ( b) PolyDEAEM homopolymers;(c) –(e) low conversion poly(PEGM-co-DEAEM)(3),(5), and (7);(f) –(h ) high conversion poly(PEGM-co-DEAEM)(3),(5), and (7) respectively.

### 2.3.6 Gel Content

The gel percent is one of the most important factors that affect the swelling of hydrogels. Highly crosslinked hydrogels have a tighter structure and swell less compared to the hydrogels, which have lower crosslinking. When the composition of PEGM and DEAEM was changed, the gel percent changed.

The gel content of the hydrogels poly(PEGM-*co*-DEAEM)(3),(5), and (7), which were synthesized at high conversion, was measured by placing them in distilled water for 48 h to ensure dissolution of all noncrosslinked components. They were then dried at 80 °C for about 48 h to constant weight. The gel percent was calculated by using equation (2.25) given below [110].

$$Gel\ \% = \frac{Wd}{Wi} \times\ 100 \qquad (2.25)$$

where: Wd is the weight of dried insoluble part and Wi is the initial weight of dried sample.

The Gel % of the poly(PEGM-*co*-DEAEM)(3), (5), and (7) are: 53.9, 58.1, and 78.5 %, respectively. As the gel content increases, the crosslinking density increases so the equilibrium swelling degree decreases as shown in Figure 2.6, and as explained later.

### 2.3.7 Equilibrium Swelling Behavior

Swelling degree affects several characteristics of hydrogels, such as the permeability, mechanical properties, surface properties, and others [144]. The swelling degree is also related to the chemical structure of the polymer network, the crosslinking density, the type of ionic groups in the polymers, the acid dissociation constant of the ionizable groups, and external factors, such as the ionic strength, pH, and temperature of the solution [141,145].

Swelling behavior of the copolymer was studied, in water [Figure 2.6(a)], 0.01 M HCl [Figure 2.6(b)], and in 0.01 M NaOH solution [Figure 2.6(c)]. Equilibrium swelling capacities increased in all solutions with increasing DEAEM fraction, and with increasing acidity of the solution. This is related to the protonation of amino groups of DEAEM and to more electrostatic repulsive force between ionized groups. Thus, more space in the polymer network, more water is allowed to diffuse into the hydrogel structure. On the other hand, the gel content reveals that the crosslinking degree of poly(PEGM-*co*-DEAEM)(3) is the minimum, so the swelling degree is expected to be the highest. SEM analysis given below reveals that this sample has got a loose network structure and larger pores (average diameter 4.5 μm) compared to the other samples. These factors contribute to the larger swelling capacity of poly(PEGM-*co*-DEAEM)(3). It reaches around 2000% for poly(PEGM-*co*-DEAEM)(3) after 1 hour in 0.01 M HCl solution.

When the swelling kinetics are considered in different pH values it can be followed from Figure 2.6(a) that at pH = 7.4 five minutes are enough for poly(PEGM-*co*-DEAEM)(3), (5), and (7) to reach a swelling degree of 613%, 429%, and 46.7%, respectively. During the first hour, the % swelling of poly(PEGM-*co*-DEAEM)(3), (5), and (7), are 904%, 565%, and 147%, respectively. Two hours are enough to reach the equilibrium swelling capacity.

Figure 2.6 (b) shows that when the pH is decreased to 2, better swelling behavior is achieved for all copolymers. Within the first five minutes, the % swelling of poly(PEGM-*co*-DEAEM)(3), (5), and (7) copolymers, are 784%, 308%, and 152%, respectively. During the first hour, the % swelling of poly(PEGM-*co*-DEAEM)(3),

(5), and (7), are 2024%, 1179%, and 315%, respectively. All copolymers need around two hours to reach equilibrium swelling capacity.

Figure 2.6 (c) shows that under alkaline conditions, when the pH is 12, the lowest swelling capacities are observed for all copolymers studied. Within the first five minutes, the % swelling of poly(PEGM-*co*-DEAEM)(3), (5), and (7)copolymers, are 289%, 220%, and 60.9%, respectively. During the first hour, the % swelling of poly(PEGM-*co*-DEAEM)(3), (5), and (7), are 382%, 346%, and 194%, respectively. All copolymers need around 2 hours to reach equilibrium swelling capacity.

Hence, the fastest and the highest % swelling degree is achieved when the pH is equal to 2, with poly(PEGM-*co*-DEAEM)(3) sample.

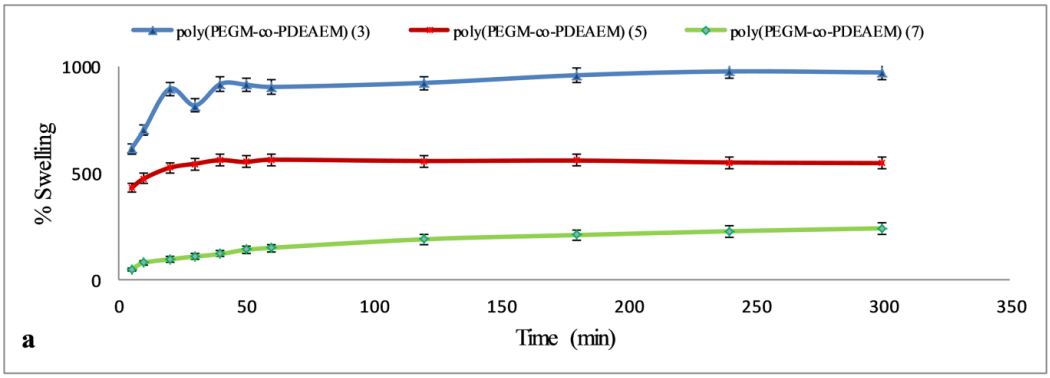


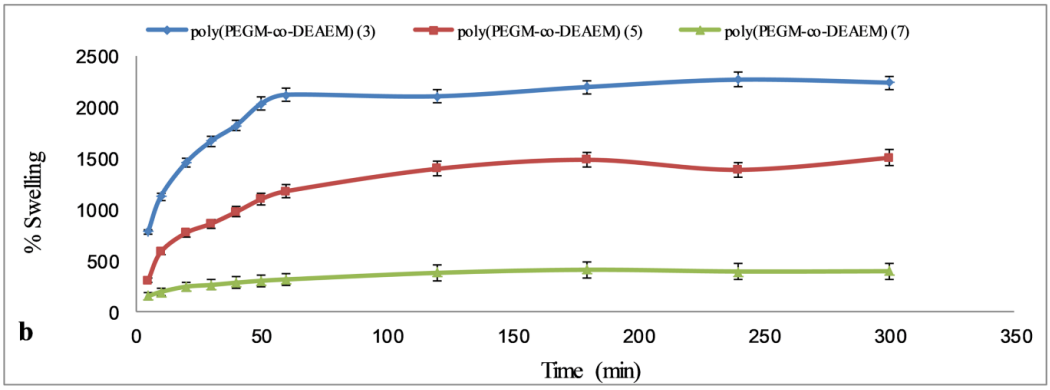


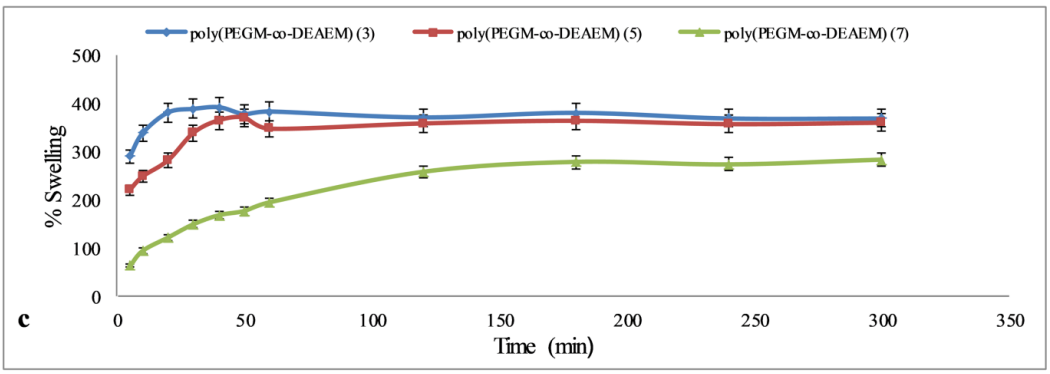


Figure 2.6: Swelling behavior of the copolymers in (a) distilled water, (b) 0.01M HCl, and (c) 0.01M NaOH.

### 2.3.8 Dye Adsorption

#### 2.3.8.1 SEM Analysis

The surface morphologies of the poly(PEGM-*co*-DEAEM)(3), (5), and (7) before and after the MO adsorption analyzed by using SEM are shown in [Figure 2.7(a-f)]. The poly(PEGM-*co*-DEAEM)(3) shows a rougher surface with bigger pores [Figure 2.7(a)] while the other copolymers exhibit smoother surfaces with smaller pores [Figure 2.7(b-c)]. Furthermore, it can be observed that increasing PEGM content from sample (3) to (5) to (7) gives tighter network structures with smaller pores and higher pore density per unit area. A two dimensional pore size analysis based on SEM pictures reveals that the average diameters of pores are 4.6±0.5 µm, 2.7±0.5 µm, and 1.8±0.5 µm in samples poly(PEGM-*co*-DEAEM) (3), (5), and (7) respectively. On the other hand the surface morphologies of the copolymers after the adsorption process [Figure 2.7(d-f)] show that most voids have been occupied by the adsorbed dye. Smoother surfaces with a noticeable layer of the MO dye can be observed.

#### 2.3.8.2 Effect of pH on MO Adsorption

Adsorption experiments were carried under different pH values (2, 3, 4, 6, 8, and 10), where the other parameters were kept constant as follows: mass of the copolymer =0.05 g, MO concentration = 20 ppm, Temperature = 298K, and the contact time = 24 h. The results are shown in Figure 2.8(a).

The maximum dye removal for all copolymer compositions was achieved at pH 3. This may be attributed to electrostatic interaction between protonated tertiary amino group of polyDEAEMA chains and negative charge of sulfonate group on the MO dye.

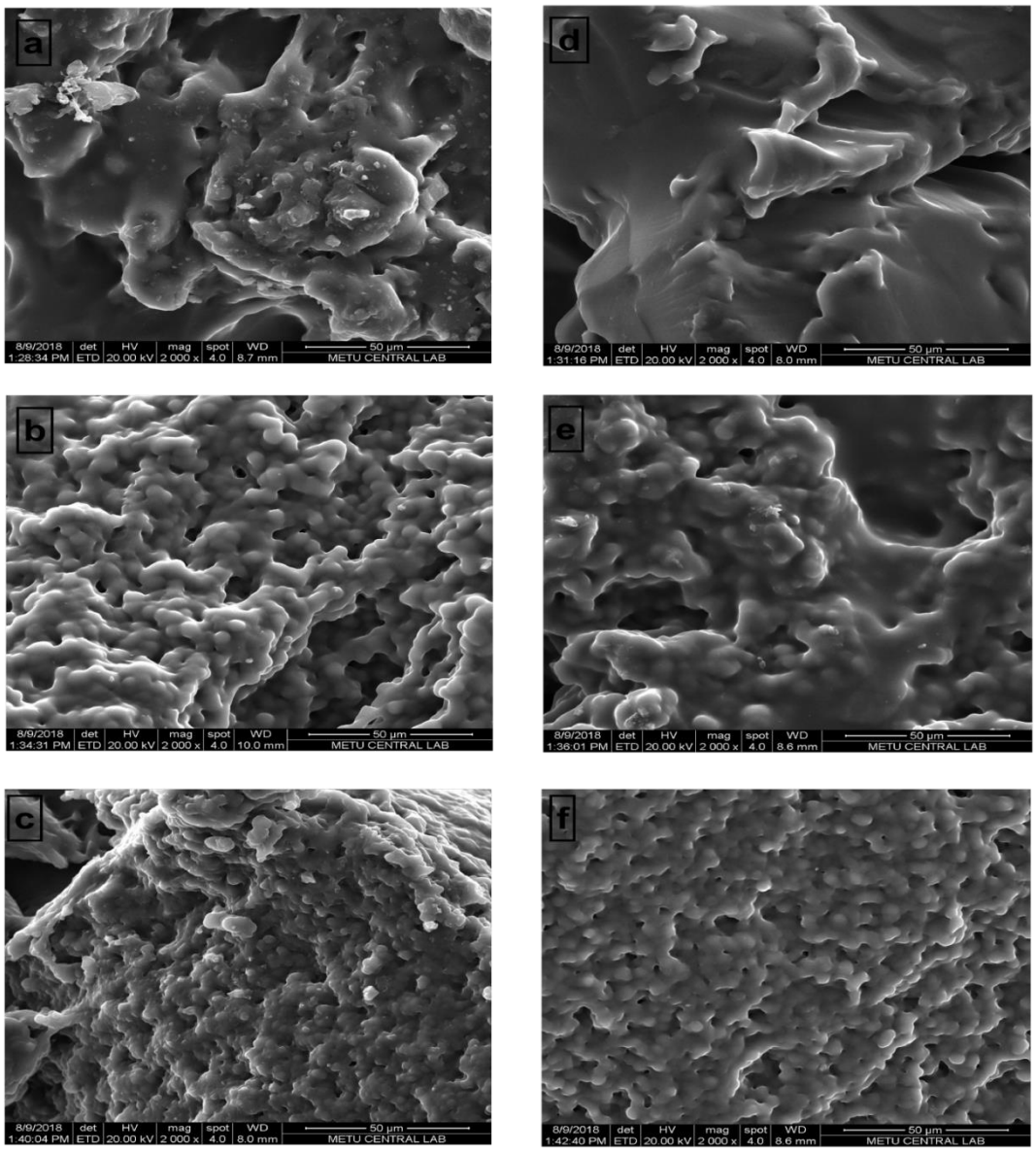


Figure 2.7: SEM micrographs (x2000); (a) –(c ) poly(PEGM-co-DEAEM)(3),(5), and (7) ( before adsorption) ; (d) –(f) poly(PEGM-co-DEAEM)(3),(5), and (7) (after adsorption) respectively.

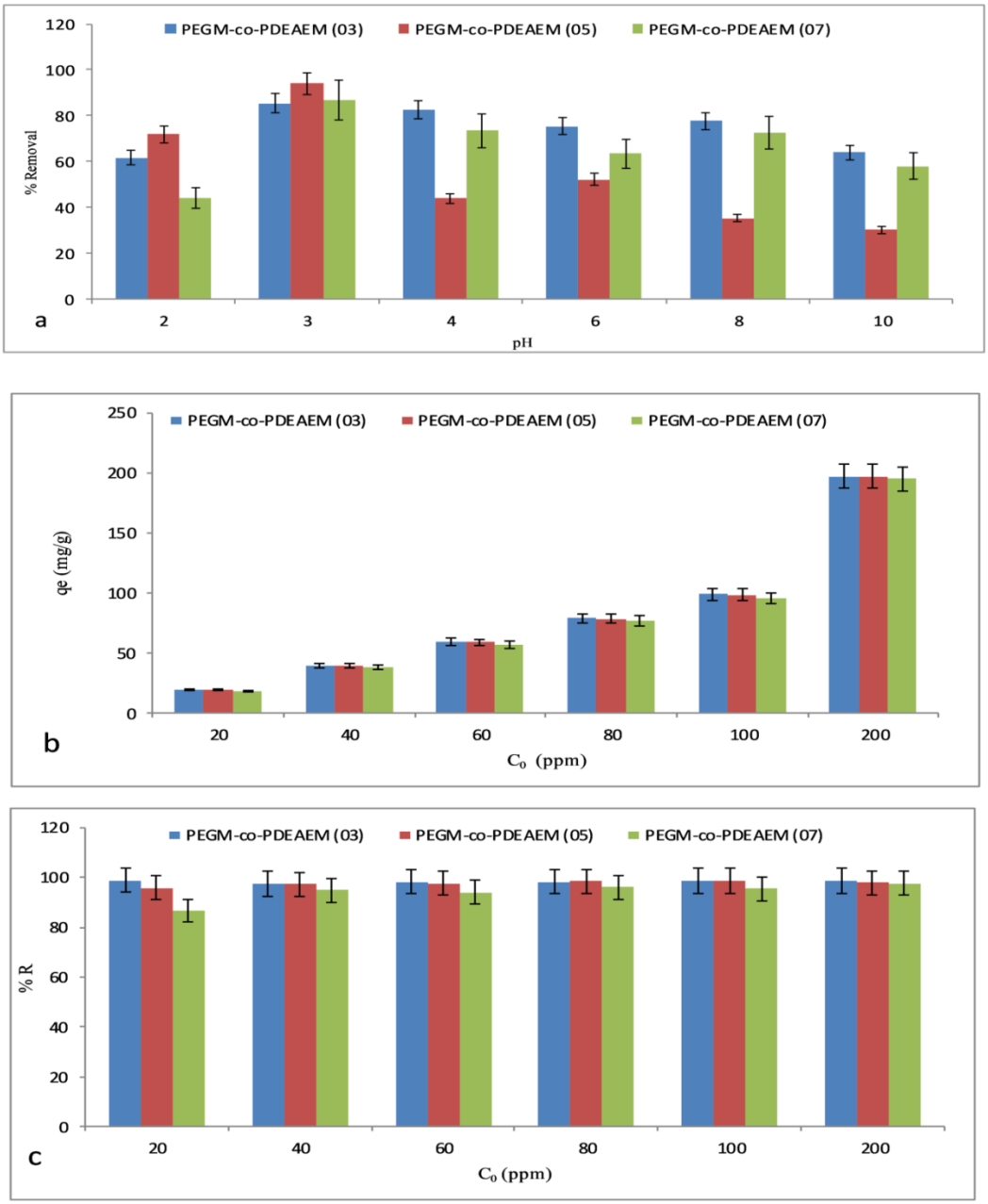


Figure 2.8: (a) The effect of pH on the MO adsorption onto copolymers; The effect of initial MO concentration (0.05 g adsorbent; 50 mL MO solution ; adsorption time 12 hrs ; room temperature; and pH value of 3) on (b) adsorption capacity, (c) on the % removal

#### 2.3.8.3 Effect of Initial Concentrations on the Adsorption Capacity, and % Removal.

Figure 2.8(b) shows that as the initial concentrations of MO, $C_o$ value, increases, the $q_e$ value increases for all samples studied. Poly(PEGM-*co*-DEAEM)(3) has a slightly higher value of $q_e$ at different initial concentrations values than the others. On the other hand, Figure 2.8(c) shows that the % removal, %R, is always more than 95%, which indicates excellent adsorbing capacity of the hydrogels towards MO dye. Poly(PEGM-*co*-DEAEM)(3) has the highest % R value even at low $C_o$, (20 ppm). As the $C_o$ value increases the differences in % R values between the hydrogels decrease.

#### 2.3.8.4 Kinetics Studies

Studying the kinetics of adsorption is important to know adsorption equilibrium time, and to design treatment systems that depend on interaction rates. The pseudo-first-order and pseudo-second-order kinetics were used to study the MO adsorption onto poly(PEGM-*co*-DEAEM)(3), (5), and (7) copolymers, the calculated parameters at different initial concentration are given in Table 2.7.

Table 2.7 shows that at all of the studied initial concentrations, the adsorption kinetics is described by pseudo second order model better than the pseudo first order model. The corresponding values of the correlation coefficient ($R^2$) of this model are higher compared to those of pseudo first order model. On the other hand, the theoretical ($q_e$) values, which were calculated from the pseudo second order model are closer to the experimental values.

From the previous observations, MO adsorption onto poly(PEGM-*co*-DEAEM) copolymers follows pseudo second order kinetic, which assumed that the rate limiting step is a chemisorption .

Table 2.7: Kinetic parameters of MO adsorption onto poly(PEGM-co-DEAEM) copolymers.

| $C_0$ (ppm) | 1st order | | | 2nd order | | | $q_e$ (Exp) (mg/g) | Copolymer |
|---|---|---|---|---|---|---|---|---|
| | $q_e$ (mg/g) | $K_1$ ($min^{-1}$) | $R^2$ | $q_e$ (mg/g) | $K_2$ (g/mg.min) | $R^2$ | | |
| 20 | 46.31 | 0.042 | 0.978 | 20.41 | 0.0027 | 0.9991 | 19.79 | **Poly(PEGM-*co*-DEAEM(3)** |
| | 24.05 | 0.0177 | 0.9392 | 20.37 | 0.00124 | 0.9979 | 19.14 | **Poly(PEGM-*co*-DEAEM(5)** |
| | 35.45 | 0.0168 | 0.8835 | 13.68 | 0.0015 | 0.9404 | 17.35 | **Poly(PEGM-*co*-DEAEM(7)** |
| 40 | 5.93 | 0.0125 | 0.6765 | 39.84 | 0.0039 | 0.9989 | 38.98 | **Poly(PEGM-*co*-DEAEM(3)** |
| | 13.03 | 0.0047 | 0.9288 | 40.16 | 0.0012 | 0.9998 | 40.00 | **Poly(PEGM-*co*-DEAEM(5)** |
| | 20.68 | 0.0065 | 0.9843 | 39.37 | 0.0008 | 0.9995 | 38.5 | **Poly(PEGM-*co*-DEAEM(7)** |
| 60 | 10.85 | 0.0044 | 0.7619 | 59.52 | 0.0014 | 0.9998 | 58.98 | **Poly(PEGM-*co*-DEAEM(3)** |
| | 25.16 | 0.0086 | 0.9834 | 59.88 | 0.00085 | 0.9997 | 62.89 | **Poly(PEGM-*co*-DEAEM(5)** |
| | 18.71 | 0.0042 | 0.9832 | 57.47 | 0.0001 | 0.9985 | 57.5 | **Poly(PEGM-*co*-DEAEM(7)** |
| 80 | 11.92 | 0.0047 | 0.5736 | 79.36 | 0.0016 | 0.9999 | 78.66 | **Poly(PEGM-*co*-DEAEM(3)** |
| | 23.64 | 0.0080 | 0.971 | 79.36 | 0.001 | 0.9999 | 78.60 | **Poly(PEGM-*co*-DEAEM(5)** |
| | 64.82 | 0.0026 | 0.8615 | 75.19 | 0.001 | 0.9999 | 74.4 | **Poly(PEGM-*co*-DEAEM(7)** |
| 100 | 18.34 | 0.0144 | 0.9303 | 99.01 | 0.0023 | 1 | 98.78 | **Poly(PEGM-*co*-DEAEM(3)** |
| | 25.62 | 0.0083 | 0.9668 | 100 | 0.0009 | 0.9999 | 99.01 | **Poly(PEGM-*co*-DEAEM(5)** |
| | 19.95 | 0.0053 | 0.8638 | 98.4 | 0.007 | 0.9993 | 92.8 | **Poly(PEGM-*co*-DEAEM(7)** |
| 200 | 29.55 | 0.017 | 0.9184 | 196.1 | 0.0019 | 1 | 197.3 | **Poly(PEGM-*co*-DEAEM(3)** |
| | 13.80 | 0.0032 | 0.9512 | 196.1 | 0.0012 | 1 | 197.24 | **Poly(PEGM-*co*-DEAEM(5)** |
| | 29.55 | 0.032 | 0.8165 | 185.2 | 0.048 | 1 | 185.4 | **Poly(PEGM-*co*-DEAEM(7)** |

Table 2.8: Adsorption isotherms Parameters of MO onto poly (PEGM-co-DEAEM) copolymers.

| Copolymer | Langmuir | | | Freundlich | | | Temkin | | |
|---|---|---|---|---|---|---|---|---|---|
| | $q_{max}$ | $K_L$ | $R^2$ | $K_F$ | n | $R^2$ | $b_T$ | $K_T$ | $R^2$ |
| **Poly(PEGM-co-DEAEM)(3)** | 212.7 | 0.52 | 0.9753 | 6.34 | 1.2 | 0.9412 | 41.5 | 4.6 | 0.7225 |
| **Poly(PEGM-co-DEAEM)(5)** | 208.3 | 0.55 | 0.9542 | 6.32 | 1.4 | 0.9880 | 35.6 | 3.1 | 0.9068 |
| **Poly(PEGM-co-DEAEM)(7)** | 178.6 | 0.18 | 0.9503 | 4.32 | 1.6 | 0.9537 | 42.6 | 1.0 | 0.8285 |

### 2.3.8.5 Adsorption Isotherms

A comparison of three isotherms, Langmuir, Temkin and Freundlich models for MO adsorption onto poly(PEGM-co-DEAEM) hydrogels , is given in Table 2.8. It can be found that Langmuir isotherm fits to the data describing the adsorption behavior of MO onto poly(PEGM-co-DEAEM)(3). On the other hand, Freundlich model describes the adsorption process better for both poly(PEGM-*co*-DEAEM)(5) and poly(PEGM-*co*-DEAEM)(7), where higher $R^2$ values were obtained.

The Langmuir isotherm [130] suggests mono-layer adsorption on a uniform surface with a finite number of adsorption sites. The main characteristic of the Langmuir isotherm can be expressed in terms of a constant called dimensionless separation factor ($R_L$)

$$R_L = \frac{1}{1+K_L C_0} \quad (2.26)$$

$R_L$ describes the shape of adsorption to be either, unfavorable ($R_L > 1$), linear ($R_L = 1$), favorable ($0 < R_L < 1$) or irreversible ($R_L = 0$) [146]. For poly(PEGM-co-DEAEM)(3), (5), and (7) results were found for $R_L$ to be between (0.009 to 0.088), (0.009 to 0.045 ), and (0.026 to 0.121), respectively which represents a favorable adsorption. Furthermore, the Low $R_L$ values indicate the strong interaction between the MO and hydrogels [147].

Freundlich isotherm [131] assumes that adsorption occurs on heterogeneous surfaces with different energy of adsorption and non-identical rare sites. The Freundlich constant n describes the favorability of the adsorption process. For favorable process n should be more than 1 and less than 10. It was found that the values of n ware greater than 1, suggesting that the adsorption of MO onto the poly(PEGM-co-DEAEM) hydrogels was a favorable.

The Temkin isotherm model is based on the assumption that the adsorption energy decreases linearly with the surface coverage due to adsorbent–adsorbate interactions [132].

From Table 2.8, the correlation coefficient ($R^2$) was less than that obtained for both Langmuir and Freundlich models, for all poly(PEGM-*co*-DEAEM) hydrogels indicating that Temkin isotherm model does not fit with experimental data as well as the other models.

Table 2.9 lists a comparison between our copolymers with other adsorbents reported in other studies [148,149,150,151] towards MO, it shows that poly(PEGM-co-DEAEM)(3), (5), and (7) hydrogels have an excellent adsorption capacity, with higher $q_{max}$ values, supporting that these hydrogels can act as alternative adsorbents to the others due to their considerably higher adsorption capacities.

**2.3.8.6 Thermodynamic Parameters**

The thermodynamic parameters, including the Gibbs free energy change (ΔG°), entropy change (ΔS°), enthalpy change (ΔH°) were calculated to examine the spontaneity of the adsorption of MO onto the poly(PEGM-co-DEAEM)(3), (5), and (7) hydrogels. Table 2.10 lists these parameters and from the data it is clear that the

negative values of ΔH° show an exothermic nature of MO adsorption where MO adsorption efficiency decreases with the increase of temperature. The negative values of ΔS° indicate decreasing of the degree of randomness of the dye molecule at the solid-liquid interface during the adsorption process. The negative values of ΔG° in all the temperature confirm that the adsorption process is spontaneous in nature.

Table 2.9: Comparison of the adsorption capacities of various adsorbents toward MO dye

| **Adsorbent** | **Adsorption conditions** | **$q_{max}$ (mg $g^{-1}$)** | **Reference** |
|---|---|---|---|
| **Poly(PEGM-*co*-DEAEM(3)** | pH 3, 298K | 212.77 | This work |
| **Poly(PEGM-*co*-DEAEM(5)** | pH 3, 298K | 208.3 | This work |
| **Poly(PEGM-*co*-DEAEM(7)** | pH 3, 298K | 178.57 | This work |
| **Graphene oxide** | pH 3, 298 K | 16.83 | [149] |
| **Chitosan** | pH 3, 298 K | 29 | [150] |
| **20CMC-Bent** | pH 6.86, 298K | 110.7 | [148] |
| **Activated carbons of corncob derived char wastes** | pH 7, 298K | 11.57 | [151] |

Table 2.10: Thermodynamic parameters of the adsorption of MO dye onto poly(PEGM-co-DEAEM) copolymers.

| | **poly(PEGM-co-DEAEM)(3)** | **poly(PEGM-co-DEAEM)(5)** | **poly(PEGM-co-DEAEM)(7)** |
|---|---|---|---|
| **ΔS° (J mol-1 K-1)** | -272.08 | -34 | -49.32 |
| **ΔH° (kJ mol-1)** | -87.05 | -11.08 | -16.14 |
| **ΔG° (kJ mol-1), T=298 K** | -5.98 | -0.942 | -1.44 |
| **ΔG° (kJ mol-1), T= 308 K** | -3.26 | -0.607 | -0.947 |
| **ΔG° (kJ mol-1), T=318 K** | -0.53 | -0.267 | -0.453 |

## 2.4 Conclusions

Photoinitiated copolymerization of PEGM and DEAEM monomers was successfully achieved at low and high conversions. Crosslinked polymers were obtained without using any chemical cross linker during polymerization in the presence of $CCl_4$ solvent. The crosslinked polymers of PEGM-*co*-PDEAEM act as superabsorbents in aqueous solution. Equilibrium swelling capacities increased in all solutions with increasing DEAEM fraction, and with increasing acidity of the solution, reaching 2000 % within an hour in 0.01 M HCl solution.

The monomers compositions in the copolymers were determined using elemental analysis method and the monomer reactivity ratio was calculated, PEGM is more reactive monomer at low and high conversions. The MO adsorption onto the copolymers was highly efficient, (% R reaches 98%), and ($q_e$=212.7 mg $g^{-1}$), favorable ($0<R_L<1$) and spontaneously occurred ($\Delta G°<0$). In addition, these poly(PEGM-*co*-DEAEM) hydrogels would exhibit less environmental negative effects due to their environment friendly nature.

# Chapter 3

# PHOTOINITIATED GRAFTING OF POLY(2-HYDROXYETHYL METHACRYLATE) ONTO POLY(VINYL CINNAMATE) FILMS FOR FLURBIPROFEN LOADING AND RELEASE

## 3.1 Introduction

Vinyl cinnamate (VCi), and especially its copolymers are well known for their photo responsive behavior including photoinitiated polymerization, photo crosslinking [95], and light induced bending of its gels [96].

Cinnamoyl groups undergo 2+2 photocylo addition to form crosslinked gels under UV light of the order of 350 nm wavelength. Photo responsive hydrogels/nanogels of PolyVCi can undergo UV induced bending or volume transition [97], which may find use in phototherapy, as drug carriers, or in medical imaging in addition to application in optoelectronics. PolyVCi and its copolymers with hydrophilic polymers can form micelles in solution and molecular arrangement leading to liquid crystal behavior [98].

Studies on either homopolymerization or copolymerization of VCi derivatives are scarce in the literature. Homopolymerization to poly(vinyl cinnamate) (PolyVCi) had

been reported [99,100]. Amphiphilic copolymers have the ability to create micelle in selective solvents [104].

Poly(2-hydroxyethyl methacrylate) (polyHEMA) has proved to be a promising polymer for applications in biomedical fields since it was first synthesized in 1960. These applications include the use of PolyHEMA in the fields of contact lenses, artificial corneas and skins, drug delivery, and degradable scaffolds for tissue engineering [87], polyHEMA hydrogels are versatile due to their non-toxicity, biocompatibility, and thermal stability [88].

Grafting is one of the most efficient methods in order to achieve well modified polymers. In principle, graft copolymerization is an attractive method to impart a variety of functional groups to a polymer backbone [61]. Photoinitiation process shows ability to control the degree of crosslinking, and the amount of the polymer yield by adjusting the dose and time of the UV irradiation [52].

Flurbiprofen is classified as nonsteroidal anti-inflammatory drug (NSAID). It is used during eye surgery and for the treatment of rheumatoid arthritis, ankylosing spondylitis, and degenerative joint disease for the reduction of pain, fever and inflammation [152].

Pulsatile drug delivery systems are developed to deliver drug according to circadian behavior of diseases. In other words, these systems will deliver drug at certain time when it is neeeded within a circadian cycle (24 hs.). In these systems, there is an initial release period followed by a lag time characterized by no release behaviour, which is followed by rapid and complete drug release. A sigmoidal release profile is

observed. These systems allow delivery of the drug to the right side, at required dose and needed time [153].

This part of the thesis work presents synthesis of poly(vinyl cinnamate)-*graft*-poly(2-hydroxyethyl methacrylate) (PolyVCi-*graft*-PolyHEMA) copolymers by UV initiation via free radical mechanism, and the physicochemical properties of the products. The significance of the work lies on the fact that synthesis of these copolymers has not been reported in the literature before. PolyVCi/PolyHEMA hybrid systems have a potential to blend the more hydrophilic nature of PolyHEMA and hydrophobicity of PolyVCi polymer. These systems may find biomedical applications as surfaces with tunable hydrophilicity.

Grafting of polyHEMA onto polyVCi backbone by UV initiation has been achieved and optimum grafting conditions have been investigated. In addition to photocrosslinking, the products were further crosslinked by ethylene glycol dimethacrylate (EGDMA). Crosslinked films with swelling capability in water and in ethanol were obtained. The products have been characterized with respect to their chemical structures, chemical compositions, and physical properties such as surface morphology and thermal properties in addition to their swelling kinetics. The PolyVCi-*graft*-PolyHEMA films proved to be suitable loading and release matrixes for flurbiprofen demonstrating pulsatile release behavior, which has not been reported for flurbiprofen before.

## 3.2 Experimental Part

### 3.2.1 Materials

HEMA (Aldrich), and EGDMA (Aldrich) were cleaned from inhibitor by passing through inhibitor removal column (Aldrich). Flurbiprofen was provided by Pharma Mondial, North Cyprus. PolyVCi (Aldrich) was purified before use as described below. Benzophenone (Aldrich), chloroform (Aldrich), ethanol (Aldrich), methanol (Aldrich), tetrahydrofuran (THF) (Aldrich), and n-hexane (Aldrich) were used as received.

### 3.2.2 Purification of PolyVCi

PolyVCi was cleaned from any poly(vinyl alcohol) impurity as follows: 0.5 g of polyVCi (Aldrich) was dissolved in 10.0 mL of chloroform. The solution was refluxed at 50°C in an oil bath for 24 h. Then the flask was cooled down, and 30.0 mL of n-hexane was added to precipitate PolyVCi. The suspension was stirred overnight, filtered and dried at 60°C.

### 3.2.3 Characterization Techniques

FTIR-ATR analysis of the films was made by using Perkin-Elmer Spectrum Two FTIR-ATR spectrometer.

Thermal Gravimetric Analysis (TGA) of the films was made using Perkin Elmer Diamond Differential Calorimeter and Perkin Elmer Pyris 1 under nitrogen atmosphere at 10°C/min heating rate in Central Laboratory of Middle East Technical University, Ankara.

Scanning Electron micrographs (SEM) of the films were taken in Central Laboratory of Middle East Technical University, Ankara using Quanta 400F field emission

scanning electron microscope using Au-Pd coating.

The original PolyVCi sample as provided by the producer and purified PolyVCi used as the backbone for PolyHEMA grafting was characterized by GPC in Middle East Technical University Central Laboratory using Malvern-OmniSEC instrument. The solvent was THF and the flow rate was set as 1 mL/min.

Optical contact angle measurements on the films were made using Attension Theta goniometer in in Central Laboratory of Middle East Technical University, Ankara, Turkey.

### 3.2.4 Photoinitiated Grafting of PolyHEMA onto PolyVCi

Purified PolyVCi was dissolved in THF to obtain a 0.125 mM solution. Then different amounts of HEMA monomer (20.6, 41.2, 82.5, 123.8 mM) the crosslinker EGDMA (13.2, 26.5, 52.9 mM), photoinitiator benzophenone ($Ph_2CO$), (6.86, 13.7, 27.4 mM), were added to the polymerization solution and closed, and connected to $N_2$ gas bubbling at room temperature for 20 min. The reaction was carried out at different time intervals. Non grafted PolyVCi film was prepared for comparison of physichochemical properties with those of PolyVCi-*graft*-PolyHEMA films. The reaction conditions are shown in Table 3.1

The homogeneous solutions (20 mL) were transferred into glass petri dishes and exposed to UV-irradiation using a Luzchem photoreactor LZC 4V equipped with 6 top and 8 side UVA lamps of 350 nm wavelength and 7670 $\mu W.cm^{-2}$ power. All samples were placed 15.0 cm distance from the lamps. Film samples were obtained after UV irradiation. The samples were taken from the chamber at given time intervals, soaked in ethanol for 2 days during which ethanol was refreshed regularly

every 6 hours. Then, the films were dried at room temperature, to constant weight. The films were insoluble in aqueous media, or in organic solvents. The grafting percentage was calculated according to equation (3.1).

$$\%\ grafting = \frac{W_2 - W_1}{W_1} x100\% \quad (3.1)$$

where $W_1$ and $W_2$ stand for the initial weight of polyVCi film, and the weight of the film after UV irradiation, respectively.

### 3.2.5 Swelling Behavior

Known masses of films were placed in water and in ethanol. Swollen samples were weighed at given time intervals after removing the excess water on the surface. Each sample was tested three times. The swelling degree was determined using equation (3.2) given below.

$$\%\ \text{Swelling Degree} = \frac{W_s - W_d}{W_d} \times\ 100\% \quad (3.2)$$

where $W_d$ is the initial weight of dried film, and $W_s$ is the final weight of the swollen film after a certain period of time.

### 3.2.6 Flurbiprofen Loading

PolyVCi was dissolved in THF to obtain a 0.125 mM solution. Then a 41.2 mM of HEMA monomer, 26.5 mM of EGDMA, 13.7 mM of $Ph_2CO$, and FB (20.5 or 10.25 mM) were added to the polymerization solution and closed, and connected to $N_2$ gas bubbling at room temperature for 20 min. The reaction was carried out for 8 h. The homogeneous solutions (20 mL) were transferred into glass petri dishes and exposed to UV irradiation using a Luzchem photoreactor LZC 4V equipped with 6 top and 8 side UVA lamps of 350 nm wavelength and 7670 $\mu W.cm^{-2}$ power. Both samples were placed 15.0 cm distance from the lamps. Loaded films were obtained after UV irradiation, washed with ethanol several times, dried at room temperature, the obtained films were labeled as $FB_1$ and $FB_2$ according to initial concentration of the

added drug; $FB_1$ for 10.25 mM of the drug, and when the initial concentration of drug is 20.5 mM the film obtained was labeled as $FB_2$.

### 3.2.7 Flurbiprofen Release

Loaded films ($FB_1$and $FB_2$) were soaked in 100-mL of ethanol at room temperature. Aliquot volume of 1.0 mL of solution was drawn from the release medium at several given time intervals, and was measured using a (UV_Win 5.0, Bejjing, T80+) UV/vis spectrometer at 249 nm. Each measurement was repeated three times, and the average results were used in calculations. The release medium was replaced with 1.0 mL pure ethanol after each draw. The UV absorbance of the aliquot taken from the release medium was evaluated according to the flurbiprofen calibration curve using the best fit linear equation (y = 0.0716 x + 0.0846, $R^2$ = 0.9914), and the concentration of flurbiprofen in the release medium was calculated. The cumulative release % was calculated according to equation (3) [152,154].

$$Cumulative\ release\ = \frac{M_T}{M_\infty} \times 100\% \qquad (3.3)$$

where $M_T$ is the amount of drug released from loaded films ($FB_1$, $FB_2$) at time t, and $M_\infty$ is the amount of drug released from the loaded films at time infinity taken as 45 h.

## 3.3 Results and Discussion

### 3.3.1 Synthesis of poly(vinylcinnamate)-*graft*-poly(2-hydroxyethylmethacrylate) Copolymers

PolyVCi-*graft*-PolyHEMA films were prepared by using PolyVCi (Aldrich) as the substrate after purification as described above. The PolyVCi sample was found to have number average molecular weight of 9.20 x $10^4$ g/mol and weight average molecular weight of 1.74 x $10^5$ by SEC analysis. Grafting of polyHEMA onto polyVCi was carried out by photoinitiation at 350 nm by simultaneous

photocrosslinking of polyVCi polymer backbone. PolyVCi-*graft*-polyHEMA films, both photocrosslinked and EGDMA crosslinked were prepared. The polyVCi-*graft*-polyHEMA samples crosslinked with EGDMA in addition to photocrosslinked polyVCi backbone may also contain some polyHEMA crosslinked with EGDMA. The synthesis route and a schematic representation of the gel system formed are given in Figure 3.1

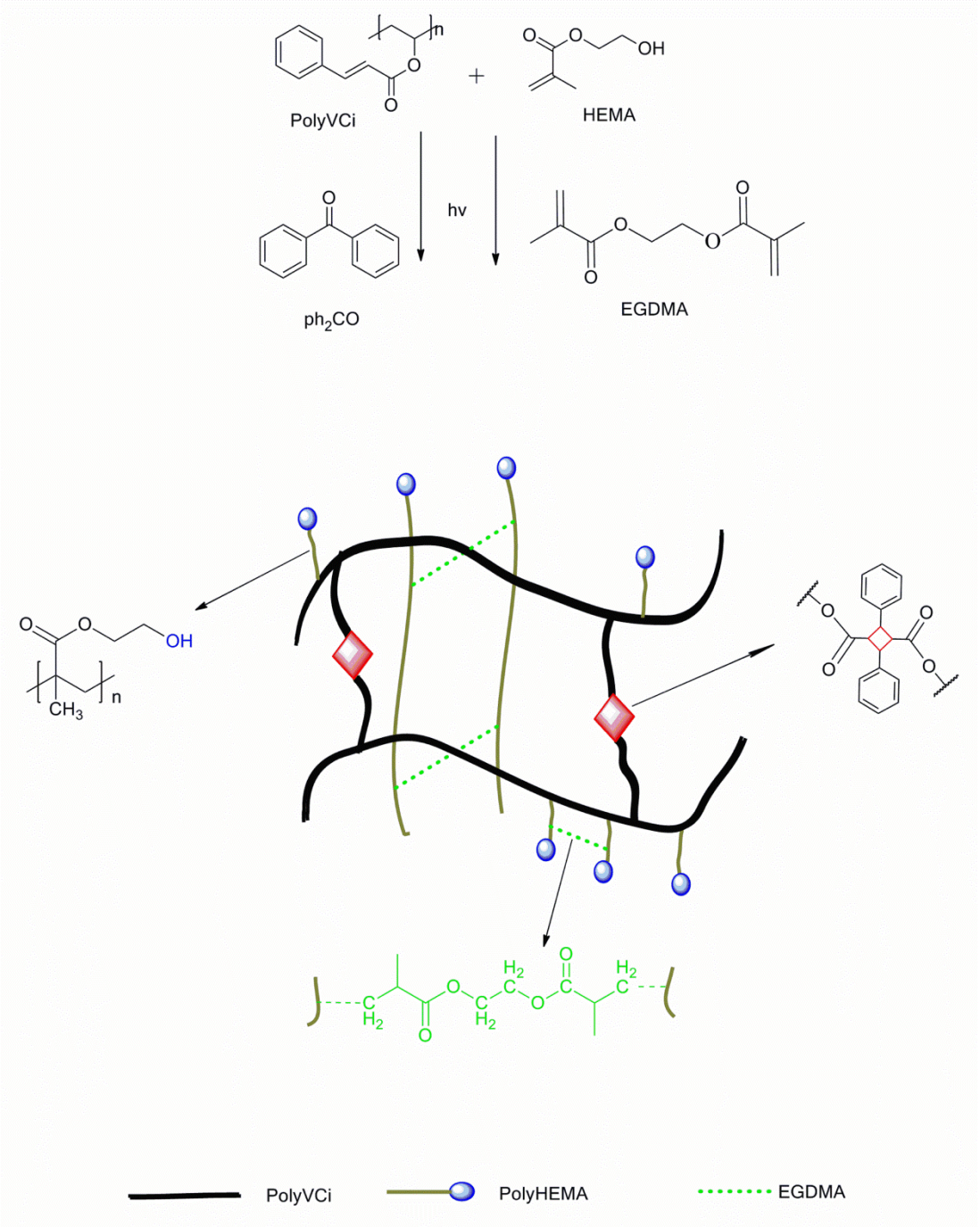


Figure 3.1: Proposed structure of PolyVCi-*graft*-PolyHEMA.

### 3.3.2 Optimization of Grafting Conditions

The grafting parameters were optimized with respect to initiator concentration, monomer and crosslinker concentrations and with respect to time. The reaction conditions and %G values are shown in (Table 3.1). The concentration of polyVCi solution was set as 0.125 mM in all experiments. A blank sample of photocrosslinked polyVCi film (Phot. PolyVCi) was prepared to establish any mass changes during photocrosslinking. No loss or gain in mass was observed after photocrosslinking of polyVCi.

Studying the effect of $Ph_2CO$ concentration on the grafting yield, Figure 3.2(a), revealed that increasing concentration of $Ph_2CO$ from 6.86 mM to 13.7 mM, results in an increase in %G value from 54% to 112%, due to higher number of active sites created in the reaction medium. Further increase in the $Ph_2CO$ concentration to 27.4 mM causes a slight decrease in %G to 90%. This effect can be an indication of radical-radical combination reactions at higher initiator concentrations causing a decrease in initiator efficiency and hence less grafting yield. Since a decreasing trend started above 27.4 mM, no higher concentrations of the photoinitiator were tested. Since 13.7 mM $Ph_2CO$ gave the highest grafting yield value as 112% (sample B), in all other experiments $Ph_2CO$ was used as 13.7 mM.

The effect of EGDMA concentration on the grafting yield is shown in Figure 3.2(b). PolyVCi grafted with polyHEMA, sample M in Table 3.1, gave 40% grafting yield value using 41.2 mM HEMA, and 13.7 mM $Ph_2CO$ after 4 h UV irradiation. Sample B prepared under the same conditions as sample M, but by adding 26.5 mM EGDMA to the system resulted in 112% grafting value providing gravimetric evidence for insertion of EGDMA in the chemical structure. While 26.5 mM (sample

B) and 13.2 mM EGDMA (sample D) result in similar grafting yields as 112% and 110% respectively, increasing EGDMA concentration to 52.9 mM does not result in any further increase in the grafting yield (90%), represented by sample E. Hence, it can be concluded that 41.2 mM HEMA: 13.2 mM EGDMA (3:1) ratio gives optimum crosslinking by EGDMA. Excess EGDMA is wasted unreacted.

It was observed that increasing HEMA concentration resulted in considerable increase in the grafting yield value at 82.5 mM HEMA concentration (sample G), as shown in Figure 3.2(c). While 41.2 mM (sample B) and 20.6 mM (sample F) HEMA gave similar grafting yields with 112 and 111% values, 82.5 mM led to a product with 175% grafting yield. Again, we observe a 3:1 optimum HEMA: EGDMA (82.5 mM: 26.5 mM) ratio. Further increase in HEMA concentration to 123.8 mM (sample Y) gives 76.8% grafting yield indicating that non crosslinked polyHEMA is formed, which is removed by ethanol extraction (Figure 3.2(c)).

Increasing time from 4 to 8 and to 12 h, increases the grafting yield from 112% (sample B) to 119 % (sample H) and to 193% (sample I) respectively, since more polymerization of HEMA is achieved at longer reaction times. But 16 h (sample Z) lead to lower % grafting yield (Figure 3.2(d) probably due to more homopolymer formation. Optimum reaction duration was taken as 4 h since increasing UV irradiation time leads to more crosslinked products with limited swelling capacities as will be discussed below.

The optical pictures of polyVCi, M, B, G, F, and I film samples are shown in Figure 3.3. Homogeneous, transparent films of average film thickness 10 μm have been obtained.

Table 3.1: Grafting Yield (%G) of PolyEMA onto PolyVCi under different conditions.

| Sample | PolyVCi (mM) | HEMA (mM) | $Ph_2CO$ (mM) | EGDMA (mM) | Time (h) | % G |
|---|---|---|---|---|---|---|
| **Phot. PolyVCi** | 0.125 | - | 13.7 | - | 4 | - |
| **M** | 0.125 | 41.2 | 13.7 | - | 4 | 40 |
| **A** | 0.125 | 41.2 | 6.86 | 26.5 | 4 | 54 |
| **B** | 0.125 | 41.2 | 13.7 | 26.5 | 4 | 112 |
| **C** | 0.125 | 41.2 | 27.4 | 26.5 | 4 | 90 |
| **D** | 0.125 | 41.2 | 13.7 | 13.2 | 4 | 110 |
| **E** | 0.125 | 41.2 | 13.7 | 52.9 | 4 | 90 |
| **F** | 0.125 | 20.6 | 13.7 | 26.5 | 4 | 111 |
| **G** | 0.125 | 82.5 | 13.7 | 26.5 | 4 | 175 |
| **Y** | 0.125 | 123.8 | 13.7 | 26.5 | 4 | 76.8 |
| **H** | 0.125 | 41.2 | 13.7 | 26.5 | 8 | 119 |
| **I** | 0.125 | 41.2 | 13.7 | 26.5 | 12 | 193 |
| **Z** | 0.125 | 41.2 | 13.7 | 26.5 | 16 | 89.4 |

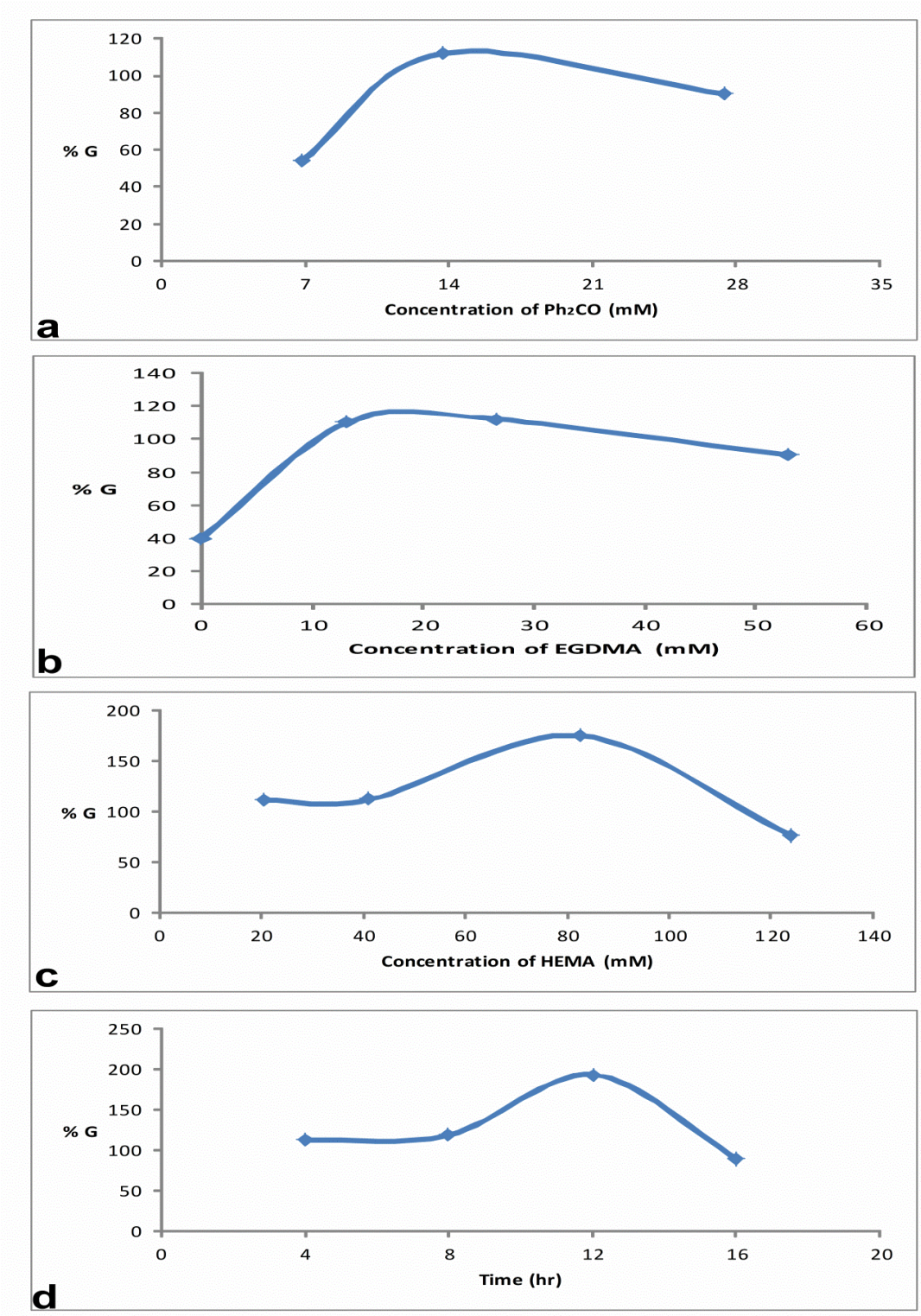


Figure 3.2: Effect of grafting parameters a) $Ph_2CO$, b) EGDMA, c) HEMA, and d) Time, onto the % grafting

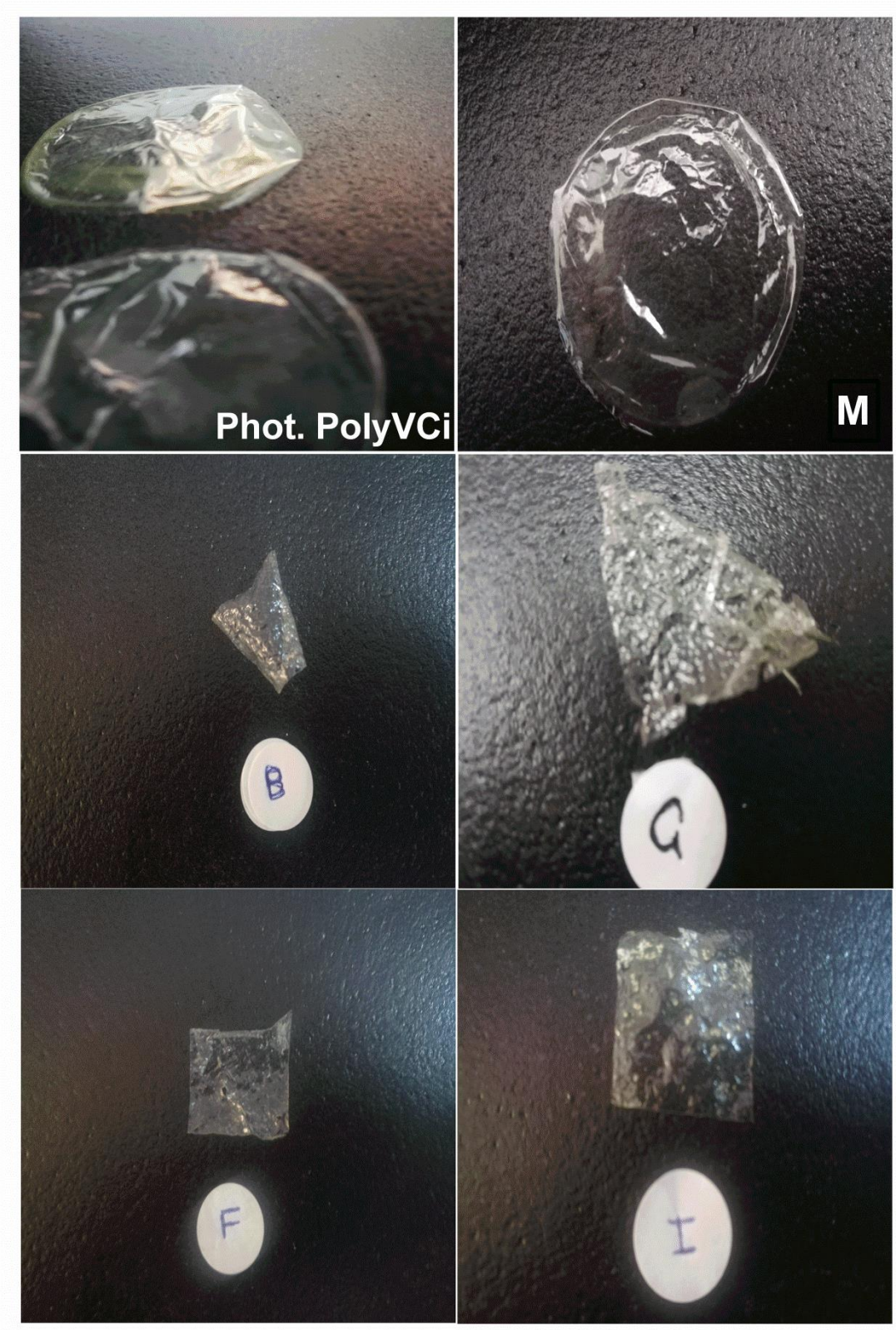


Figure 3.3: Optical photos of Phot. PolyVCi, M, B, G, F, and I films.

### 3.3.3 Swelling Kinetics

Swelling kinetics of the films was followed in distilled water and in ethanol. Figure 3.4(a) shows the swelling behavior of the films in distilled water. All samples reach equilibrium swelling within an hour. Sample M shows the highest equilibrium swelling value (550%) even though the grafting yield of polyHEMA is low with 40%. PolyVCi backbone, which is photocrosslinked gains a hydrophilic nature due to polyHEMA chains grafted. Sample G exhibits an equilibrium swelling value comparable to that of sample M with 500%. Although it is expected that crosslinking with EGDMA should limit the equilibrium swelling capacity to lower values, higher amount of polyHEMA grafted (175%) overcomes this effect. Photocrosslinked PolyVCi-*graft*-polyHEMA samples crosslinked with EGDMA and with increasing %G values (sample B, %G=112, and sample G, %G=175) demonstrate that increasing polyHEMA in the network structure results in higher equilibrium swelling capacities with 151% and 500% respectively. Sample I (%G=193) that has been exposed to UV irradiation for 12 h, bear smaller equilibrium swelling capacity (56%) than the others showing that longer exposure to UV light increases the crosslinking density leading to smaller degree of swelling. It is interesting to note that the equilibrium swelling capacity of photocrosslinked PolyVCi is unexpectedly high and comparable to those of polyHEMA grafted samples (307%) even though it is more hydrophobic than polyHEMA grafted PolyVCi samples. This behavior should be due to the microporous morphology of the PolyVCi sample as revealed by SEM analysis discussed below.

Figure 3.4(b) shows that the maximum % swelling values in ethanol are higher compared to the values in water. This may be attributed to lower polarity of ethanol

than water, which results in more favorable interactions with the hydrophobic polyVCi backbone. PolyVCi film exhibits the highest swelling capacity in ethanol with 907% equilibrium swelling percentage. Grafting polyHEMA and crosslinking with EGDMA result in a decrease in equilibrium swelling capacities in ethanol. Increasing the UV exposure time causes decrease in the equilibrium % swelling values, due to higher crosslinking density, as was observed in water. The equilibrium swelling capacities of the samples studied are as follows: Phot. PolyVCi, M, B, F, G, H, I exhibit values 907%, 565%, 255%, 297%, 197, 176, and 175% respectively.

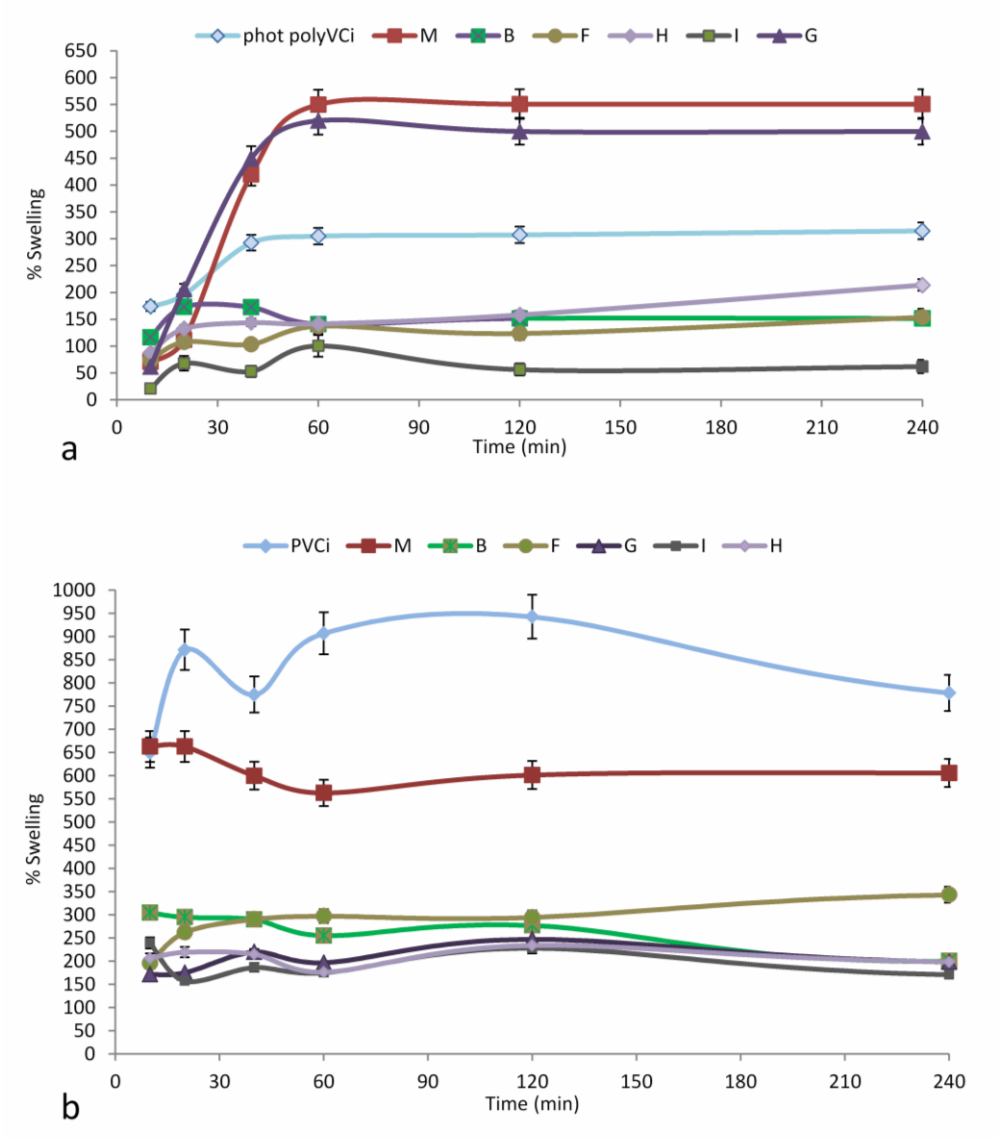


Figure 3.4: Swelling behavior of films in a) water, b) ethanol.

### 3.3.4 FTIR Analysis

Figure 3.5(a) shows the FTIR spectrum of PolyVCi film. An absorption band at 1636 $cm^{-1}$ corresponds to exocyclic C=C stretching of cinnamate moieties [155]. Aromatic C-C and C-H stretchings are observed at 703 and 766 $cm^{-1}$ respectively. C=O stretching of unsaturated ester can be observed at 1710 $cm^{-1}$ [156].

Two characteristic peaks of polyHEMA (Figure 3.5(c)) are at 3400 $cm^{-1}$ and 1720 $cm^{-1}$ corresponding to hydroxyl (OH) and carbonyl (C=O) stretching vibration bands, respectively [157]. Figure 3.5(b) that belongs to a PolyVCi-*graft*-PolyHEMA sample B (G%=112 ) shows a carbonyl band at 1724 $cm^{-1}$, and the absorption band of PolyVCi at 1636 $cm^{-1}$ besides overlap of PolyVCi and polyHEMA bands in the region of 1000-1200 $cm^{-1}$ represented by a broader band for C-O-C stretching at 1151 $cm^{-1}$. Furthermore, the peak intensity of C=C stretching vibration at 1636 $cm^{-1}$ has decreased. All of these characteristics provide evidence for successful of the grafting of PolyHEMA onto PolyVCi.

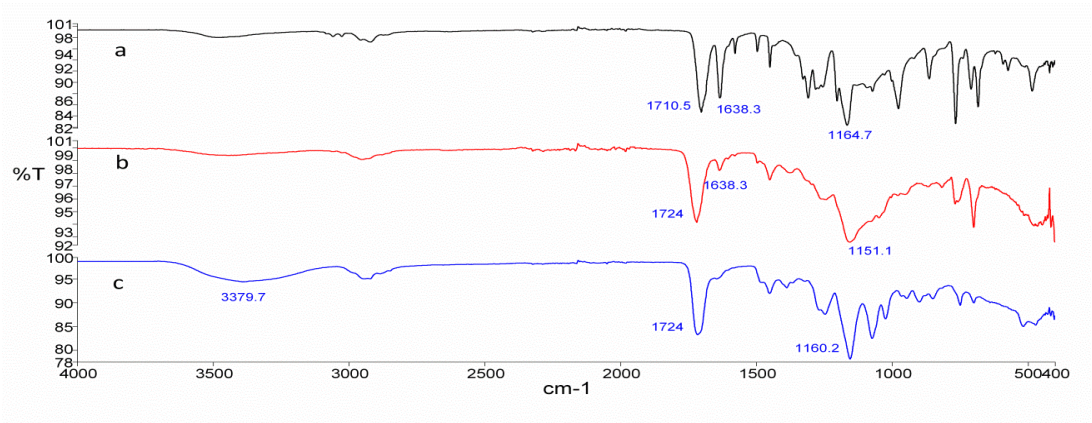


Figure 3.5: FTIR spectrum a) PolyVCi film; b) B film, and c) PolyHEMA

### 3.3.5 Thermal Analysis

Figure 3.6(a) shows the TGA thermogram of polyVCi film. The first decomposition peak is observed at 180°C with around 45% weight loss, while the main mass loss occurs at a temperature around 330 °C. These observations indicate the decomposition of the polymer from the cinnamate groups are mainly occurred at 330 °C, and the detached cinnamates groups are evaporated, resulting in the weight loss [95, 158]. For polyHEMA (Figure 3.6(b)) the decomposition takes place in three stages. In the first stage, around 7% weight loss occurs at 180 °C. The second stage and third stages where the main weight loss is observed are in the range of 300-400 °C. The first peak is at 300 °C and refers to the decomposition of C-O backbone, while the peak at 370°C, can be presumed as the decomposition of the methacrylate component. The general mechanism of the thermal degradation of the polymethacrylates involves the loss of the ester side group to form methacrylic acid followed by cross-linking.

Figure 3.6(c) shows the thermogram of the film M that has been prepared in the absence of the crosslinker EGDMA. It has two decomposition peaks. The first one appears at 120°C with 30% weight loss, which refers to water loss. On the other hand, the main decomposition is peak observed at 330°C. For sample B (Figure 3.6(d)) three decomposition peaks at 120 °C, 330 °C and 400 °C are observed indicating further crosslinking by EGDMA in addition to grafting of polyHEMA onto polyVCi backbone. For both films G and I (Figure 3.6(e-f)) similar thermal stability has been observed as for film B, with an increase in the % weight loss at 400 °C due to more crosslinking.

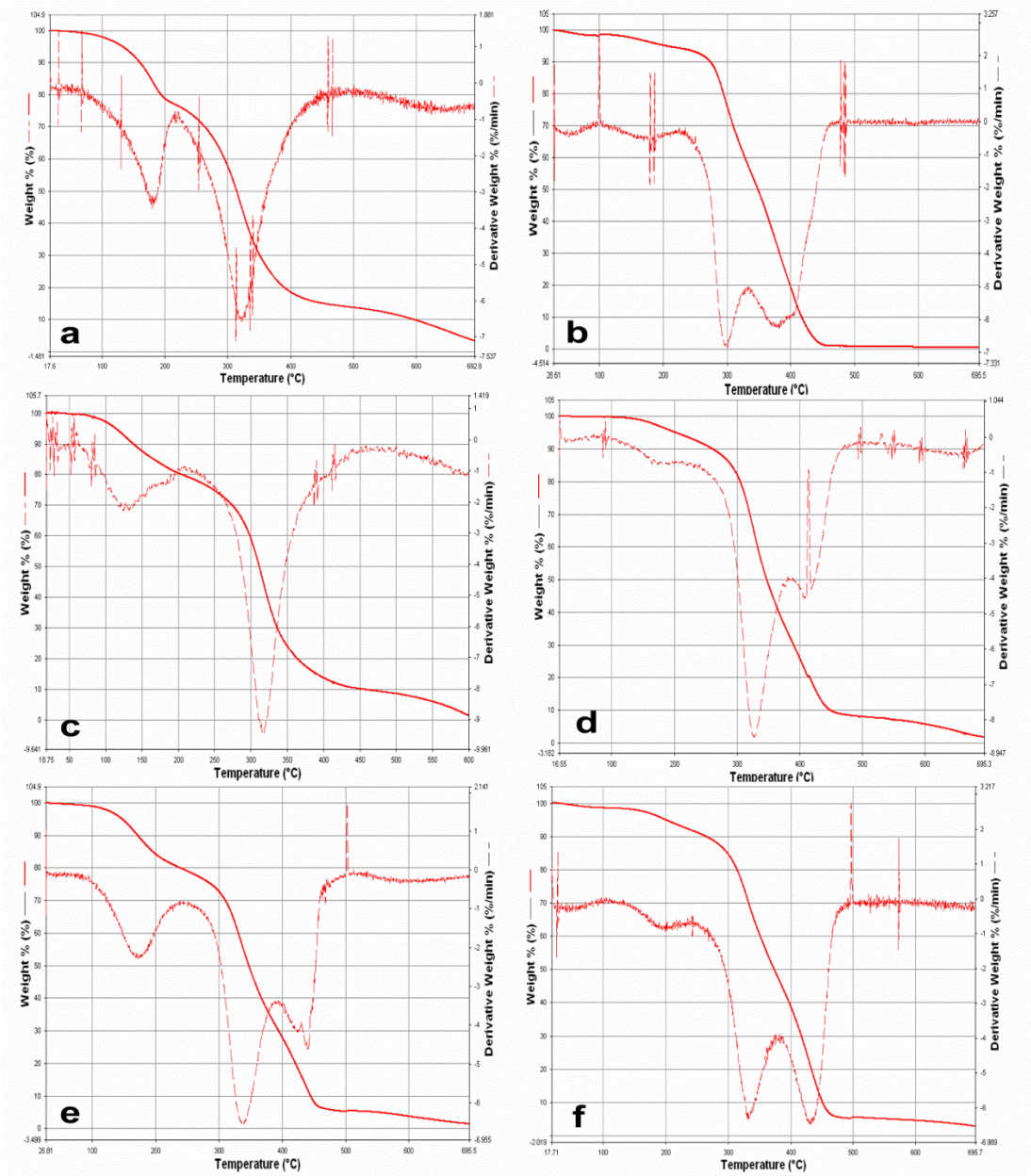


Figure 3.6: TGA thermogram of a) phot.polyVCi film; b) polyHEMA; c) M film; d) B film; e) G film and f) I film.

### 3.3.6 SEM Analysis

Figure 3.7 shows the surface morphology of polyVCi film and polyVCi-*graft*-polyHEMA films. The surface of polyVCi film shown in Figure 3.7(a) exhibits regular fine pores. The pore size as measured from the SEM picture is of the order of 1-2 microns. The formation of pores has been attributed to the evaporation of THF solvent during the photopolymerization. The surfaces of the grafted films exhibit

heterogeneity. The grafted regions are observed as islands in continuous PolyVCi phase in all B, H, and G films (Figure 3.7 (b-d)).

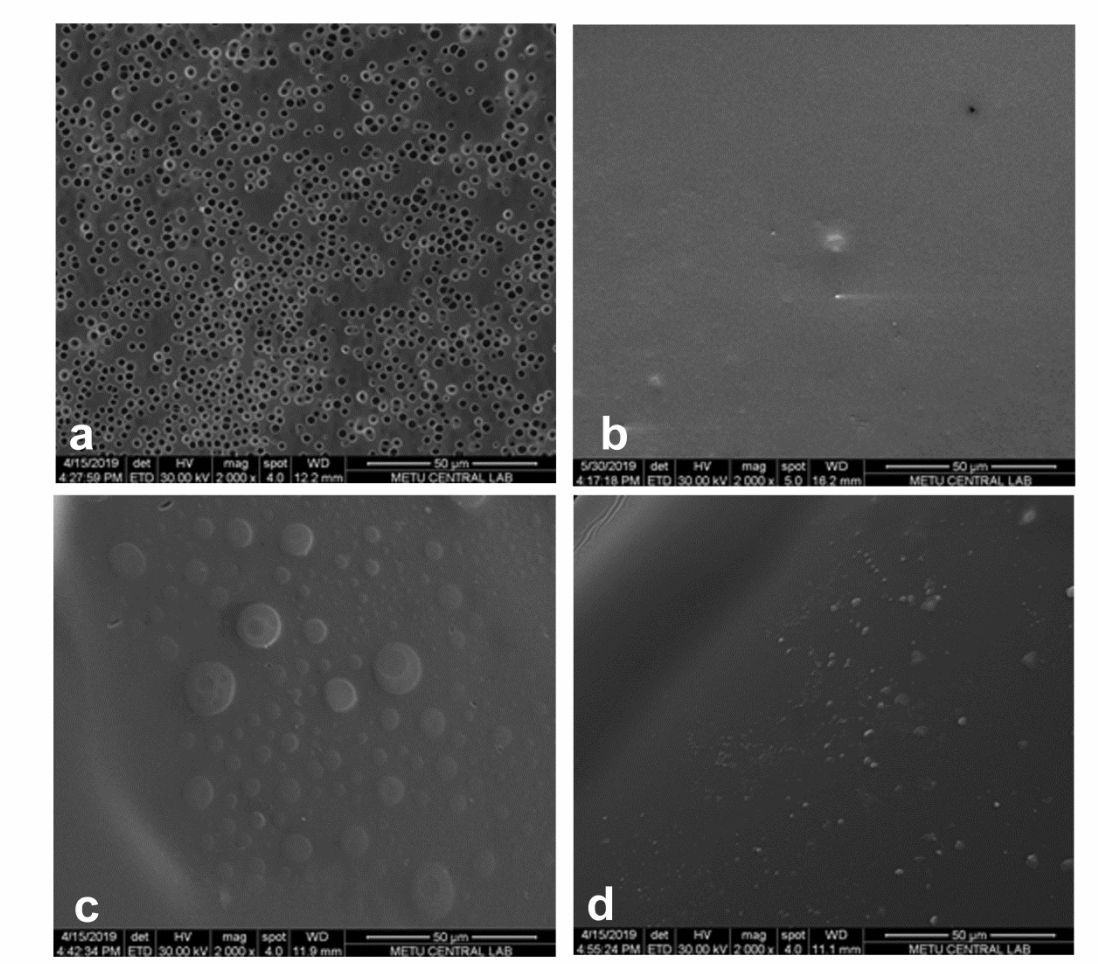


Figure 3.7: SEM micrographs (X2000) of a) Phot. PolyVCi, b) B film, c) H film, and d) G film

### 3.3.7 Contact Angle

Figure 3.8 shows that grafting with polyHEMA modifies the surface of polyVCi film into a more hydrophilic one. The contact angle of polyVCi film decreases from 77.23° to 64.11° after being grafted with polyHEMA (sample B G%= 112) (Figure 3.8(a-b)). Film I (Figure 3.8(c)) shows more hydrophilicity than polyVCi, but less than that of B film with a contact angle of 70°. This may be due to more hydrophobicity (due to the 2+2 photocycloaddition) inserted during

photocrosslinking process of polyVCi backbone as a result of more time of UV irradiation (12 h).

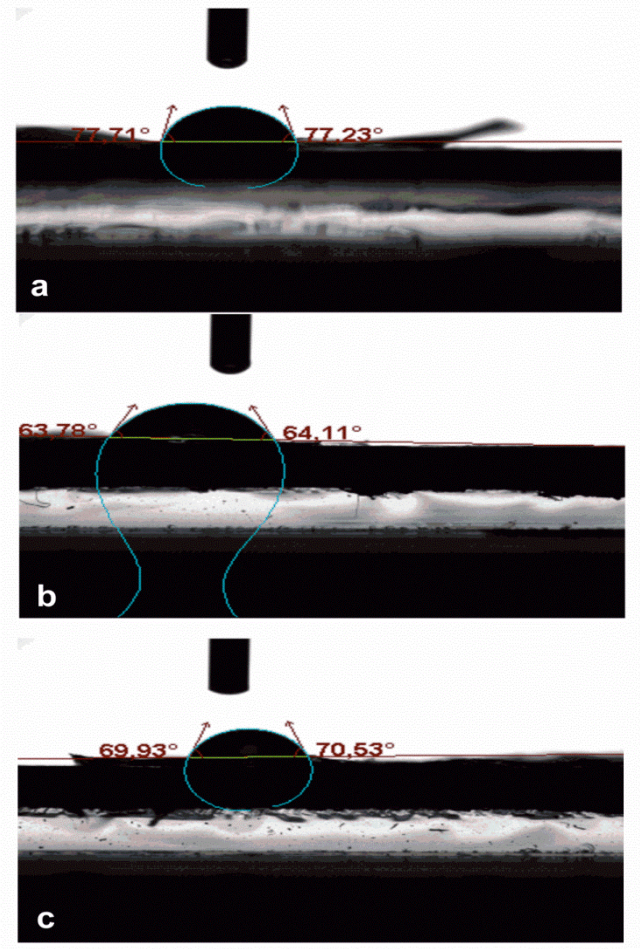


Figure 3.8: Contact angle of a) Phot. PolyVCi, b) B film, and c) I film.

### 3.3.8 Flurbiprofen Loading and Release

Flurbiprofen was loaded into polyVCi-*graft*-polyHEMA matrix during photografting process. Two film samples loaded with flurbiprofen $FB_1$ and $FB_2$ were used in the release study. The amount of flurbiprofen encapsulated into the film was assumed to be the same as the amount of drug released from the loaded films at time infinity ($m_\infty$). These values are 36.5 mg and 43.6 mg $FB_1$and $FB_2$ respectively. Accordingly,

the encapsulation efficiency of $FB_1$ and $FB_2$ has been calculated as 73% and 43.6% respectively.

As can be observed from Figure 3.9(a), the drug release from $FB_1$ shows a fast release within first 5 h with a total of 32% cumulative release, followed by no release for a period of 15 h that can be identified as lag time period. After the lag time period, a second release period begins at 20 h which is completed at 35 h. A similar behavior has been observed for $FB_2$ film, except that the total release at the first release stage, within the first 5 h, is 22% (Figure 3.9(b)). In both cases, it is clear that a time controlled flurbiprofen release system is obtained by loading it into polyVCi-*graft*-polyHEMA films.

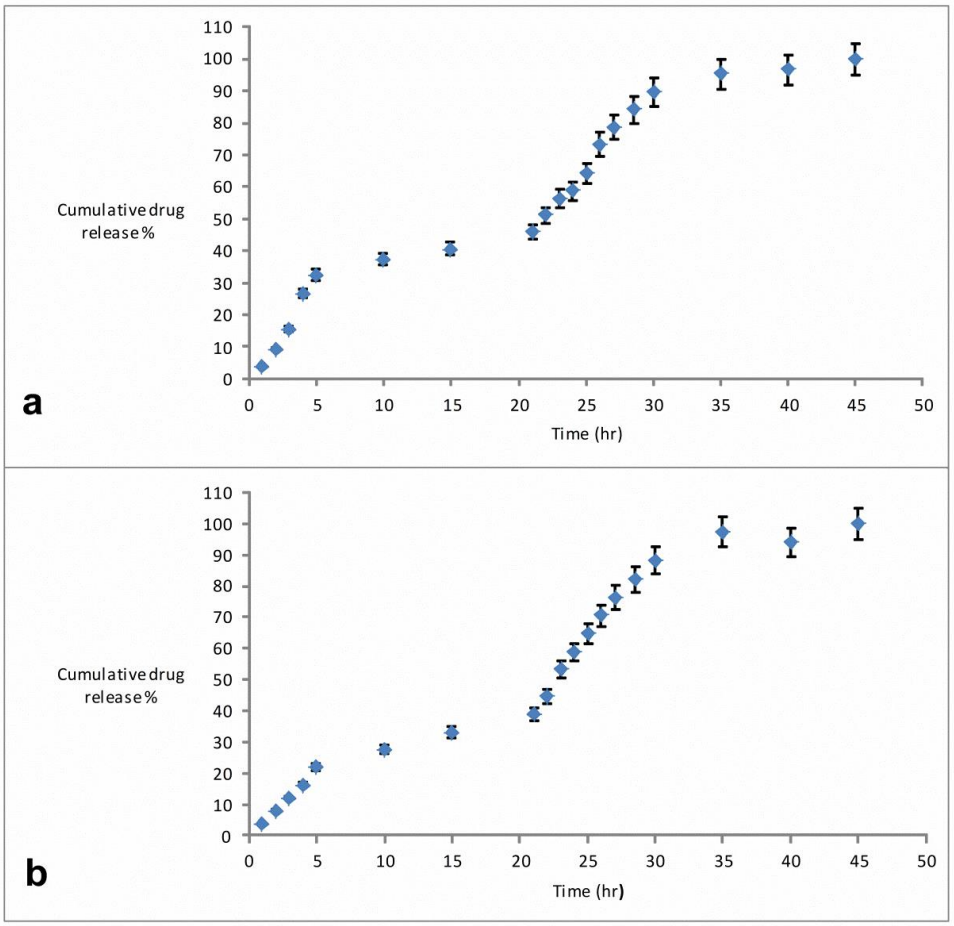


Figure 3.9: Flurobiprofen release profile from a) $FB_1$, b) $FB_2$ films (mean±SD, n=3).

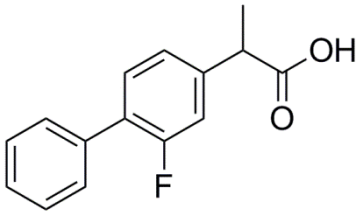

Figure 3.10: Chemical structure of flurbiprofen.

### 3.3.9 Flurbiprofen Release Kinetics

The obtained release results were studied for two periods of release separately. The first one was from (time 0-5) h and denoted by PI, while the second period, PII, was used for the second release (20-30) h. The data were fit into different kinetic equations such as: zero order model (plotting cumulative % drug released versus time), first order (plotting log cumulative % drug remained versus time), Higuchi (plotting cumulative % released versus √time), and Korsmeyer Peppas (plotting log of cumulative % drug released versus log time, where the slope represents the n value). The kinetic model that best fits the dissolution data was estimated by comparing the correlation coefficient ($R^2$) values obtained in various models. In the Peppas (Fickian diffusion) model, mechanisms of drug release are characterized using the release exponent (*n* value). An *n* value of 1 corresponds to zero-order release kinetics (case II transport); $0.5 < n < 1$ indicates an anomalous (non-Fickian) diffusion release model; when $n = 0.5$ indicates Fickian diffusion, and $n > 1$ indicates a super case II transport relaxational release [159]. In flurbiprofen loaded polyVCi-*graft*-polyHEMA films studied in this work, it has been established that these systems obey zero order release kinetics, which is an important advantage. Zero-order release is the ideal in controlled drug release and has an advantage of delivering drugs at a constant rate. Usually, zero order release kinetics is not observed in matrix systems. This behavior has been related to the changes in the

concentration of the drug in the as it is released from the matrix in time. Another factor is the diffusional path length [160].

Table 3.2 shows that the most probable release mechanism for the flurbiprofen loaded films ($FB_1$, and $FB_2$) in both periods (PI, and PII), are zero order since a higher "$R^2$" values were obtained. The zero-order rate describes systems where drug release rate is independent of its concentration. This mechanism is confirmed by its Ritger-Peppas "n" value (1.00 to 1.41), which indicates super case II release mechanism.

Two factors can be considered to explain the lag time behavior. These are the drug-matrix interaction nature and the morphology of the polyVCi-*graft*-polyHEMA matrix. Carbonyl functionalities available both on polyHEMA and polyVCi interact with flurbiprofen molecule via dipole-dipole interactions. Secondary interactions such as dispersion forces and dipole-dipole interactions are also available between benzene rings that exist in both polyVCi and flurbiprofen. Flurbiprofen, shown in Figure 3.10, and polyHEMA component of the matrix may interact via hydrogen bonding interaction between the -OH groups available on both molecules or via strong dipole-dipole interaction between the fluorine atom and the hydroxyl group. So, it may be concluded that there are stronger favorable interactions between polyHEMA component of the copolymer than between polyVCi and flurbiprofen. Furthermore, polyVCi-*graft*-polyHEMA films show two phase morphology as can be observed in the SEM pictures given in Figure 3.7. The islands embedded in the continuous polyVCi matrix have been attributed to the polyHEMA grafted regions. Two types of crosslinked areas are available in the matrix; the photocrosslinked and EGDMA crosslinked areas. Flurbiprofen is distributed randomly in the polyVCi-

*graft*-polyHEMA matrix during the photo encapsulation process. Hence, diffusion rate of the flurbiprofen molecule through these two different regions with different chemical nature and crosslinking density should be different resulting in the two-stage release behavior.

Table 3.2: Drug release kinetic data.

| | **$FB_1$** | | **$FB_2$** | |
|---|---|---|---|---|
| | **Period I (0-5 h)** | **Period II (20-30 h)** | **Period I (0-5 h)** | **Period II (20-30 h)** |
| **Zero order** | $R^2$=0.8867 | $R^2$=0.9456 | $R^2$=1 | $R^2$=1 |
| **First order** | $R^2$=0.8568 | $R^2$=0.8118 | $R^2$=0.9997 | $R^2$=0.9994 |
| **Higuchi** | $R^2$=0.8087 | $R^2$=0.9356 | $R^2$=0.9129 | $R^2$=0.9993 |
| **Korsmeyer Peppas** | $R^2$=0.7508 | $R^2$=1 | $R^2$=0.9089 | $R^2$=1 |
| | n=1.42 | n=1.12 | n=1.28 | n=1.0 |

## 3.4 Conclusions

Photoinitiated grafting of polyHEMA onto polyVCi backbone was successfully achieved and optimized. The polyVCi-*graft*-polyHEMA films are homogenous at the macroscopic level, and they are transparent film material. Hydrophilicity of the polyVCi-graft-polyHEMA films increases with increasing polyHEMA grafting as demonstrated by contact angle measurements and equilibrium swelling capacities in water and in ethanol. The films are thermally stable up to around 300 °C, as revealed by TGA.

Successful photo-encapsulation of flurbiprofen into the film matrixes was achieved. The PolyVCi-*graft*-PolyHEMA films proved to be suitable release matrixes for flurbiprofen demonstrating pulsatile release behavior. As a result polyVCi-*graft*-

PolyHEMA films are promising devices for a time-pulsatile controlled release of flurbiprofen.

# Chapter 4

# CONCLUSION

Photoinitiated copolymerization of PEGM and DEAEM monomers can be achieved at low and high conversions. Crosslinked polymers are obtained without using any chemical cross linker during polymerization in the presence of $CCl_4$ solvent. There is a solvent effect operation on copolymer composition. The crosslinked polymers of PEGM-*co*-PDEAEM act as superabsorbents in aqueous solution. Increasing DEAEM fraction results in higher equilibrium swelling capacities. Equilibrium swelling capacities are higher in acidic solution due the protonation of DEAEM fraction of the copolymer. Monomer reactivity ratios at low conversions are $r_1$(PEGM) = 0.90, $r_2$(DEAEM) = 0.14. At high conversions the monomer reactivity ratios are 1.01, 0.4, respectively.The MO adsorption onto the copolymers was highly efficient, (% R reaches 98%), and ($q_e$=212.7 mg $g^{-1}$), favorable ($0<R_L<1$) and spontaneously occurred ($\Delta G°<0$). In addition, these poly(PEGM-*co*-DEAEM) hydrogels would exhibit less environmental negative effects due to their environment friendly nature.

Photoinitiated grafting of polyHEMA onto polyVCi backbone can be achieved in THF solvent. The polyVCi-*graft*-polyHEMA films are homogenous at the macroscopic level, and they are transparent film material. Hydrophilicity of the polyVCi-graft-polyHEMA films increases with increasing polyHEMA grafting as demonstrated by contact angle measurements and equilibrium swelling capacities in

water and in ethanol. The films are thermally stable up to around 300 °C, as revealed by TGA. SEM pictures reveal two-phase morphology.

Successful photo-encapsulation of flurbiprofen into the film matrixes can be achieved. The polyVCi-*graft*-polyHEMA films are suitable release matrixes for flurbiprofen demonstrating pulsatile release behavior. As a result polyVCi-*graft*-polyHEMA films are promising devices for a time-pulsatile controlled release of flurbiprofen.

# REFERENCES


[1] Y. Luo, X. Wei, and P. Huang, "3D bioprinting of hydrogel-based biomimetic microenvironments," *J. Biomed. Mater. Res. Part B Appl. Biomater.*, vol. 107, no. 5, pp. 1695–1705, 2019.

[2] S. P. Miguel, A. F. Moreira, and I. J. Correia, "Chitosan based-asymmetric membranes for wound healing: A review," *Int. J. Biol. Macromol.*, 2019.

[3] M. El-Sayed, M. Sorour, N. Abd El Moneem, H. Talaat, H. Shalaan, and S. El-Marsafy, "Synthesis and properties of natural polymers-grafted-acrylamide," *World Appl Sci J*, vol. 13, no. 2, pp. 360–368, 2011.

[4] O. Wichterle and D. Lim, "Hydrophilic gels for biological use," *Nature*, vol. 185, no. 4706, p. 117, 1960.

[5] M. M. Elsayed, "Hydrogel Preparation Technologies: Relevance Kinetics, Thermodynamics and Scaling up Aspects," *J. Polym. Environ.*, vol. 27, no. 4, pp. 871–891, 2019.

[6] M. P. Lutolf and J. A. Hubbell, "Synthetic biomaterials as instructive extracellular microenvironments for morphogenesis in tissue engineering," *Nat. Biotechnol.*, vol. 23, no. 1, p. 47, 2005.

[7] M. W. Tibbitt and K. S. Anseth, "Hydrogels as extracellular matrix mimics for 3D cell culture," *Biotechnol. Bioeng.*, vol. 103, no. 4, pp. 655–663, 2009.

[8] J. Kopeček, “Hydrogel biomaterials: a smart future?,” *Biomaterials*, vol. 28, no. 34, pp. 5185–5192, 2007.

[9] B. Chen and X. Hu, “An injectable composite gelatin hydrogel with pH response properties,” *J. Nanomater.*, vol. 2017, 2017.

[10] L. S. M. Teixeira, J. Feijen, C. A. van Blitterswijk, P. J. Dijkstra, and M. Karperien, “Enzyme-catalyzed crosslinkable hydrogels: emerging strategies for tissue engineering,” *Biomaterials*, vol. 33, no. 5, pp. 1281–1290, 2012.

[11] S. Garg and A. Garg, “Hydrogel: Classification, Properties, Preparation and Technical Features,” *Asian J. Biomater. Res.*, vol. 2, no. 6, pp. 163–170, 2016.

[12] M. F. Passos *et al.*, “PHEMA Hydrogels Obtained by Infrared Radiation for Cartilage Tissue Engineering,” *Int. J. Chem. Eng.*, vol. 2019, pp. 1–9, 2019.

[13] S. Benamer, M. Mahlous, A. Boukrif, B. Mansouri, and S. L. Youcef, “Synthesis and characterisation of hydrogels based on poly (vinyl pyrrolidone),” *Nucl. Instruments Methods Phys. Res. Sect. B Beam Interact. with Mater. Atoms*, vol. 248, no. 2, pp. 284–290, 2006.

[14] L. Christensen, V. Breiting, J. Vuust, and E. Hogdall, “Adverse reactions following injection with a permanent facial filler polyacrylamide hydrogel (Aquamid): causes and treatment,” *Eur. J. Plast. Surg.*, vol. 28, no. 7, pp. 464–471, 2006.

[15] M. J. Zohuriaan and K. Kabiri, “Superabsorbent Polymer Materials: A Review,” *Iran. Polym. J.*, vol. 17, no. 6, pp. 451–477, 2008.

[16] C. Gong *et al.*, “Synthesis and characterization of PEG-PCL-PEG thermosensitive hydrogel,” *Int. J. Pharm.*, vol. 365, no. 1–2, pp. 89–99, 2009.

[17] B. Kim and N. A. Peppas, “Poly (ethylene glycol)-containing hydrogels for oral protein delivery applications,” *Biomed. Microdevices*, vol. 5, no. 4, pp. 333–341, 2003.

[18] Y. Wang, Y. Li, X. Yu, Q. Long, and T. Zhang, “Synthesis of a photocurable acrylated poly (ethylene glycol)-co-poly (xylitol sebacate) copolymers hydrogel 3D printing ink for tissue engineering,” *RSC Adv.*, vol. 9, no. 32, pp. 18394–18405, 2019.

[19] Y. S. Lipatov, “Polymer blends and interpenetrating polymer networks at the interface with solids,” *Prog. Polym. Sci.*, vol. 27, no. 9, pp. 1721–1801, 2002.

[20] F. Ardeshiri, A. Akbari, M. Peyravi, and M. Jahanshahi, “PDADMAC/PAA semi-IPN hydrogel-coated PVDF membrane for robust anti-wetting in membrane distillation,” *J. Ind. Eng. Chem.*, vol. 74, pp. 14–25, 2019.

[21] L. Li, R. Wang, X. Xing, W. Qu, S. Chen, and Y. Zhang, “Preparation of porous semi-IPN temperature-sensitive hydrogel-supported nZVI and its application in the reduction of nitrophenol,” *J. Environ. Sci.*, vol. 82, pp. 93–102, 2019.

[22] D. Quintanar-Guerrero, B. N. Zorraqu\'\in-Cornejo, A. Ganem-Rondero, E. Piñón-Segundo, M. G. Nava-Arzaluz, and J. M. Cornejo-Bravo, "Controlled release of model substances from pH-sensitive hydrogels," *J. Mex. Chem. Soc.*, vol. 52, no. 4, pp. 272–278, 2008.

[23] M. A. Saleem, S. K. Azharuddin, S. Ali, and C. C. Patil, "Studies on different chitosan polyelectrolyte complex hydrogels for modified release of diltiazem hydrochloride," *Int J Pharm Pharm Sci*, vol. 2, no. 4, pp. 6467–6479, 2010.

[24] J. J. K. Derwent and W. F. Mieler, "Thermoresponsive hydrogels as a new ocular drug delivery platform to the posterior segment of the eye," *Trans. Am. Ophthalmol. Soc.*, vol. 106, p. 206, 2008.

[25] S. Gunasekaran, T. Wang, and C. Chai, "Swelling of pH-sensitive chitosan--poly (vinyl alcohol) hydrogels," *J. Appl. Polym. Sci.*, vol. 102, no. 5, pp. 4665–4671, 2006.

[26] J. Bünsow and D. Johannsmann, "Electrochemically produced responsive hydrogel films: Influence of added salt on thickness and morphology," *J. Colloid Interface Sci.*, vol. 326, no. 1, pp. 61–65, 2008.

[27] A. A. Aimetti, A. J. Machen, and K. S. Anseth, "Poly (ethylene glycol) hydrogels formed by thiol-ene photopolymerization for enzyme-responsive protein delivery," *Biomaterials*, vol. 30, no. 30, pp. 6048–6054, 2009.

[28] L. G. J. De Leede, A. G. De Boer, E. Pörtzgen, J. Feijen, and D. D. Breimer,

"Rate-controlled rectal drug delivery in man with a hydrogel preparation," *J. Control. release*, vol. 4, no. 1, pp. 17–24, 1986.

[29] R. Masteikova, Z. Chalupova, and Z. Sklubalova, "Stimuli-sensitive hydrogels in controlled and sustained drug delivery," *Medicina (B. Aires).*, vol. 39, no. 2, pp. 19–24, 2003.

[30] T. Miyazaki, Y. Takeda, S. Akane, T. Itou, A. Hoshiko, and K. En, "Role of boric acid for a poly (vinyl alcohol) film as a cross-linking agent: Melting behaviors of the films with boric acid," *Polymer (Guildf).*, vol. 51, no. 23, pp. 5539–5549, 2010.

[31] E. A. Kamoun, E.-R. S. Kenawy, and X. Chen, "A review on polymeric hydrogel membranes for wound dressing applications: PVA-based hydrogel dressings," *J. Adv. Res.*, vol. 8, no. 3, pp. 217–233, 2017.

[32] E. S. Abdel-Halim and S. S. Al-Deyab, "Hydrogel from crosslinked polyacrylamide/guar gum graft copolymer for sorption of hexavalent chromium ion," *Carbohydr. Polym.*, vol. 86, no. 3, pp. 1306–1312, 2011.

[33] K. S. Soppirnath and T. M. Aminabhavi, "Water transport and drug release study from cross-linked polyacrylamide grafted guar gum hydrogel microspheres for the controlled release application," *Eur. J. Pharm. Biopharm.*, vol. 53, no. 1, pp. 87–98, 2002.

[34] T. Hongbo, L. Yanping, S. Min, and W. Xiguang, "Preparation and property

of crosslinking guar gum," *Polym. J.*, vol. 44, no. 3, p. 211, 2012.

[35] R. López-Cebral, P. Paolicelli, V. Romero-Caamaño, B. Seijo, M. A. Casadei, and A. Sanchez, "Spermidine-cross-linked hydrogels as novel potential platforms for pharmaceutical applications," *J. Pharm. Sci.*, vol. 102, no. 8, pp. 2632–2643, 2013.

[36] X. Xu, Y. Weng, L. Xu, and H. Chen, "Sustained release of Avastin®from polysaccharides cross-linked hydrogels for ocular drug delivery," *Int. J. Biol. Macromol.*, vol. 60, pp. 272–276, 2013.

[37] N. S. Raut, P. R. Deshmukh, M. J. Umekar, and N. R. Kotagale, "Zinc cross-linked hydroxamated alginates for pulsed drug release," *Int. J. Pharm. Investig.*, vol. 3, no. 4, p. 194, 2013.

[38] M. O. Taha, W. Nasser, A. Ardakani, and H. S. AlKhatib, "Sodium lauryl sulfate impedes drug release from zinc-crosslinked alginate beads: Switching from enteric coating release into biphasic profiles," *Int. J. Pharm.*, vol. 350, no. 1–2, pp. 291–300, 2008.

[39] T. Hussain, M. Ansari, N. M. Ranjha, I. U. Khan, and Y. Shahzad, "Chemically cross-linked poly (acrylic-co-vinylsulfonic) acid hydrogel for the delivery of isosorbide mononitrate," *Sci. World J.*, vol. 2013, 2013.

[40] M. M. El-Sayed, G. A. Al Bazedi, and M. A. Abdel-Fatah, "Development of a Novel Hydrogel Adsorbent for Removal of Reactive Dyes from Textile

Effluents," *Res. J. Pharm. Biol. Chem. Sci.*, vol. 8, no. 3, pp. 945–955, 2017.

[41] F. H. A. Rodrigues *et al.*, "Superabsorbent hydrogel composites with a focus on hydrogels containing nanofibers or nanowhiskers of cellulose and chitin," *J. Appl. Polym. Sci.*, vol. 131, no. 2, 2014.

[42] E. M. Ahmed, F. S. Aggor, A. M. Awad, and A. T. El-Aref, "An innovative method for preparation of nanometal hydroxide superabsorbent hydrogel," *Carbohydr. Polym.*, vol. 91, no. 2, pp. 693–698, 2013.

[43] K. Kabiri, H. Omidian, M. J. Zohuriaan-Mehr, and S. Doroudiani, "Superabsorbent hydrogel composites and nanocomposites: a review," *Polym. Compos.*, vol. 32, no. 2, pp. 277–289, 2011.

[44] J. Kuang, K. Y. Yuk, and K. M. Huh, "Polysaccharide-based superporous hydrogels with fast swelling and superabsorbent properties," *Carbohydr. Polym.*, vol. 83, no. 1, pp. 284–290, 2011.

[45] T. Yoshimura, K. Matsuo, and R. Fujioka, "Novel biodegradable superabsorbent hydrogels derived from cotton cellulose and succinic anhydride: Synthesis and characterization," *J. Appl. Polym. Sci.*, vol. 99, no. 6, pp. 3251–3256, 2006.

[46] T. Yoshimura, I. Uchikoshi, Y. Yoshiura, and R. Fujioka, "Synthesis and characterization of novel biodegradable superabsorbent hydrogels based on chitin and succinic anhydride," *Carbohydr. Polym.*, vol. 61, no. 3, pp. 322–

326, 2005.

[47] T. Yoshimura, R. Yoshimura, C. Seki, and R. Fujioka, “Synthesis and characterization of biodegradable hydrogels based on starch and succinic anhydride,” *Carbohydr. Polym.*, vol. 64, no. 2, pp. 345–349, 2006.

[48] A. T. Paulino, M. R. Guilherme, A. V Reis, G. M. Campese, E. C. Muniz, and J. Nozaki, “Removal of methylene blue dye from an aqueous media using superabsorbent hydrogel supported on modified polysaccharide,” *J. Colloid Interface Sci.*, vol. 301, no. 1, pp. 55–62, 2006.

[49] G. B. Marandi, K. Esfandiari, F. Biranvand, M. Babapour, S. Sadeh, and G. R. Mahdavinia, “pH sensitivity and swelling behavior of partially hydrolyzed formaldehyde-crosslinked poly (acrylamide) superabsorbent hydrogels,” *J. Appl. Polym. Sci.*, vol. 109, no. 2, pp. 1083–1092, 2008.

[50] M. Sadeghi, N. Ghasemi, and M. Kazemi, “Synthesis and swelling behavior of carrageenans-graft-poly (sodium acrylate)/kaolin superabsorbent hydrogel composites,” *World Appl. Sci. J.*, vol. 16, no. 1, pp. 113–118, 2012.

[51] E. Su, M. Yurtsever, and O. Okay, “A Self-Healing and Highly Stretchable Polyelectrolyte Hydrogel via Cooperative Hydrogen Bonding as a Superabsorbent Polymer,” *Macromolecules*, 2019.

[52] M. Alokour and E. Yilmaz, “Photoinitiated synthesis of poly(poly(ethylene glycol) methacrylate- *co* - diethyl amino ethyl methacrylate) superabsorbent

hydrogels for dye adsorption," *J. Appl. Polym. Sci.*, vol. 136, no. 26, p. 47707, Jul. 2019.

[53] A. Li, J. Zhang, and A. Wang, "Utilization of starch and clay for the preparation of superabsorbent composite," *Bioresour. Technol.*, vol. 98, no. 2, pp. 327–332, 2007.

[54] K. Kabiri, H. Omidian, S. A. Hashemi, and M. J. Zohuriaan-Mehr, "Synthesis of fast-swelling superabsorbent hydrogels: effect of crosslinker type and concentration on porosity and absorption rate," *Eur. Polym. J.*, vol. 39, no. 7, pp. 1341–1348, 2003.

[55] J. Chen and K. Park, "Synthesis and characterization of superporous hydrogel composites," *J. Control. Release*, vol. 65, no. 1–2, pp. 73–82, 2000.

[56] F. A. Dorkoosh, J. C. Verhoef, G. Borchard, M. Rafiee-Tehrani, and H. E. Junginger, "Development and characterization of a novel peroral peptide drug delivery system," *J. Control. release*, vol. 71, no. 3, pp. 307–318, 2001.

[57] P. Nesvadba, *Radical Polymerization in Industry*. 2012.

[58] C. J. Hawker, "10 Nitroxide-Mediated Living Radical Polymerizations," *Handb. Radic. Polym.*, p. 463, 2002.

[59] R. O. Ebewele, *Polymer science and technology*. CRC press, 2000.

[60] K. Matyjaszewski, M. J. Ziegler, S. V Arehart, D. Greszta, and T. Pakula, "Gradient copolymers by atom transfer radical copolymerization," *J. Phys. Org. Chem.*, vol. 13, no. 12, pp. 775–786, 2000.

[61] A. Bhattacharya and B. N. Misra, "Grafting: A versatile means to modify polymers: Techniques, factors and applications," *Prog. Polym. Sci.*, vol. 29, no. 8, pp. 767–814, 2004.

[62] I. Kaur, R. Barsola, A. Gupta, and B. N. Misra, "Graft copolymerization of acrylonitrile and methacrylonitrile onto gelatin by mutual irradiation method," *J. Appl. Polym. Sci.*, vol. 54, no. 8, pp. 1131–1139, 1994.

[63] T. Yamaki *et al.*, "Radiation grafting of styrene into crosslinked PTEE films and subsequent sulfonation for fuel cell applications," *Radiat. Phys. Chem.*, vol. 67, no. 3–4, pp. 403–407, 2003.

[64] G. Odian, *Principles of polymerization*. John Wiley & Sons, 2004.

[65] H. T. Ban *et al.*, "Methylaluminoxane as a new catalyst for alternating copolymerization between 1, 3-butadiene and methyl methacrylate," *Macromolecules*, vol. 33, no. 19, pp. 6907–6909, 2000.

[66] W. Schnabel, *Polymers and light: fundamentals and technical applications*. John Wiley & Sons, 2007.

[67] A. C. Borges, A. Jayakrishnan, P.-E. Bourban, C. J. G. Plummer, D. P.

Pioletti, and J.-A. E. Månson, “Synthesis and photopolymerization of tween 20 methacrylate/N-vinyl-2-pyrrolidone blends,” *Mater. Sci. Eng. C*, vol. 32, no. 8, pp. 2235–2241, 2012.

[68] P. Glöckner, *Radiation curing*. Vincentz Network GmbH & Co KG, 2009.

[69] L. S. Gonçalves, R. R. Moraes, F. A. Ogliari, L. Boaro, R. R. Braga, and S. Consani, “Improved polymerization efficiency of methacrylate-based cements containing an iodonium salt,” *Dent. Mater.*, vol. 29, no. 12, pp. 1251–1255, 2013.

[70] C. Esposito Corcione, A. Greco, and A. Maffezzoli, “Photopolymerization kinetics of an epoxy-based resin for stereolithography,” *J. Appl. Polym. Sci.*, vol. 92, no. 6, pp. 3484–3491, 2004.

[71] J. V Crivello and E. Reichmanis, “Photopolymer materials and processes for advanced technologies,” *Chem. Mater.*, vol. 26, no. 1, pp. 533–548, 2013.

[72] F. Liu, Y. Zhang, and G. Zhou, “Grafting pH-sensitive poly [2-(diethylamino) ethyl methacrylate] modification of vesicular silica with activator regenerated by electron transfer atom transfer radical polymerisation for controlled drug release,” *Micro Nano Lett.*, vol. 10, no. 4, pp. 187–191, 2015.

[73] P. de Wetering, J.-Y. Cherng, H. Talsma, D. J. A. Crommelin, and W. E. Hennink, “2-(Dimethylamino) ethyl methacrylate based (co) polymers as gene transfer agents,” *J. Control. release*, vol. 53, no. 1–3, pp. 145–153, 1998.

[74] Y. Sun, B. Lin, Q. Wang, X. Zhang, and R. Zhuo, "Preparation of Poly (2-aminoethyl methacrylate-co-2-(diethylamino) ethyl methacrylate) by Atom Transfer Radical Polymerization for Gene Delivery," *Acta Polym. Sin.*, no. 1, pp. 113–119, 2015.

[75] B. C. Anderson and S. K. Mallapragada, "Synthesis and characterization of injectable, water-soluble copolymers of tertiary amine methacrylates and poly (ethylene glycol) containing methacrylates," *Biomaterials*, vol. 23, no. 22, pp. 4345–4352, 2002.

[76] A. R. Shirin-Abadi, P. G. Jessop, and M. F. Cunningham, "In Situ Use of Aqueous RAFT Prepared Poly (2-(diethylamino) ethyl methacrylate) as a Stabilizer for Preparation of CO2 Switchable Latexes," *Macromol. React. Eng.*, vol. 11, no. 1, p. 1600035, 2017.

[77] X. Xu, C. Liu, and J. Huang, "Synthesis, characterization, and stimuli-sensitive properties of triblock copolymer poly (ethylene oxide)-b-poly (2-(diethylamino) ethyl methacrylate)-b-poly (N-isopropylacrylamide)," *J. Appl. Polym. Sci.*, vol. 108, no. 4, pp. 2180–2188, 2008.

[78] P. D. Topham *et al.*, "Controlled growth of poly (2-(diethylamino) ethyl methacrylate) brushes via atom transfer radical polymerisation on planar silicon surfaces," *Polym. Int.*, vol. 55, no. 7, pp. 808–815, 2006.

[79] E. Çakal and S. Cavus, "Novel poly (N-vinylcaprolactam-co-2-(diethylamino) ethyl methacrylate) gels: characterization and detailed Investigation on their

stimuli-sensitive behaviors and network structure," *Ind. Eng. Chem. Res.*, vol. 49, no. 22, pp. 11741–11751, 2010.

[80] Á. Szabó, A. Wacha, R. Thomann, G. Szarka, A. Bóta, and B. Iván, "Synthesis of poly(methyl methacrylate)-poly(poly(ethylene glycol) methacrylate)-polyisobutylene ABCBA pentablock copolymers by combining quasiliving carbocationic and atom transfer radical polymerizations and characterization thereof," *J. Macromol. Sci. Part A Pure Appl. Chem.*, vol. 52, no. 4, pp. 252–259, 2015.

[81] N. M. Tsegay, X.-Y. Du, S.-S. Liu, C.-F. Wang, and S. Chen, "Frontal polymerization for smart intrinsic self-healing hydrogels and its integration with microfluidics," *J. Polym. Sci. Part A Polym. Chem.*, vol. 56, no. 13, pp. 1412–1423, 2018.

[82] I. Yati, K. Karadag, and H. B. Sonmez, "Amphiphilic poly (ethylene glycol) gels and their swelling features," *Polym. Adv. Technol.*, vol. 26, no. 6, pp. 635–644, 2015.

[83] S. Hemmilä, J. V Cauich-Rodr\'\iguez, J. Kreutzer, and P. Kallio, "Rapid, simple, and cost-effective treatments to achieve long-term hydrophilic PDMS surfaces," *Appl. Surf. Sci.*, vol. 258, no. 24, pp. 9864–9875, 2012.

[84] M. Verma, A. K. Biswal, S. Dhingra, A. Gupta, and S. Saha, "Antibacterial response of polylactide surfaces modified with hydrophilic polymer brushes," *Iran. Polym. J.*, pp. 1–12, 2019.

[85] J. Hu, W. Wang, B. Zhou, Y. Feng, X. Xie, and Z. Xue, “Poly (ethylene oxide)-based composite polymer electrolytes embedding with ionic bond modified nanoparticles for all-solid-state lithium-ion battery,” *J. Memb. Sci.*, vol. 575, pp. 200–208, 2019.

[86] S. Louguet *et al.*, “Poly (ethylene glycol) methacrylate hydrolyzable microspheres for transient vascular embolization,” *Acta Biomater.*, vol. 10, no. 3, pp. 1194–1205, 2014.

[87] G. Su, T. Zhou, Y. Zhang, X. Liu, and A. Zhang, “Microdynamics mechanism of D 2 O absorption of the poly(2-hydroxyethyl methacrylate)-based contact lens hydrogel studied by two-dimensional correlation ATR-FTIR spectroscopy,” *Soft Matter*, vol. 12, no. 4, pp. 1145–1157, 2016.

[88] O. S. Kukolevska, I. I. Gerashchenko, M. V Borysenko, E. M. Pakhlov, M. Machovsky, and T. I. Yushchenko, “Synthesis and Examination of Nanocomposites Based on Poly(2-hydroxyethyl methacrylate) for Medicinal Use.,” *Nanoscale Res. Lett.*, vol. 12, no. 1, p. 133, Dec. 2017.

[89] N. S. Reddy and K. K. Rao, “Polymeric hydrogels: recent advances in toxic metal ion removal and anticancer drug delivery applications,” *Indian J. Adv. Chem. Sci*, vol. 4, no. 2, 2016.

[90] C. Zanardi *et al.*, “Development of a redox polymer based on poly (2-hydroxyethyl methacrylate) for disposable amperometric sensors,” *Electrochem. commun.*, vol. 62, pp. 34–37, 2016.

[91] G. S. Chauhan, S. Chauhan, U. Sen, and D. Garg, “Synthesis and characterization of acrylamide and 2-hydroxyethyl methacrylate hydrogels for use in metal ion uptake studies,” *Desalination*, vol. 243, no. 1–3, pp. 95–108, 2009.

[92] Z. Yu *et al.*, “Quasi-solid-state dye-sensitized solar cell fabricated with poly ($β$-hydroxyethyl methacrylate) based organogel electrolyte,” *Energy Environ. Sci.*, vol. 4, no. 4, pp. 1298–1305, 2011.

[93] P. A. Faccia and J. I. Amalvy, “Synthesis, characterization, and swelling behavior of new pH-sensitive hydrogels derived from copolymers of 2-hydroxyethyl methacrylate and 2-(diisopropylamino) ethylmethacrylate,” *J. Appl. Polym. Sci.*, vol. 127, no. 3, pp. 1974–1980, 2013.

[94] P. A. Faccia, F. M. Pardini, and J. I. Amalvy, “Evaluation of pH-sensitive poly(2-hydroxyethyl methacrylate-co-2-(diisopropylamino)ethyl methacrylate) copolymers as drug delivery systems for potential applications in ophthalmic therapies/ocular delivery of drugs,” *Express Polym. Lett.*, vol. 9, no. 6, pp. 554–566, 2015.

[95] H. Du and J. Zhang, “The synthesis of poly(vinyl cinnamates) with light-induced shape fixity properties,” *Sensors Actuators, A Phys.*, vol. 179, pp. 114–120, 2012.

[96] M. H. Wang and J. C. Kim, “Nanogels Composed of Cinnamoyl Alginate and Cinnamoyl Pluronic F127,” *J. Dispers. Sci. Technol.*, vol. 36, no. 3, pp. 377–

383, 2015.

[97] H. Esen, S. Küsefoğlu, and R. Wool, “Photolytic and free-radical polymerization of monomethyl maleate esters of epoxidized plant oil triglycerides,” *J. Appl. Polym. Sci.*, vol. 103, no. 1, pp. 626–633, 2007.

[98] D. Iqbal and M. H. Samiullah, “Photo-responsive shape-memory and shape-changing liquid-crystal polymer networks,” *Materials (Basel).*, vol. 6, no. 1, pp. 116–142, 2013.

[99] A. H. Ali and K. S. V. Srinivasan, “Synthesis, characterization, and studies on the solid-state crosslinking of functionalized vinyl cinnamate polymers,” *J. Appl. Polym. Sci.*, vol. 67, no. 3, pp. 441–448, 2002.

[100] C. Sheng, B. Wenting, T. Shijian, and W. Yuechuan, “Electrochromic Behaviors of Poly ( 3-n-octyloxythiophene ),” *Polymer (Guildf).*, vol. 108, pp. 900–903, 2008.

[101] J. Zou, Y. Liu, B. Shan, A. Chattopadhyay, and L. L. Dai, “Early damage detection in epoxy matrix using cyclobutane-based polymers,” *Smart Mater. Struct.*, vol. 23, no. 9, p. 95038, 2014.

[102] M. T. Ramesan, V. Nidhisha, and P. Jayakrishnan, “Synthesis, characterization and conducting properties of novel poly (vinyl cinnamate)/zinc oxide nanocomposites via in situ polymerization,” *Mater. Sci. Semicond. Process.*, vol. 63, pp. 253–260, 2017.

[103] M. T. Ramesan, P. Jayakrishnan, T. Sampreeth, and P. P. Pradyumnan, "Temperature-dependent AC electrical conductivity, thermal stability and different DC conductivity modelling of novel poly (vinyl cinnamate)/zinc oxide nanocomposites," *J. Therm. Anal. Calorim.*, vol. 129, no. 1, pp. 135–145, 2017.

[104] Y. Zhang, Y. M. Lam, and W. S. Tan, "Poly(ethylene oxide)-poly(propylene oxide)-poly(ethylene oxide)-g-poly(vinylpyrrolidone): Association behavior in aqueous solution and interaction with anionic surfactants," *J. Colloid Interface Sci.*, vol. 285, no. 1, pp. 74–79, 2005.

[105] N. Sahiner, W. T. Godbey, G. L. McPherson, and V. T. John, "Microgel, nanogel and hydrogel--hydrogel semi-IPN composites for biomedical applications: synthesis and characterization," *Colloid Polym. Sci.*, vol. 284, no. 10, pp. 1121–1129, 2006.

[106] S.-E. Park, Y.-C. Nho, and H.-I. Kim, "Preparation of poly (polyethylene glycol methacrylate-co-acrylic acid) hydrogels by radiation and their physical properties," *Radiat. Phys. Chem.*, vol. 69, no. 3, pp. 221–227, 2004.

[107] O. Okay, "Macroporous copolymer networks," *Prog. Polym. Sci.*, vol. 25, no. 6, pp. 711–779, 2000.

[108] T. Serizawa, H. Sakaguchi, M. Matsusaki, and M. Akashi, "Polyelectrolyte multilayers prepared on hydrogel surfaces," *J. Polym. Sci. Part A Polym. Chem.*, vol. 43, no. 5, pp. 1062–1067, 2005.

[109] D. Pathania *et al.*, "Novel nanohydrogel based on itaconic acid grafted tragacanth gum for controlled release of ampicillin," *Carbohydr. Polym.*, vol. 196, no. December 2017, pp. 262–271, 2018.

[110] W. Wang, H. Zhang, J. Shen, and M. Ye, "Facile preparation of magnetic chitosan/poly (vinyl alcohol) hydrogel beads with excellent adsorption ability via freezing-thawing method," *Colloids Surfaces A Physicochem. Eng. Asp.*, vol. 553, no. April, pp. 672–680, 2018.

[111] X. Allonas, J. P. Fouassier, L. Angiolini, and D. Caretti, "Excited-state properties of camphorquinone based monomeric and polymeric photoinitiators," *Helv. Chim. Acta*, vol. 84, no. 9, pp. 2577–2588, 2001.

[112] E. Jabbari and S. Nozari, "Swelling behavior of acrylic acid hydrogels prepared by γ-radiation crosslinking of polyacrylic acid in aqueous solution," *Eur. Polym. J.*, vol. 36, no. 12, pp. 2685–2692, 2000.

[113] E. Andrzejewska, E. Socha, and M. Andrzejewski, "Cross-linking photocopolymerization of dodecyl methacrylate with oxyethylene glycol dimethacrylates: Kinetics and reactivity ratios," *Polymer (Guildf).*, vol. 47, no. 19, pp. 6513–6523, 2006.

[114] C. Soykan, A. Delibaş, and R. Coşkun, "Novel copolymers of N-(4-bromophenyl)-2-methacrylamide with glycidyl methacrylate: Synthesis, characterization, monomer reactivity ratios and thermal properties," *React. Funct. Polym.*, vol. 68, no. 1, pp. 114–124, 2008.

[115] S. Lotfy and M. F. A. Taleb, “Free radical polymerization of polyvinyl butyral/polyethylene glycol diacrylate copolymer for removing organic dyes from waste water,” *Polym. Bull.*, vol. 75, no. 7, pp. 2865–2885, 2018.

[116] Z. Yang *et al.*, “Highly efficient adsorbent for organic dyes based on a temperature- and pH-responsive multiblock polymer,” *J. Appl. Polym. Sci.*, vol. 135, no. 34, pp. 1–8, 2018.

[117] V. Rizzi *et al.*, “A comprehensive investigation of dye–chitosan blended films for green chemistry applications,” *J. Appl. Polym. Sci.*, vol. 135, no. 10, pp. 1–14, 2018.

[118] G. Capar, U. Yetis, and L. Yilmaz, “Membrane based strategies for the pre-treatment of acid dye bath wastewaters,” *J. Hazard. Mater.*, vol. 135, no. 1–3, pp. 423–430, 2006.

[119] A. Y. Zahrim, C. Tizaoui, and N. Hilal, “Coagulation with polymers for nanofiltration pre-treatment of highly concentrated dyes: A review,” *Desalination*, vol. 266, no. 1–3, pp. 1–16, 2011.

[120] C. H. Liu, J. S. Wu, H. C. Chiu, S. Y. Suen, and K. H. Chu, “Removal of anionic reactive dyes from water using anion exchange membranes as adsorbers,” *Water Res.*, vol. 41, no. 7, pp. 1491–1500, 2007.

[121] S. Sheshmani, A. Ashori, and S. Hasanzadeh, “Removal of Acid Orange 7 from aqueous solution using magnetic graphene/chitosan: A promising nano-

adsorbent," *Int. J. Biol. Macromol.*, vol. 68, pp. 218–224, 2014.

[122] Z. Zhao *et al.*, "PH-Responsive polymeric Janus containers for controlled drug delivery," *Polym. Chem.*, vol. 6, no. 22, pp. 4144–4153, 2015.

[123] Y. Q. Yang *et al.*, "PH-sensitive micelles self-assembled from multi-arm star triblock co-polymers poly(ε-caprolactone)-b-poly(2-(diethylamino)ethyl methacrylate)-b-poly(poly(ethylene glycol) methyl ether methacrylate) for controlled anticancer drug delivery," *Acta Biomater.*, vol. 9, no. 8, pp. 7679–7690, 2013.

[124] X. Qiu, X. Ren, and S. Hu, "Fabrication of dual-responsive cellulose-based membrane via simplified surface-initiated ATRP," *Carbohydr. Polym.*, vol. 92, no. 2, pp. 1887–1895, 2013.

[125] Á. Szabó, G. Szarka, and B. Iván, "Synthesis of poly(poly(ethylene glycol) methacrylate)-polyisobutylene ABA block copolymers by the combination of quasiliving carbocationic and atom transfer radical polymerizations," *Macromol. Rapid Commun.*, vol. 36, no. 2, pp. 238–248, 2015.

[126] A. Mathew, H. Cao, E. Collin, W. Wang, and A. Pandit, "Hyperbranched PEGmethacrylate linear pDMAEMA block copolymer as an efficient non-viral gene delivery vector," *Int. J. Pharm.*, vol. 434, no. 1–2, pp. 99–105, 2012.

[127] A. M. L. Fernández, M. A. Villa-García, M. Rendueles, and M. Díaz,

"Synthesis of the Ion-Exchanger Based on 2-(diethylamino)ethyl Methacrylate-co-Ethyleneglycol Dimethacrylate Beads: Physico-Chemical Characterization and Chromatographic Performance for Sulfonamide Adsorption," *Solvent Extr. Ion Exch.*, vol. 33, no. 3, pp. 295–312, 2015.

[128] L. A. Manzanares-Guevara, A. Licea-Claverie, and F. Paraguay-Delgado, "Preparation of stimuli-responsive nanogels based on poly(N,N-diethylaminoethyl methacrylate) by a simple 'surfactant-free' methodology," *Soft Mater.*, vol. 16, no. 1, pp. 37–50, 2018.

[129] P. Quiñonez-Angulo, J. Ruiz-Villegas, Á. Licea-Claveríe, A. Ramirez-Jiménez, V. Miranda-Soto, and I. Zapata-González, "A kinetic study, thermal analysis and kinetic modeling on homo and copolymerization of 2-(N,N-diethylamino)ethyl methacrylate and PEGMA," *Eur. Polym. J.*, vol. 109, no. July, pp. 347–359, 2018.

[130] F. A. Ngwabebhoh, A. Erdem, and U. Yildiz, "Synergistic removal of Cu(II) and nitrazine yellow dye using an eco-friendly chitosan-montmorillonite hydrogel: Optimization by response surface methodology," *J. Appl. Polym. Sci.*, vol. 133, no. 29, pp. 1–14, 2016.

[131] S. Jana, J. Ray, S. K. Bhanja, and T. Tripathy, "Removal of textile dyes from single and ternary solutions using poly(acrylamide-co-N-methylacrylamide) grafted katira gum hydrogel," *J. Appl. Polym. Sci.*, vol. 135, no. 10, pp. 1–20, 2018.

[132] M. A. Kamal, S. Bibi, S. W. Bokhari, A. H. Siddique, and T. Yasin, "Synthesis and adsorptive characteristics of novel chitosan/graphene oxide nanocomposite for dye uptake," *React. Funct. Polym.*, vol. 110, pp. 21–29, 2017.

[133] A. E. Muftuoglu, B. Saner, A. Levent Demirel, and Y. Yagci, "Synthesis and characterization of graft and branched polymers via type-II photoinitiation," *Des. Monomers Polym.*, vol. 8, no. 6, pp. 645–658, 2005.

[134] K. T. Nguyen and J. L. West, "Photopolymerizable hydrogels for tissue engineering applications," *Biomaterials*, vol. 23, no. 22, pp. 4307–4314, 2002.

[135] J. M. Rosiak and P. Ulański, "Synthesis of hydrogels by irradiation of polymers in aqueous solution," *Radiat. Phys. Chem.*, vol. 55, no. 2, pp. 139–151, 1999.

[136] N. Zeng *et al.*, "Facile synthesis of branched polyvinyl acetate: Via redox-initiated radical polymerization," *Polym. Chem.*, vol. 9, no. 23, pp. 3215–3222, 2018.

[137] S. M. Sayyah, S. S. Abd El-Rehim, S. M. Kamal, M. M. El-Deeb, and R. E. Azooz, "Electropolymerization kinetics of a binary mixture of o-phenylenediamine and 2-aminobenzothiazole and characterization of the obtained polymer films," *J. Appl. Polym. Sci.*, vol. 119, no. 1, pp. 252–264, 2011.

[138] A. Ju, S. Guang, and H. Xu, “Molecular design and stabilization mechanism of acrylonitrile bipolymer,” *J. Appl. Polym. Sci.*, vol. 129, no. 6, pp. 3255–3264, 2013.

[139] G. V. R. Reddy, N. G. Devi, and J. Panda, “Microemulsion and conventional emulsion copolymerizations of styrene with methyl methacrylate,” *J. Appl. Polym. Sci.*, vol. 105, no. 6, pp. 3391–3401, 2007.

[140] A. Kanellou, A. Spilioti, G. V Theodosopoulos, I. Choinopoulos, and P. Marinos, “Statistical copolymers of benzyl methacrylate and diethylaminoethyl methacrylate: monomer reactivity ratios and thermal properties,” *J. Org. Inorg. Chem*, vol. 1, no. 1, pp. 1–11, 2015.

[141] B. Li, Q. Zhong, D. Li, K. Xu, L. Zhang, and J. Wang, “Influence of Ethylene Glycol Methacrylate to the Hydration and Transition Behaviors of Thermo-Responsive Interpenetrating Polymeric Network Hydrogels,” *Polymers (Basel).*, vol. 10, no. 2, p. 128, 2018.

[142] H. Sun, L. Zhang, X. Zhu, C. Kong, C. Zhang, and S. Yao, “Poly(PEGMA) magnetic nanogels: Preparation via photochemical method, characterization and application as drug carrier,” *Sci. China, Ser. B Chem.*, vol. 52, no. 1, pp. 69–75, 2009.

[143] H. E. Kissinger, “Reaction kinetics in differential thermal analysis,” *Anal. Chem.*, vol. 29, no. 11, pp. 1702–1706, 1957.

[144] F. M. Pardini and J. I. Amalvy, “Synthesis and swelling behavior of pH-responsive polyurethane/poly[2- (diethylamino)ethyl methacrylate] hybrid materials,” *J. Appl. Polym. Sci.*, vol. 131, no. 2, pp. 1–8, 2014.

[145] O. Okay, *Macroporous copolymer networks*, vol. 25, no. 6. 2000.

[146] S. Akgöl, N. Tüzmen, and A. Denizli, “Porous dye affinity beads for albumin separation from human plasma,” *J. Appl. Polym. Sci.*, vol. 105, no. 3, pp. 1251–1260, 2007.

[147] L. Xiong *et al.*, “Adsorption behavior of methylene blue onto titanate nanotubes,” *Chem. Eng. J.*, vol. 156, no. 2, pp. 313–320, 2010.

[148] W. Li *et al.*, “Tunable adsorption properties of bentonite/carboxymethyl cellulose-g-poly(2-(dimethylamino) ethyl methacrylate) composites toward anionic dyes,” *Chem. Eng. Res. Des.*, vol. 124, no. Cmc, pp. 260–270, 2017.

[149] D. Robati *et al.*, “Removal of hazardous dyes-BR 12 and methyl orange using graphene oxide as an adsorbent from aqueous phase,” *Chem. Eng. J.*, vol. 284, pp. 687–697, 2016.

[150] F.-N. Allouche, N. Yassaa, and H. Lounici, “Sorption of Methyl Orange from Aqueous Solution on Chitosan Biomass,” *Procedia Earth Planet. Sci.*, vol. 15, pp. 596–601, 2015.

[151] X. X. Hou, Q. F. Deng, T. Z. Ren, and Z. Y. Yuan, “Adsorption of Cu2+ and

methyl orange from aqueous solutions by activated carbons of corncob-derived char wastes," *Environ. Sci. Pollut. Res.*, vol. 20, no. 12, pp. 8521–8534, 2013.

[152] L. Donnelly, J. G. Hardy, S. P. Gorman, D. S. Jones, N. J. Irwin, and C. P. McCoy, "Photochemically Controlled Drug Dosing from a Polymeric Scaffold," *Pharm. Res.*, vol. 34, no. 7, pp. 1469–1476, 2017.

[153] A. Singh, H. Dubey, I. Shukla, and D. P. Singh, "Pulsatile drug delivery system: An approach of medication according to circadian rhythm," *J. Appl. Pharm. Sci.*, vol. 2, no. 3, pp. 166–176, 2012.

[154] S. Jafari, M. Soleimani, and R. Salehi, "Nanotechnology-based combinational drug delivery systems for breast cancer treatment," *Int. J. Polym. Mater. Polym. Biomater.*, vol. 68, no. 14, pp. 859–869, 2018.

[155] C. D. Petruczok, E. Armagan, G. O. Ince, and K. K. Gleason, "Initiated chemical vapor deposition and light-responsive cross-linking of poly(vinyl cinnamate) thin films," *Macromol. Rapid Commun.*, vol. 35, no. 15, pp. 1345–1350, 2014.

[156] Y. Ni and S. Zheng, "A novel photocrosslinkable polyhedral oligomeric silsesquioxane and its nanocomposites with poly(vinyl cinnamate)," *Chem. Mater.*, vol. 16, no. 24, pp. 5141–5148, 2004.

[157] Y. Kodama, M. Barsbay, and O. Güven, "Poly(2-hydroxyethyl methacrylate)

(PHEMA) grafted polyethylene/polypropylene (PE/PP) nonwoven fabric by γ-initiation: Synthesis, characterization and benefits of RAFT mediation," *Radiat. Phys. Chem.*, vol. 105, pp. 31–38, 2014.

[158] H. T. Kim and J. K. Park, "Thermal degradation of poly (vinyl cinnamate)," *Polym. Bull.*, vol. 41, no. 3, pp. 325–331, 1998.

[159] K. C. Ofokansi, M. U. Adikwu, and V. C. Okore, "Preparation and evaluation of mucin-gelatin mucoadhesive microspheres for rectal delivery of ceftriaxone sodium," *Drug Dev. Ind. Pharm.*, vol. 33, no. 6, pp. 691–700, 2007.

[160] N. C. Obitte, A. Chukwu, and I. V. Onyishi, "The use of a pH-dependent and Non pH-dependent natural hydrophobic biopolymer (Landolphia owariensis latex) as capsule coating agents in in vitro controlled release of metronidazole for possible colon targeted delivery," *Int. J. Appl. Res. Nat. Prod.*, vol. 3, no. 1, pp. 1–17, 2010.